Checks and Balances: Transcriptional Regulation of Myeloid Innate Immunity and Dendritic Cell Maturation

Rodolfo Nazitto

A dissertation submitted in partial fulfillment of the requirements for the degree of
Doctor of Philosophy

University of Washington
2021

Reading Committee:
Alan Aderem, Chair
Jessica Hamerman
Ram Savan

Program Authorized to Offer Degree:
Immunology

University of Washington

ABSTRACT

Checks and Balances: Transcriptional Regulation of Myeloid Innate Immunity and Dendritic Cell Maturation

Rodolfo Nazitto

Doctor of Philosophy in Immunology

Dr. Alan Aderem, Chair

Antigen presenting cells such as myeloid dendritic cells (DCs) are key sentinels of the innate immune system. In response to pathogen recognition and innate immune stimulation, DCs transition from an immature to a mature state that is characterized by widespread changes in host gene expression, which include the upregulation of cytokines, chemokines, and costimulatory factors to protect against infection. Several transcription factors are known to drive these gene expression changes, but the mechanisms that negatively regulate DC maturation are less well understood. Here, we identify the transcription factor Interleukin Enhancer Binding Factor 3 (ILF3) as a negative regulator of innate immune responses and DC maturation. Depletion of ILF3 in primary human monocyte-derived DCs (MDDCs) led to increased expression of maturation markers and potentiated innate responses during stimulation with viral mimetics or classic innate agonists. Conversely, overexpression of short or long ILF3 isoforms (NF90 and NF110) suppressed DC maturation and innate immune responses. Through mutagenesis experiments, we found that a nuclear localization sequence in ILF3, and not its dual double-stranded RNA-binding domains (dsRBDs), was required for this function. Mutation of the domain associated with zinc finger (DZF) motif of ILF3's NF110 isoform blocked its ability to

suppress DC maturation. Moreover, RNA-seq analysis indicated that ILF3 regulates genes associated with cholesterol homeostasis in addition to genes associated with DC maturation. Together, our data establish ILF3 as a transcriptional regulator that restrains DC maturation and limits innate immune responses through a mechanism that may intersect with lipid metabolism.

TABLE OF CONTENTS

LIST OF FIGURES

Chapter 3:

Chapter 4:

Summary:

ACKNOWLEDGEMENTS

First, I would like to deeply thank my P.I. Alan Aderem for being a mentor that has guided my success as a graduate student during my time in his lab. He has always taken the time for any requests for help I may have needed throughout my training, even well up past midnight. He is one of the most dedicated and caring mentors I have ever encountered during my academic career. Alan has always supported my scientific and career goals wherever they may lead me. Apart from his scientific guidance, I have appreciated his commitment to the mental health and well-being of his lab members as first and foremost. Graduate school is often a time of many difficulties and hardships beyond the laboratory. Alan has always understood how important and meaningful family is to me. I am forever grateful for his understanding and never hesitating to let me see my family on their birthdays, holidays, and during times of stress.

I would also like to thank my scientific mentor Jarrod Johnson for going above and beyond in being one of the best mentors a graduate student could ask for. Having someone so invested in your academic success and keeping a positive attitude even when you think things have all gone wrong has been an invaluable part of my scientific training. I am forever appreciative of all his mentorship in learning new skills, techniques, traits of a good scientist, and time taken to review grants and manuscripts. I also want to thank Sasha Lucas and Stephanie Skelton for also being incredibly supportive team members in the lab who always had smiles on their faces and encouraged me throughout their time in lab to press on in the darker times.

I want to also thank Alan Diercks for taking on the role of scientific mentor when Jarrod moved on to bigger and bigger things. He is one of the most talented computational biologists and immunologists; having been trained in physics and adapted into an innate immunity lab. His

support, like others in the lab, has extended beyond the science into my personal well-being as well during the challenges brought about in 2020 by COVID-19. I am forever grateful for his contribution to my training as a graduate student and as a human being.

I want to thank the rest of the Aderem lab, about which I could write an entire chapter. Greg Olson has been the best graduate student partner to have in the lab and will always be thankful for our discussions. Alissa Rothchild has been an extremely caring and talent scientist to work with and I am so appreciative of her knowledge and expertise, especially in flow cytometry. Thank you to Liz Gold for being there to keep me on track and a voice of reason in the lab. Thank you to Lynn Amon for being a patient and wonderful bioinformatic mentor in my first introduction to sequencing analysis. Thank you to Dat Mai, Ana Jahn, Irina Podolskaia, Tara Murray, Drew Dover, Angie Solomon, Rosa Suen, Rebecca Podyminogin, Vincent Tam, Mary Young, and Peter Asokovich for all their collective contributions to my training over the years.

As part of the Molecular Medicine Training Certificate program, I want to thank my mentor Kevin Urdahl for taking me on as his mentee. His clinical expertise provided invaluable insight into my own project. I also thank Nancy Maizels and Conrad Liles for their contributions to make success in the certificate program.

I thank the Department of Immunology for supporting me during my time as a graduate student. In particular, Sandy Turner, Sarah Bland, and Peggy McCune for making sure I kept on top of all my requirements and documents.

I want to thank my thesis committee members Ram Savan, Jessica Hamerman, and Deborah Fuller for their constant guidance and support of my thesis project and growth as a graduate student. I have appreciated their comments and suggestions.

I am grateful for my rotation lab mentors Marion Pepper and Jessica Hamerman. Though I did not join their labs, I enjoyed being a part of their teams and learned many skills that I still use and take forward with me to this day. They are wonderful mentors and their contributions continue to impact my work in an extremely positive way.

My cohort colleagues Annelise Snyder, Rebecca Olson, Kerri Thomas, and Jared Delahaye have been the most wonderful and talented set of individuals to have as a support system. I am truly honored to know and call them my friends. I am excited to see what great things they all will achieve in their respective fields.

I also want to acknowledge the contributions to my various mentors outside of academia. Joanne Cuomo and her team at ICON Central Labs for teaching me flow cytometry in high school, Mark Sandberg and Antony Symons during my time at Amgen, Lola Martinez at the Spanish National Cancer Research Center in Madrid, Spain, William Golde at Plum Island Animal Disease Center, and Carrie Rosenberger at Genentech. Thank you all for imparting your skills and mentorship onto me to provide me with invaluable perspective. I also want to thank my teachers in K-12 that were 100% committed to their students and their ultimate success.

Lastly, but most importantly, I want to thank my entire family. I cannot stress enough how impactful and important their collective presence has been in my life. Most of all, I dedicate and owe my success to this entire work to my parents, Benjamin and Sara Nazitto. What they have done in raising and guiding me to this point in my life, in addition to the struggles of their own lives growing up, dwarfs any accomplishment I have made during my life thus far. They are the strongest people I know in this world and I want them to know for perpetuity that I love them beyond condition. No one could have done better raising their child and imparting onto them the value of higher education. We have been through a lot in my 30 years so far, but I want them to

know that I have always appreciated everything they have sacrificed and done for me. My only wish is that I could repay them 10 times over for it, and that I would have expressed this more growing up. Thank you for being my best friends, my mentors, my teachers, and my everything, Mom and Dad, I love you. Thank you.

CHAPTER 1: INTRODUCTION

DC Development and Maturation

Dendritic cells (DCs) are key antigen presenting sentinels of the innate immune (1). They are the cellular bridges between a pathogen and the adaptive immune response to eliminate and establish T- and B-cell mediated immune memory (2). Much of our understanding of myeloid DC biology, and dendritic cell development, subset characterization, and function stems from experiments started in mouse models (3, 4). In mice, DCs undergo a process of development in the bone marrow and differentiation from progenitor cell types beginning with hematopoietic stem cells, to common myeloid progenitors, macrophage/DC progenitors, and common DC progenitors (4). Common DC progenitors give rise to DC subsets such as plasmacytoid (pDC) and pre-DCs which are capable of differentiating into conventional cDC1 (to prime CD8 T-cell responses, efficient cross-presentation) and cDC2 (to prime CD4 T-cell responses) subsets.

Macrophage/DC progenitors can give rise to circulating monocytes through differentiation into common monocyte progenitors. In humans, these monocytes can then be further differentiated *in vivo* into the monocyte-derived DC (MDDC) (5, 6). Human monocytes have been used *in vitro* as a well-established as a cell type to model myeloid DCs when derived into monocyte-derived dendritic cells (7). *In vitro,* MDDCs are derived by the incubation of the cytokines IL-4 and GM-CSF over the course of several days to generate immature MDDCs (8, 9). Importantly, circulating DC subsets have been increasingly studied in humans in an effort to provide greater insight into the equivalency of DC subsets between human and mouse (10).

Differentiation and maintenance of these DC subsets require key transcription factors that assist in these processes to give rise to various DC subsets. Transcription factors such as PU.1 can broadly and positively affect the fate and development of multiple subsets of myeloid

dendritic cells (11, 12). XBP-1 is another such broad-acting transcription factor that is required for DC development of both classical and plasmacytoid DCs (13). Other transcription factors are more specific to certain DC subsets, such as the transcription factors E2-2 and SPI-B to plasmacytoid DCs for their proper development and maintenance (14, 15). Classical cDC1 DCs require transcription factors IRF8 (16, 17) and BATF3 (18) while cDC2 DCs require IRF4 (19) and KLF4 (20, 21). Interestingly, while ID2 is upregulated across multiple DC subsets, it is required for the maintenance of Langerhans cells as well as cross presenting CD8α+ DCs (22, 23). Human monocyte-derived DCs utilize AHR, IRF4, and NCOR2 for their differentiation (8, 9).

Once differentiated, immature DCs are poised to respond to pattern-recognition receptor (PRR) and interferon (IFN) stimuli to undergo a process of maturation, a hallmark of DCs. This process confers morphological and functional changes altering antigen processing and presentation by increasing MHC class II molecules such as HLA-DR to the surface loaded with phagocytized and processed antigen. Chemokine receptors such as CCR7 are also upregulated to begin the journey of trafficking to the proximal lymph node from the site of infection, ultimately to prime naïve T-cells with newly presented antigen (24). In cooperation with MHC class II presentation, DCs also upregulate a variety of costimulatory surface molecules such as CD80 and CD86 that can engage receptors on T-cells such as CD28 to activate or CTLA-4 to help resolve the innate immune response to a vanquished pathogen by initiating an anti-inflammatory program (25).

To develop the quality and specificity in T-cell priming, maturation also enables mature DCs to secrete various cytokines depending on the context of the insult (viral, fungal, helminth, etc.). IL-12p70 (the biologically active form derived from IL-12p35 and IL-12p40) and type I

interferons can skew T-cell differentiation toward a Th1 phenotype combat viral and bacterial infections (26). For Th17 differentiation, IL-23 (composed of IL-12-p40 and IL-12p19) and IL-1β secreted by DCs can skew T-cells towards this phenotype against extracellular bacteria and fungi (27). The anti-inflammatory cytokines TGF-β (28) and IL-10 (29, 30) secreted by DCs can aid in the development of immunosuppressive regulatory T-cells, preferentially generated by immature or partially mature DCs (31).

But what regulates this process of maturation that orchestrates the delicate balance between inflammation and immune suppression? Many host molecules on myeloid DCs can contribute to this process of resolution and suppression such as *trans* surface receptor engagement of CD80/CD86-CTLA4 and cytokines like IL-10 and TGB-β. However, transcription factors control broad transcriptomic changes that make them ideal candidates as gatekeepers of DC maturation. Numerous transcription factors are already known to promote or restrain DC maturation. T-bet and Interferon Regulatory Factor 3 (IRF3) are examples of master transcription factors that are required for optimal myeloid DC maturation in response to innate stimulation (32-34). Nuclear factor–kB1 (NF-kB1) and Foxo3 are transcription factors that can temper and suppress inflammatory DC activation (35, 36). NF-kB1 can be engaged through IL-10 or TLR ligand stimulation, while Foxo3 can be activated upon engagement of CD80/86 with CTLA-4 on activated T-cells. Discovery of additional transcription factors that either act as master regulators or factors that fine-tune DC maturation is key to our understanding of human innate immunity in not only programming efficient adaptive immune responses, but also how these responses are eventually resolved and kept in check from aberrant hyperinflammation.

Intracellular Nucleic Acid Sensing in MDDCs

In the context of viral infection, DCs have the ability to undergo maturation through recognition of viral nucleic acids by intracellular nucleic acid sensors and the production of type I interferons (IFN-Is). Enveloped RNA viruses generate RNA nucleic acid species or create cDNA through reverse transcription in the case of retroviruses that can be sensed by intracellular nucleic acid sensors. RNA species can be detected through RIG-I-like receptor (RLR) sensors such as RIG-I that can detect *in vitro* transcribed or short double-stranded RNA species, or through MDA5 detecting 5' tri-phosphate single-stranded RNA and the agonist PolyI:C (37). Differential detection of viruses also occurs between RIG-I and MDA5 with RIG-I recognizing paramyxoviruses, influenza virus and Japanese encephalitis virus and MDA5 recognizing picornaviruses (37). Both of these sensors signal through the mitochondrial antiviral-signaling protein (MAVS) localized to the mitochondrial outer membrane. Phosphorylation events following MAVS via TBK1 lead to the phosphorylation and dimerization of the transcription factor IRF3 that drives IFN production, along with inflammatory cytokines through the recruitment of NF-κB (38).

Complementing the detection of viral RNA species, intracellular DNA sensors detect viral DNA species, as well as host DNA, to initiate a variety of innate immune responses including IFN induction, pro-inflammatory cytokine secretion, and cell death. Sensors of double-stranded DNA (dsDNA) such as cyclic GMP-AMP synthase (cGAS) and the Absent in melanoma 2(AIM2)-like receptor (ALR) IFI16 can contribute to the production of IFN-Is using similar adapters as previously described downstream of MAVS such as TBK1. In myeloid DCs, it has been established that IFI16 is dispensable and plays no significant role in innate immune activation, in contrast to macrophages (34, 39). Once dsDNA is bound by cGAS, a secondary

messenger is produced called 2’3’-cGAMP (cyclic [G(2',5')pA(3',5')p) and activates the stimulator of interferon genes (STING) localized at the endoplasmic reticulum (40-42). Signaling then uses adapter proteins ofthe RLR pathway at the level of TBK1 and IRF3 phosphorylation and dimerization. This also results in the production of IFN, which signals through the interferon alpha receptor (IFNAR), comprised of IFNAR1 and IFNAR2. This signaling then recruits Signal transducer and activator of transcription 1 and 2 (STAT1, STAT2), along with IRF9 to form the interferon-stimulated γ factor 3 (ISGF3) transcriptional complex that binds to the Interferon-stimulated response element (ISRE) (43). This complex can induce a battery of interferon-stimulated genes (ISGs) which confers protective antiviral immunity within the cell and to the local environment.

Shared with the RLR and cGAS/STING sensing pathways, activation of NF-κB occurs downstream of MAVS and STING, respectively, signaling to produce a slew of inflammatory cytokines (44, 45). Transcription of *IL1B, IL6, TNFA,* and other inflammatory genes are expressed upon sensing of nucleic acid species to aid in the antiviral response. Notably in monocyte-derived DCs, endosomal sensing of viral ssRNA via TLR8 signals through the adapter MyD88 to activate NF-κB, but does not induce activation of IRF3 to express type I IFNs alone (34). Only upon activation of the cGAS/STING pathway can endosomal TLR signaling boost dsDNA-primed IFN responses in MDDCs (34). Thus, NF-κB activation via endosomal TLR sensing is insufficient to induce type I IFNs alone in MDDCs, but is required for the induction of pro-inflammatory cytokines downstream of either endosomal or nucleic acid sensing pathways.

HIV-1 & Sensing by Myeloid Dendritic Cells

A viral pathogen that has been extensively studied in the context of its ability to stimulate innate immune responses through intracellular nucleic acid sensing is Human Immunodeficiency Virus 1 (HIV-1). HIV-1 affects approximately 1.2 million people in the United States and approximately 38 million people worldwide (46). There is no current cure for HIV-1 though many significant strides have been made in controlling viral loads with the development of antiretroviral therapy drugs and their use in pre- and post-exposure prophylaxis in uninfected individuals. However, a vaccine against HIV-1 does not currently exist, underscoring the need for continued research into how HIV-1 evades the immune system and leads to chronic, hyperinflammatory conditions.

HIV-1 is a positive-sense single-stranded RNA lentivirus of the retrovirus virus family. HIV-1 enters its primary immune cell target CD4+ T-cells, though it can also infect macrophages, monocytes, and dendritic cells using the CD4 receptor and CCR5 or CXCR4 co-receptor engaged with HIV-1's trimer of gp120 and gp41 glycoproteins (47). Once inside the cell, the ssRNA is converted to viral cDNA via its reverse transcriptase within the viral capsid. Once the capsid reaches and passes through the nuclear envelope in close association with cyclophilin A in MDDCs, the viral cDNA forms an intasome with integrase bound each of the long terminal repeats (LTRs) (33, 48). The viral cDNA is then integrated into the genome of the cell where transcription of HIV-1 RNA species and subsequent translation of viral proteins such as Gag can occur to produce new infectious virions within the infected host cell.

In the context of myeloid DCs and induction of antiviral IFN, HIV-1 is able to go largely undetected by these key antigen presenting cells ultimately resulting in a dysregulated and cytopathic antiviral response (49). The vast majority of DCs are not productively infected and

while evidence of cDNA from the closely related simian immunodeficiency virus (SIV) has been found *in vivo* within DCs in non-human primate tissue, this likely is the result of phagocytosed infected target cells (50). IFNs have been studied *in vitro* and *in vivo* with great interest as a means to combat and cure HIV-1 infection. Work done with the SIV in rhesus macaques has shown that systemic IFN acts as a double-edged sword in controlling infection (51). Blocking IFNAR systemically with an anti-IFNAR antibody during SIV infection leads to significantly increased viral loads and rapid depletion of the CD4 T-cell compartment. Interestingly, when IFN (specifically IFN-α2a) is provided at the time of SIV infection, there is a rapid induction of ISGs and protection from acquisition of SIV (51). Importantly, when administration of IFN was prolonged representing chronic infection, there was pronounced desensitization to IFN. SIV infection is able to take hold resulting in viral loads and T-cell depletion similar to that seen with IFNAR blocking antibody. This mirrors what has been show in humans infected with HIV-1 where during the chronic phase of infection there is a direct correlation with levels of IFN and viral load and an inverse correlation between IFN and CD4+ T-cell count (52). Thus, both the timing and robustness in the IFN response against HIV-1 is of critical importance and understanding the mechanism by which HIV-1 dysregulates this process within innate immune cells charged with the responsibility to program adaptive immunity like myeloid DCs is critical.

Examining infection in myeloid DCs, previous work has shown that an array of host factors prevent detection of viral cDNA by cGAS, the DNA sensor of HIV-1 in myeloid DCs. The exonuclease TREX1 deficient in Aicardi-Goutiere Syndrome patients, is responsible for eliminating both self and unmasked HIV-1 dsDNA from detection by cGAS (53). More recently, NONO was discovered to work in tandem with cGAS to detect incoming viral capsid in the nucleus, allowing for the specific detection of HIV-2 cDNA and not self, genomic DNA (54).

The capsid of HIV-1 is of important interest as differences to closely related HIV-2 reveal differential association and binding to the DC host factor cyclophilin A (CypA). HIV-2's interaction with CypA allows for the escape, replication, and potential detection of viral cDNA made within the capsid (55, 56). HIV-1 has a high affinity for CypA stabilizing the capsid (57), thus preventing most pre-integration cGAS-mediated sensing of cDNA (58). Post-integration, there may be additional mechanisms by which HIV-1 cDNA is sensed by cGAS, potentially involving newly synthesized Gag molecules, CypA, and the capsid to unmask cDNA (33). Recent work has shown exciting new evidence that during reverse transcription, viral double-stranded cDNA can be extruded through patches in the stabilized capsid structure highlighting the relevance for examining DNA sensing in myeloid DCs (59).

Sensing of HIV-1 cDNA via cGAS/STING, under certain permissive conditions, induces DC maturation during HIV-1 infection in myeloid DCs that is dependent on the master transcription factor IRF3 (34). In DCs lacking IRF3, these cells fail to induce IFN and upregulate costimulatory molecules such as CD80 and CD86, markers of DC maturation (33, 34). Discovery of other transcription factors key to this process will aid in illuminating how myeloid DCs balance potent antiviral interferon signaling and DC maturation.

HIV-1-GFP as a viral mimetic of HIV-1 infection, bypassing host restriction in MDDCs

Myeloid DCs express several host restriction factors that limit innate immune sensing and viral replication. These include factors such as TRIM5α (premature uncoating of the virion core and activates E3 ubiquitin ligase activity) (60, 61), APOBEC3G (a cytidine deaminase that edits HIV-1 cDNA) (62), MxB (prevents nuclear import for HIV-1 cDNA) (63), SLFN11 (inhibits translation of HIV-1 RNA) (64), Tetherin (inhibits budding of HIV virions from the cell surface)

(65, 66), and IFITM1-3 (incorporated into virions and impairs viral entry) (67). HIV-1 accessory proteins can aid in overcoming these restriction factors such as Vif disabling APOBEC3G (68, 69) and Vpu disabling Tethrin (65). SAMHD1 is another host restriction factor that depletes the pool of dNTPs available for reverse transcription of HIV-1 ssRNA (70). SAMHD1-mediated restriction can be overcome by the HIV-2 and SIV accessory protein Vpx.

Taking advantage of this relationship, a system utilizing SIV Vpx in monocyte-derived DCs can examine the regulation of innate immune responses and DC maturation (71, 72). HIV-1-GFP is a single-cycle, VSV-G pseudotyped, attenuated form of HIV-1 lacking l *env*, *vif*, *vpr*, and *vpu* accessory protein-coding genes and has GFP in place of *nef* as a proxy to track integration (73, 74). Vpx is delivered *in trans* prior to infection to disable SAMHD1 via recruitment of a cullin4A-RING E3 ubiquitin ligase to target Vpx for proteasomal degradation (75). This then allows for productive infection of myeloid DCs. Together, this system allows for the discovery of potential novel regulators of innate immune sensing and DC maturation in myeloid DCs.

Interleukin Enhancer Binding Factor 3 (ILF3)

This work uncovers the role of a dual transcription factor/RNA-binding protein as a negative regulator of myeloid DC maturation. *ILF3*, located on chromosome 19 in humans, encodes 2 major protein isoforms, NF90 and NF110, caused by an alternative splicing event causing the inclusion of 3 coding exons (exons 19, 20, and 21) in NF110 (76-78). These isoforms are identical through the C-terminus of NF110 that extends beyond NF90, which contains a GQSY-repeat motif that has been found to be essential from protein aggregation (79). NF90 and NF110 share several other domains in common such as a Nuclear Export Signal (NES) that is

located with the Domain Associated with Zinc Finger domain (DZF) containing a C2H2 zinc finger (80). The DZF has largely been associated with binding with its stabilization partner ILF2 (encoded by *ILF2*) as well as transcriptional activity (81). Strikingly, there is a high degree of conservation of amino acid residues within the DZF across vertebrates, suggesting evolutionary selective pressure to retain DZF structure and function (Fig. 1A). Apart from interspecies conservation of the DZF domain, within humans, there are only 4 gene families that encode a DZF: *ILF3*, *ILF2* (ILF3's stabilization binding partner), *SPNR* (a testes-specific paralogue of *ILF3*), and *ZFR* (81). The DZF domain has high structural homology to the family of template-free nucleotidyltransferases such as poly (A) polymerases, 2′–5′ oligoadenylate synthase (OAS) (an interferon stimulated gene family), and tRNA nucleotidyltransferase (81). However, key catalytic residues from these transferases are not conserved in ILF3 thus forming a "pseudotransferase" which might give rise to new biological function. NF90 and NF110 also share a Nuclear Localization Signal (NLS) essential for its localization to the nucleus at steady state conditions (82). Also common to both isoforms are two double-stranded RNA-binding domains (dsRBDs) which are essential for its function as an RNA-binding protein . An RGG-repeat motif follows the dsRBDs and is a domain that supports coordination of broader RNA-binding by the dual dsRBDs (83). Both NF90 and NF110 have been given alternative names such as NFAR-1 and NFAR-2, DRBP76, or ILF3, respectively.

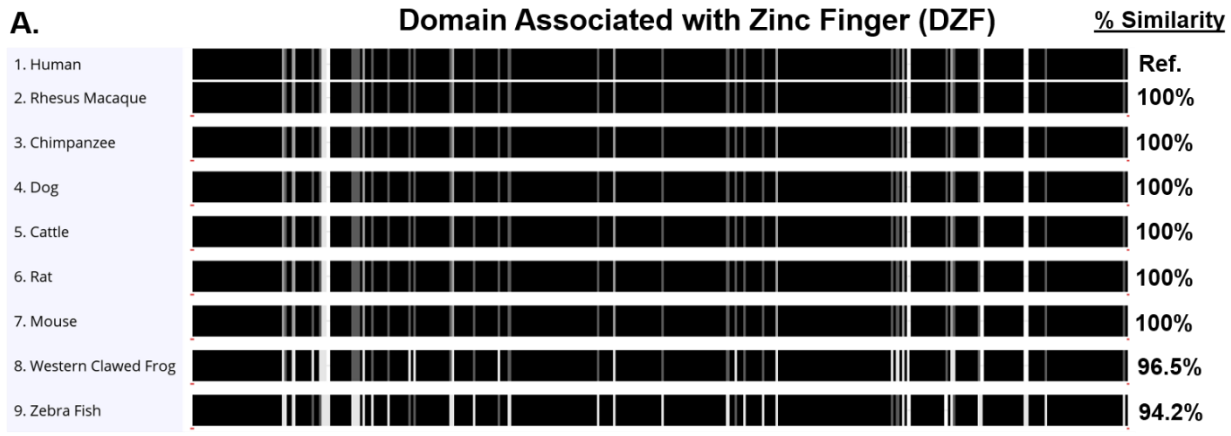

Figure. 1. ILF3's DZF domain is highly conserved across multiple vertebrate species. A. MUSCLE alignment of the DZF domain (amino acid residues 89-342) of human ILF3 to full length ILF3 sequences of indicated vertebrate species, trimmed after alignment. Similarity score calculated using human ILF3 as the reference calculated using Blosum45 with threshold 0.

ILF3 was first discovered in the human Jurkat T-cell cell line as a subunit of the Nuclear Factor of Activated T-cells (NF-AT) enhanceosome, along with its stabilization partner Interleukin Enhancer Binding Factor 2 (ILF2) (84-86). ILF3 was found to be bound at the region of the promoter of interleukin 2 (*IL2*) known as the antigen receptor response element 2 (ARRE-2) where the NF-AT complex is required to bind for *IL2*'s transcription following T-cell activation. Later work has also shown that ILF3 as an enhancer of *IL13* transcription, using a similar DNA-binding sequence to the ARRE-2 promoter of *IL2* (CTGTT) (87). Following these works, ILF3 has been shown to be a transcriptional regulator of other genes aside from the family of interleukins such as *FOS* and *HLA-DRA* (88, 89). Apart from the NF-AT complex, ILF3 is also a member of other transcriptional complexes such as DNA-PK, primarily composed of Ku70, Ku80, and DNA-PKcs involved in DNA-damage repair (84, 90). Studies have revealed that a transcriptional complex of isoform NF90, Ku70, Ku80, and DNA-PKcs can also bind to the ARRE-2 of *IL2* to enhance its induction (84). Interestingly, though there is evidence that ILF3 can be found bound to dsDNA (91), neither NF90 or NF110 contains a *bona fide* DNA-binding domain. This implies that ILF3 could harbor a noncanonical DNA-binding domain or

require association with transcription factors with DNA-binding domains in order to execute its regulatory role.

Apart from ILF3's role as a transcriptional regulator, its secondary function involves its capacity to function as an RNA-binding protein utilizing its dual dsRBDs targeting not only host, but also viral pathogen RNA species. ILF3 can bind the 3' UTR of various host mRNAs to cause either their stabilization for subsequent translation or promote their degradation. In the case of *IL2* following its role as a transcriptional enhancer, ILF3 binds to the 3' UTR of *IL2* within a region of four "AUUUA" motifs, common to many cytokines and chemokine transcripts (80, 92). This binding is required for the stabilization of the mature *IL2* transcript during export of the ILF3/*IL2* complex from the nucleus for translation. Like *IL2,* NF90 can also control the expression of *HLA-DRA* at both the transcriptional and mRNA level by stabilizing its 3' UTR. 3' UTR NF90-mediated regulation is also seen in the MHC Class II genes *HLA-DRB1* and *HLA-DQA1* (93). Apart from protein-coding genes, ILF3 is also essential in regulating a variety of host non-coding mRNAs (ncRNAs) such as the family of small-NF90 associating RNAs (snaRs) (94), LincIN (95), LINC00470 (96), HOXA-AS3 (97), TPT1-AS1 (98), and ELDR (99). ILF3 can also influence the maturation of microRNAs, another class of non-coding RNAs. miR-133a-1 (100), miR-7 (101, 102), pri-miR-590 (103), miR-548k (104), and miR-Let-7a(105) have all been found to have differentially expressed forms of their pri-, pre-, or mature miRNA upon perturbation of ILF3. ILF3 can positively regulate a different class of host RNAs known as circular RNAs (circRNA) as part of circRNA ribonuclear protein complexes in the nucleus during homeostasis, but is abrogated during viral infection where ILF3 is retargeted from the host to the pathogen (106). Interestingly, this study found that upon viral infection with a

negative-sense RNA virus (vesicular stomatitis virus), ILF3 translocates out of the nucleus to bind viral RNA to inhibit translation as an antiviral mechanism.

Within its capacity to act as an RNA-binding protein, ILF3 regulates viral RNAs to influence and regulate viral replication directly. ILF3 was first found to bind viral RNA species in adenoviruses encoding two virus-associated (VA) RNAs, VA RNAI and VA RNAII (107). Hepatitis B virus (HBV) replication was found to be positively regulated by ILF3 via binding to the encapsidation signal (epsilon) of HBV, along with other host proteins as part of a heterodimeric complex, to assist HBV polymerase in binding to this sequence (108). The related hepatitis C virus (HCV) is also positively affected by ILF3 through promoting the circularization of the viral genome through 5' and 3' UTR binding (109). Influenza A is negatively affected by ILF3 expression through two independent mechanisms. ILF3 can antagonize viral replication through association with the viral nucleoprotein (NP) and promote phosphorylation of PKR to aid in the antiviral response (110, 111). Additionally, ILF3 can act to negatively impact viral polymerase in expression new viral RNA species (112). Similar effects on viral replication are also seen in the case of ILF3 binding to dengue virus genome 3' UTR to promote replication, interacting with Ebola viral polymerase (VP35) to inhibit replication, and positively regulating replication of influenza B virus (113-115).

ILF3's role in regulating HIV-1 replication

In the context of HIV-1 infection, there have been several studies examining the role of ILF3 in regulating HIV-1 replication. NF90, in concert with ILF2, can promote HIV-1 viral replication and gene expression specifically through its dual dsRBDs (116). However, there have been several studies examining replication of HIV-1 that utilize a likely dominant-negative

variant of ILF3 termed NF90 C-terminal variant (NF90ctv). This variant contains a CT insertion within exon 15 of *ILF3* that is not caused by alternative splicing and results in a frameshift mutation causing a C-terminus that is rich in acidic residues (77, 117). As the other isoforms of ILF3 do not contain enrichment for these acidic residues, it is possible that this mutation could alter the observed phenotype of overexpression studies using NF90ctv. Thus far, there has been no evidence to support that this variant exists in the mammalian genome. Results from these studies should consider the possibility of a dominant negative effect due to this CT-insertion. Studies manipulating NF90ctv in the context of HIV-1 have found that NF90ctv inhibits HIV-1 transcription via competition for the trans activation response element (TAR) RNA with the trans-activator of transcription (TAT) during infection (118). Binding of TAT to TAR is essential for HIV-1 gene transcription. NF90ctv binding to TAR blocks available TAT from being able to bind to the TAR element. NF90ctv can also inhibit HIV-1 Rev protein activity to in inhibit viral RNA export in addition to being able to bind to the Rev-responsive element of HIV-1 (119). Similar to the TAR element, the RRE requires Rev to bind to its secondary structure so that Rev can export HIV-1 unspliced and partially spliced viral RNA from the nucleus to the cytoplasm for translation of HIV-1 viral proteins. Further work examining the comparative effects of NF90 vs. NF90ctv as well as the expression of each in vertebrate genomes should be considered to determine their relative biological relevance.

ILF3's role in regulating Type I Interferon

Critical to HIV-1 infection, type I IFN (IFN) plays both an antiviral and deleterious role in controlling HIV-1 infection that is dependent on both timing and robustness of the IFN response (120). We know much about how ILF3 can regulate viral fitness and replication

directly, but what is ILF3's role within innate immunity and the antiviral IFN response? NF90ctv was found to be a positive regulator of a variety of ISGs downstream of interferon signaling during HIV-1 infection of such as ISG15, IFI27, and MxA at the level of transcription (117). However, given the literature, it is likely that ILF3-dependent IFN and subsequent ISG responses are dependent on several key factors: ILF3 isoform, pathogen, and cell type. In studies examining mammalian expressed NF90 and NF110, there is evidence that ILF3 can either suppress, promote, or fail to impact IFN induction. Within primary human bronchial epithelial cells challenged with a ΔNS1 influenza A virus, shRNA knockdown of ILF3 resulted in potentiated IFN (121). This is in contrast to the studies done in cell lines which have resulted in no difference or decreased potentiation of IFN. In a different study examining influenza A infection *in vitro* in 293T cells, NF90 knockdown showed no difference in levels of *IFNB1* mRNA following infection compared to controls (110). Knockdown of ILF3 in Sendai virus infected A549 cells *in vitro* resulted in suppressed IFN production (115). With the use of an RNA mimetic Poly I:C, ILF3 siRNA knockdown showed no difference at the level of *IFNB1* mRNA *in vitro* in HeLa cells (122). A more recent study on ILF3 and its effect on IFN and ISGs is perhaps the most revealing in terms of the complex mechanism behind these divergent results. Analysis of ILF3 siRNA knockdown HeLa cells stimulated with Poly I:C versus controls revealed no differences in *IFNB1* transcription yet decreased expression in select ISGs such as *ISG15*, *IFIT2*, *CCL5*, and *CXCL10* at the level of mRNA (123). These differences were found to be due to association of ILF3 with active polysomes. When examining *IFNB1* between actively translating polysomes and subpolysomal pools, the group found a differential affect when targeting either NF90 or NF110. Knockdown of NF110 significantly decreased *IFNB1* in polysomal pools compared to knocking down NF90 that lead to an increase in *IFNB1* in

polysomal pools. This difference led to differential translation of certain ISGs. It is important to note that this study, as with others previously detailed here, explore ILF3's role in non-immune cell lines. Protein expression and relative ratios of NF90 and NF110 within this study appear to vary, potentially giving a clue to a stochiometric influence on regulation of IFN between NF90 and NF110 (123). Vast differences in signaling pathways and gene expression exist between primary cells and cell lines, in addition to cells of immune or non-immune origin. Further studies examining the role of ILF3 in primary human immune cells might reveal significant biological roles potentially masked in other systems.

Dissertation objectives and significance

DC maturation is a hallmark process inherent to antigen presenting cells such as myeloid dendritic cells. This process is what drives an efficient adaptive immune response leading to priming of naïve T-cells, specifically programmed to combat the diversity of pathogens encountered by the innate immune system. This can be achieved through recognition of pattern-associated molecular patterns (PAMPs) by innate immune sensors such as surface Toll-like receptors, C-type lectin receptors, or intracellular nucleic acid sensors like cGAS. Cytokines such as IFN can drive this process stemming from these signaling events through pathways that converge on transcription factors that drive IFN expression like IRF3. We know that transcription factors play essential roles in regulating innate immune responses and DC maturation, both in the capacity to promote and restrain these processes. What remains less well understood is which host transcription factors help to temper these responses, in an effort to prevent hyperinflammation or promote resolution of the innate immune response. The primary objective of this work is to define a new node in human myeloid DCs that helps restrain potent

antiviral innate immune responses and DC maturation to better understand how human innate immunity is regulated at the level of transcription.

The focus of this work surrounds the discovery of negative transcriptional regulators of innate immune responses and DC maturation. Previous work utilizing ATAC-seq and microarray data of HIV-1-GFP-infected myeloid DCs revealed induction of IFN, ISGs, and subsequent DC maturation-related gene expression. We took this data to ask whether we could identify additional regulators of these pathways by examining timepoints where decreased expression of potential candidates coincide with changes in promoter accessibility and gene expression of these processes. This led to the identification of Interleukin Enhancer Binding Factor 3 as a candidate negative transcriptional regulator of myeloid innate immunity. The phenotypic observations and dissection of key domains required for ILF3's mechanism of restraining these responses will be discussed in Chapter 3.

Chapter 4 will discuss the broader implications of ILF3's role elaborated by the work in Chapter 3. ILF3 gene expression varies across a variety of cell types and tissues. Beyond HIV-1, how is innate immune sensing impacted by other viral pathogens that APCs like myeloid dendritic cells encounter? Is this universal to DNA and RNA species? Beyond pathogens, could ILF3 regulate autoimmune and hyperinflammatory diseases that are dependent on type I IFNs and inflammatory cytokines? Related to each of these contexts, this chapter will also explore therapeutic interventions by current and unexplored small molecules that might more specifically target and fine-tune innate immune signaling and cytokine secretion.

CHAPTER 2: MATERIALS AND METHODS

Materials and Methods

Primary Human Cells and Cell Lines

We generated immature MDDCs as previously described (34). Briefly, leukocytes from anonymized healthy human donors were acquired under the Bloodworks Donor Products for Research and Test Development/Standardization – External Investigators Protocol (Western Institutional Review Board - WIRB protocol 20150119) and informed consent was obtained from all subjects. CD14+ monocytes from PBMC buffy coats were isolated with anti-human CD14 magnetic beads (Miltenyi Cat:130-050-201) and cultured in RPMI (Thermo Fisher) containing 10% heat-inactivated fetal bovine serum (FBS, Peak Serum, Inc), 50 U/mL penicillin, 50 μg/mL streptomycin (pen/strep, Thermo Fisher), 10 mM HEPES (Sigma), 2-mercaptoethanol (Thermo Fisher), and 2 mM L-glutamine (Thermo Fisher), in the presence of recombinant human GM-CSF at 10 ng/mL and IL-4 at 50 ng/mL (Peprotech). The day following isolation and transduction with lentiviral vectors, fresh media and cytokines were added to cells (50% by volume.) On the fourth day post-isolation, cells were resuspended in fresh media and cytokines for subsequent experiments. 293FT cells (Life Technologies Cat# R70007, RRID:CVCL_6911) were cultured in Dulbecco's modified Eagle's medium (DMEM, Thermo Fisher) supplemented with 10% FBS, pen/strep, 10 mM HEPES, and with 0.1 mM MEM non-essential amino acids (Thermo Fisher), 6 mM glutamine, and 1 mM sodium pyruvate (Thermo Fisher). HL116 cells were cultured similar to 293FT cells, except with the addition of HAT supplement (Thermo Fisher Cat: 21060-017). THP-1 cells (ATCC Cat# TIB-202, RRID:CVCL_0006) were cultured in RPMI with 10% heat-inactivated fetal bovine serum, pen/strep, 10 mM HEPES, 2-mercaptoethanol, and 2 mM glutamine and kept at a density between 250,000 and 1,000,000

cells per mL. All cells were maintained at 37°C and 5% CO2 and used at early passage numbers (< 20 for 293FT, or < 8 weeks for HL116 and THP-1 cells. Mycoplasma contaminant checks were performed every 6 months. THP-1 experiments were performed on biological replicates from independent cultures and MDDC experiments were performed using individual donors as biological replicates.

Plasmids and Mutagenesis

HIV-1-GFP is *env- vpu- vpr- vif- nef-*, with the GFP open reading frame in place of *nef* (33). Vpx-containing virus like particles were generated from the plasmid pSIV3+ (124). Overexpression vectors for wild-type isoforms of ILF3, dual dsRNA-binding domain deletion mutants, Domain associated with zinc finger deletion mutants, and nuclear localization signal deletion mutants were generated in-house using overlap extension mutagenesis to modify NF90 cDNA (GE Dharmacon) or directly synthesized (Thermo Fischer GeneArt) (NF90b mutants and NF110b forms) or GE Dharmacon (NF90b cDNA) in a pLKO.1 vector backbone. lentiCRISPR sgRNAs (single guide RNAs) were designed using the E-CRISP algorithm (http://www.e-crisp.org/E-CRISP/), selecting for the highest scoring guides in target specificity and efficiency for *ILF3.* Oligos spanning the sgRNA sequence were annealed and ligated into the lentiCRISPRv2 backbone (125) (Addgene plasmid #52961, Gift from Feng Zhang). (ILF3 Target Sequence #1: GCTGGAGGCAGTCCAGAACA. ILF3 Target Sequence #2: GCCTCCAGCTCCTCTTGTGT). The parental control vector (LCV2) was created from lentiCRISPRv2 digested with BsmBI and re-ligated, removing the 2 kb stuffer. All lentiviral constructs were transformed into Stbl3 bacteria (ThermoFisher Cat: C737303) for propagation of plasmid DNA. All plasmids were prepared using a Nucleobond Xtra Maxi Kit (Takara

Cat:740414.100). Coding sequences of overexpression constructs, shRNA hairpins, and sgRNAs were confirmed by automated sequencing (Genewiz).

Virus and Virus-Like Particle Production

As described (34), lentivirus stocks were produced by PEI-mediated transfection into 293FT cells. For lentiviral vectors, plasmid amounts were 3.4 μg CMV-VSV-G (Addgene plasmid #8454), 9 μg psPax2 (Addgene plasmid #12260), and 10.1 μg transgene (LKO.1 control (Addgene Cat:10878), LKO ILF3 overexpression vector, shRNA control (Sigma Cat:SHC002), ILF3 shRNA, or lentiCRISPRv2 constructs). For HIV-1-GFP, plasmid amounts were 3.4 μg CMV-VSV-G and 19.1 μg HIV-1-GFP cassette. Virus-like particles containing Vpx were produced using 3.4 μg CMV-VSV-G and 19.1 μg pSIV3+. Media was washed and refreshed the morning after transfection, and virus supernatants were harvested after 32 h later. Sufficient p24 levels were verified using Lenti-Go Stix Plus (Takara Cat:631280). Supernatants were passed through 0.45 μm syringe filters (Corning), transferred to thin-wall Conical tubes (Beckman), and concentrated by ultracentrifugation at 24k rpm for 2 hr at 4 °C in a SW28 swing-bucket rotor (Beckman). Pellets were resuspended in RPMI-DC media without cytokines and insoluble material was clarified by centrifuging at 700 rcf for 4 min. 50X concentrated viral stocks were frozen at -80 °C and titered on 293FT and THP-1 cells.

Perturbation of DCs and Cell Lines

MDDCs were modified by lentiviral shRNA and overexpression constructs similar to previously described protocols (Johnson et al., 2018). Isolated CD14+ monocytes were resuspended in media with cytokines and polybrene (Sigma, 1 μg/mL) and aliquotted to 96-well U-Bottom

plates with 200,000 cells in 150 μL per well. Supernatant containing virus-like particles packaging Vpx was added to overcome the block to reverse transcription ~30 min prior to adding lentiviral vectors. 10 μL of concentrated lentiviral stocks were used to transduce 200,000 CD14+ cells. shRNA clones for targeting ILF3 were used independently (Sigma: ILF3 sh1: TRCN0000329787, ILF3 sh2: TRCN0000329786). THP-1 monocytic cells were transduced with shRNA or lentiCRISPR constructs in 6-well cluster plates using 1,000,000 cells per well in 2 mL media with polybrene (2 μg/mL) and concentrated viral stocks (150 μL of shRNA or 250 μL of lentiCRISPR per well). Cells were placed under selection with puromycin (1 μg/mL, Invivogen) two days after transduction for 1 week and puromycin-resistant populations were allowed to expand. lentiCRISPR-transduced cells were used at day 8 for infection. shRNA-transduced cells were used for experiments beginning 2 weeks after selection. Independent transductions were performed for biological replicates, unless otherwise indicated. Perturbation of ILF3 expression was confirmed by qPCR or immunoblot.

Infections and Stimulations

MDDCs were infected with HIV-1-GFP for 48 hours beginning on day 4 after differentiation. DCs were spun down on day 4 and resuspended in fresh medium with GM-CSF, IL-4, and polybrene (1 μg/mL). For most assays, DCs were plated in round bottom 96-well plates in 75 μL. Infections and stimulations were performed by diluting virus in MDDC media (without cytokines or polybrene) to a final volume normalized to control (150 μL per well). Antiretroviral drugs (NIH AIDS Reagent Program or Selleck Chemicals Cat:S2005) were added prior to virus infection at the following concentrations: efavirenz (EFV) (20 nM); raltegravir (RAL) (25 μM). Innate and inflammatory stimuli – Immunostimulatory DNA or control DNA complexed with

LyoVec (InvivoGen Cat: tlrl-isdc/tlrl-isdcc), 2'3'-cGAMP (InvivoGen Cat: tlrl-cga23-s), and R848 (InvivoGen Cat: tlrl-r848) – were used as indicated in Fig. 3. THP-1 monocytic cells were infected in the absence of Vpx at a density of 70,000 cell per 150 µL in complete RPMI medium with polybrene (2 µg/mL). B18R (R&D Systems Cat: 8185-BR-025) for IFN neutralization was used for flow cytometry analysis of CD86 by adding B18R at a concentration of 100 ng/mL after the media refresh on day 4 and once again 24 h later. Treatment of MDDCs of day 4 with YM155 (Cayman Chemical Cat: 11490) was prepared in diH2O and incubated for 48 hours prior to flow cytometry.

Flow Cytometry

Infected or stimulated MDDCs were washed with phosphate buffered saline (PBS, Corning), cell pellets were incubated for 15 minutes at 4 °C with 2µL of Fc Block (BD Biosciences Cat: 564219), and then exposed to LIVE/DEAD violet (ThermoFisher Cat: L34955) in PBS for 15 min at 4 °C in the dark. Cells were either simultaneously stained for surface markers (CD40 Thermo Fisher Cat: CD4004, CD80 eBioscience Cat:15-0809-42, CD86 eBioscience Cat: 15-0869-42, HLA-DR Biolegend Cat: 307607/Biolegend Cat:307619, CD1c eBioscience Cat:331505, CD83 eBioscience Cat: 305307) or were then washed with PBS and fixed with 0.4% paraformaldehyde (Electron Microscopy Sciences) diluted in PBS. Cells were analyzed on an LSR II flow cytometer (BD Biosciences). For intracellular staining using anti-human ISG15 (R&D Systems Cat: IC8044P) in MDDCs and THP-1 monocytic cells, cells were first exposed to LIVE/DEAD violet and surface markers as described above, washed in PBS, then fixed and permeabilized using a cytofix/cytoperm kit (BD Biosciences Cat: 554714), blocked with 2µL Fc block for 10 min at room temperature, and stained according to the manufacturer's instructions.

Cells were washed and resuspended in PBS with 1% BSA and data were acquired on an LSR II flow cytometer (BD Biosciences) and analyzed using FlowJo software (FlowJo LLC). ArC Amine Reactive Compensation Bead Kit (Thermo Fisher Cat:A10346), UltraComp eBeads Plus Compensation Beads (Thermo Fisher Cat: 01-3333-41), and GFP BrightComp eBeads (Thermo Fisher Cat: A10514) were used for compensation.

Nucleic Acid Isolation and Quantitative PCR

~200,000 DCs were lysed in TRIzol reagent (Thermo Fisher Cat: 15596026) and RNA was isolated according to the manufacturer's instructions with the following modifications: two sequential chloroform extractions were performed and Glycoblue (Thermo Fisher Cat: AM9516) was added as a carrier prior to precipitation. cDNA was converted using Superscript IV VILO with ezDNase treatment (ThermoFisher Cat: 11766050). Quantitative PCR reactions were carried out using TaqMan primer probes (Thermo Fisher) and TaqMan Fast Universal PCR Master Mix (ThermoFisher) in a CFX96 thermocycler (BioRad) or QuantStudio3 (Thermo Fisher) in a volume of 10 μL according to the following cycling conditions: 50 °C for 2 min, 95 °C for 2 min, then 50 cycles each of 95 °C for 3 sec, to 60 °C for 30 sec, followed by 95 °C for 5 sec. For total *ILF3* Sybr green qPCR, PowerUp Sybr Green Master Mix (Thermo Fisher Cat: A25742) was used in a total volume of 10uL with the following cycling protocol: 50 °C for 2 min, , 95 °C for 2 min, 95 °C for 15 sec, 58 °C for 15 sec, and 72°C for 15 sec, repeated for 40 cycles. Data were plotted as $2^{-(\Delta Ct)}$•1000 relative to *GAPDH*. For experiments with larger number of samples, Direct-Zol 96-well RNA isolation kits (Zymo Cat: R2056) were used as per manufacturer's instructions, utilizing the optional DNase step and forgoing the ezDNase step with the SSIV VILO master mix.

Microarrays

Monocyte-derived dendritic cells from three unique donors were transduced with either a control shRNA, ILF3 sh1, or ILF3 sh2 in the presence of Vpx. RNA was extracted using TRIzol on day 5. Purified RNA was labeled and hybridized to SurePrint G3 8x60K Microarrays (Agilent) and data were acquired at the Institutes for Systems Biology. Probe sequences were mapped against the Ensembl transcript database (ensembl.org, GRCh37.74) and sequences that mapped to more than one gene or had more than five mismatches from the database sequence were removed for a total of 37,623 unique probes. Probe-specific logarithmically transformed expression was quantile-normalized. Duplicate probe sequences were averaged. Gene-specific expression was computed by using the probe that showed the highest average expression across all samples in cases in which multiple probes mapped to a single gene for a total of 26,319 gene-specific probes. Statistical significance of the coefficients were computed with the LIMMA R package (https://bioconductor.org/packages/release/bioc/html/limma.html). p values were adjusted for multiple hypothesis testing with the Benjamini-Hochberg method for controlling the false discovery rate. These data have been deposited in NCBI's Gene Expression Omnibus (Nazitto et al., 2020) and are accessible through GEO Series accession number GSE159458 (https://www.ncbi.nlm.nih.gov/geo/query/acc.cgi?acc=GSE159458). Data from our previous publications (34, 126) that were re-analyzed as indicated in Fig. S1 can be accessed through accession number GSE100374 (microarray) and GSE125918 (ATAC-seq).

Gene Set Enrichment Analysis (GSEA)

For ILF3 shRNA knockdown microarray, 37,913 gene features for each construct were ranked by the t-test metric of GSEA using the mean values computed for ILF3 sh1 and sh2 compared to the control shRNA. The analysis was performed using the weighted enrichment statistic, ranking genes using the t-test metric, against the C2 Curated gene sets containing *x* number of genes (with $15 > x > 200$) within the Molecular Signature Database. The Normalized Enrichment Score (NES) was calculated using 1000 gene set permutations. For NF110 overexpression RNA-Seq, a pre-ranked list of fold changes of NF110 wt compared to LKO control was ranked by t-test metric containing 13,125 gene features. The analysis was performed using the standard weighted enrichment statistic against the C1 Hallmark gene sets with $15>x>200$ gene membership within the Molecular Signature Database. The Normalized Enrichment Score (NES) was calculated using 1000 permutations.

RNA-Seq and analysis

RNA isolated from TRIzol lysates as described above and converted to cDNA libraries using the Illumina TruSeq stranded mRNA Kit per the manufacturer's instructions. Libraries were amplified and then sequenced on an Illumina NovaSeq (2 x 150, paired-end). Reads with more that 67% identical bases were discarded prior to alignment. The remaining read pairs were aligned to the human genome (hg19, GRCh37 Genome Reference Consortium Human Reference 37 (GCA_000001405.1)) using the gsnap aligner (v. 2016-08-24) allowing for novel splicing. Concordantly mapping read pairs (average 17 million per sample) that aligned uniquely were assigned to exons using the subRead program and gene definitions from GRCh38.87. Genes with low expression were filtered using the filterByExpr function in the edgeR package from

Bioconductor.org resulting in a total of 13,125 genes in the final dataset. Differential expression was calculated using the edgeR package. The data discussed in this publication have been deposited in NCBI's Gene Expression Omnibus and are accessible through GEO Series accession number GSE159143 (https://www.ncbi.nlm.nih.gov/geo/query/acc.cgi?acc=GSE159143). (Nazitto et al., 2020)

Immunoblotting

Samples were prepared as previously described (34). Blots were incubated with primary ILF3 antibody ILF3 (Abcam Cat:92355) (1:3000). After incubating blots overnight at 4 °C, or for at least 1 hr at room temp, they were washed with TBS/tween, then incubated with the corresponding HRP-conjugated anti-rabbit secondary antibody (1:10,000) for 1 hr at room temperature. To confirm equal protein loading, blots were incubated with an anti-actin-HRP antibody (directly conjugated) (Abcam Cat:AB20272) (1:100,000) for 30 min at room temperature. Alternatively, blots were incubated with primary GAPDH antibody (Cell Signaling Cat:5174T) (1:1000) to confirm equal protein loading in samples taken over the course of differentiation from monocytes to MDDCs, as actin expression is not constant during differentiation. After incubation with primary antibodies, blots were washed with TBS/tween, then incubated with the corresponding HRP-conjugated anti-rabbit secondary antibody (1:10,000) for 1 hr at room temperature. Blots were then washed in TBS/tween, reacted with Wesfemto ECL kit (Thermo Fisher Cat: 34095), and developed using a FluorChem E Imager (Protein Simple).

Immunofluorescence

On day 5 after transduction, 75 µl of MDDCs were plated into a chamber of an 8-chamber mounting slide (MatTek Life Sciences). Cells were collected onto the coverglass by centrifugation for 7 min at 1500 RPM at room temperature. The supernatant was aspirated and cells were fixed with 2% paraformaldehyde for 30 min at room temperature. After washing the cells with PBS the cells were then permeabilized and blocked with a solution of PBS + 0.1% Triton X-100 + 5% FBS (Perm/Block, 0.2 µm filtered) for 1 h at room temperature. The Perm/Block solution was then aspirated and anti-ILF3 antibody was added at a concentration of 1:1000 in Perm/Block solution. Cells were washed 3× for 5 min each with Perm/Block and then incubated with Alexa Fluor 594 goat anti rabbit secondary antibody (Thermo Fisher Cat:A-11012) at 1:750 in Perm/Block for 1 h at room temperature. Cells were washed twice for 5 min each at room temperature in the dark with Perm/Block. 1.25 µl of phalloidin (Thermo Fisher Cat: R415) was added to 200 µl of PBS per chamber and incubated for 20 min at room temperature in the dark, except for where indicated. Cells were washed twice with PBS and then mounted with ProLong anti-fade diamond with DAPI (Thermo Fisher Cat: P36962) and left to cure for 24 h before imaging on a DeltaVision Elite (Cytiva) widefield microscope. Images were collected with a 100× 1.4 NA objective (Olympus) on a CoolSnapHQ2 CCD camera (Photometrics). The sides of each pixel are 6.45 µm. Images were deconvolved using algorithms provided by Huygens Software (Scientific Volume Imaging BV, The Netherlands). For deconvolution, three-dimensional data sets were processed to remove noise and reassign blur by an iterative Classic Maximum Likelihood Estimation widefield algorithm using an experimentally derived point spread function. Image processing was performed using Imaris (Bitplane). Cells were segmented

using the “Cells” command, which identifies cells and their nuclei. For each cell, the ratio between nuclear and cytoplasmic ILF3 fluorescence signal intensity was determined.

ELISAs

IFNβ in DC supernatants was determined by ELISA (R&D Systems Cat: DIFNB0) according to the manufacturer’s instructions. Supernatants (50 μL) from MDDCs infected with HIV-1-GFP for 32 h were mixed with 50μL assay diluent reagent per well and measured in duplicate compared to a standard curve of IFNβ ranging from 7.81pg/mL to 500pg/mL. IFNβ was also measured in supernatants of ILF3 knockdown MDDC supernatants using high-sensitivity ELISA IFNβ (PBL Cat: 41435) on mock, 2’3’-cGAMP, and B18R-treated MDDCs (R&D Systems Cat: 8185-BR-025) (Added at 100ng/mL 1 hour before 2’3’-cGAMP treatment) 7 hours post treatment, measured in duplicate compared to a standard curve of IFNβ ranging from 150 pg/mL to 2.34 pg/mL.CXCL10 and IL-6 were measured in the supernatants of mock or ILF3 knockdown MDDC supernatants using ELISAs for CXCL10 (Abcam Cat: 173194) and IL-6 (Abcam Cat:178013) on mock, 2’3’-cGAMP, and B18R-treated MDDCs for 7 hours, measured in duplicate compared to a standard curve ranging from 800 pg/mL to 12.5 pg/mL for CXCL10 and 500 pg/mL to 7.8 pg/mL for IL-6. CCL23 was measured in the supernatants of either ILF3 knockdown or NF90/NF110 overexpressing MDDCs compared to relevant controls 48 hours post media refresh on Day 4 using a CCL23 ELISA assay (Abcam Cat: 216169), measured in duplicate compared to a standard curve of CCL23 ranging from 450 pg/mL to 7.03 pg/mL. All duplicates were averaged per donor, represented as the mean.

Bioassays for Type I IFN

IFN activity in HL116 cells was measured as previously described (34). Briefly, 20,000 HL116 cells were incubated with supernatants from MDDC cultures for 7 hours before passively lysing the cells and scoring firefly luciferase activity in the presence of luciferin.

Quantification and Statistical Analysis

Statistical tests were performed as indicated in the figure legends or otherwise using Prism 8.0.1 (GraphPad) to calculate a mixed model two-tailed t-test using paired samples and setting an alpha value of 0.05. In this study, n is defined in the figure legends and represents the number of biological replicates performed of unique donors for MDDC experiments or the number of independent, non-technical replicates for THP-1 experiments, unless otherwise indicated.

Illustrations

All graphical illustrations were done using BioRender.com

CHAPTER 3: ILF3 is a negative transcriptional regulator of innate immune responses and myeloid dendritic cell maturation

Introduction

Engagement of the innate immune system in response to an invading pathogen is a central element of host defense. Viral, bacterial, and fungal pathogens can be detected by a wide variety of innate immune cells. Myeloid DCs play key roles in this response by initiating local innate responses and programing subsequent adaptive immune responses (2). Immature DCs are poised to respond to pathogen components and inflammatory cytokines, which trigger morphological and functional changes that facilitate antigen presentation, cytokine/chemokine secretion, and expression of costimulatory molecules. These functional changes are characteristic of mature DCs, which have the capacity to prime naive T cells and program adaptive immunity (127). Many aspects of DC biology are governed by transcription factors that regulate gene expression signatures and influence cell behavior, including DC maturation. While efficient DC maturation may be beneficial for controlling an active infection, sustained or excessive innate responses following maturation can have deleterious pathologic effects (128). Thus, it is important to decipher the complex molecular mechanisms that regulate innate immune responses and DC maturation and understand their function in health and disease.

DCs express an array of pattern recognition receptors (PRRs) that serve as "sensors" positioned to detect extracellular pathogens (e.g. TLR3, TLR4) and intracellular pathogens (e.g. cGAS, IFI16, and RIG-I). Viral nucleic acids within infected cells are detected by DNA and RNA sensors such as cGAS and RIG-I, respectively. These sensors activate signaling cascades that lead to phosphorylation of transcription factors such as IRF3 and NF-κB that drive induction of inflammatory cytokines, including a potent class of antiviral signaling molecules known as type I interferons (IFNs). Autocrine and paracrine signaling of IFNs through the IFN receptor

and the JAK-STAT pathway induce a battery of IFN-stimulated genes (ISGs) that can act to directly restrict viral replication or modify cellular processes to establish an antiviral state. During chronic infection with viruses such as HIV-1, sustained production of type I IFNs and expression of ISGs can exacerbate non-specific inflammation, increase target cell susceptibility to the virus, and contribute to pathogenesis (51, 129). Given the pivotal role of DCs in linking innate and adaptive immunity, a deeper understanding of the mechanisms that restrain IFN responses or negatively regulate DC maturation during infection could lead to treatments that engage protective antiviral immune responses during viral transmission and may guide the development of therapies for late-stage disease.

Numerous transcription factors essential for DC differentiation and maturation have been identified, yet the factors that restrain and fine-tune this response remain poorly understood (130). In this report, we have identified ILF3 as one such factor. ILF3 was originally discovered as a positive regulator of *IL2* transcription as part of the NFAT-AP1-NF-κB enhanceosome and a positive regulator of *IL2* mRNA stabilization via 3'UTR binding (80, 86, 131-133). Subsequent studies have uncovered diverse functions for ILF3 that include a role in host RNA decay as a component of a messenger ribonucleoprotein (mRNP) complex, and a role as a transcriptional modulator for interleukins in addition to IL-2, such as IL-13 (87), and the oncogene uPA (134). Additionally, ILF3 can interact directly with viral nucleic acids to modulate replication of dengue virus (113), hepatitis C virus (109), bovine viral diarrhea virus (135), human rhinovirus, and Zaire ebolavirus (114). Despite these known roles in regulating transcription, mRNA stabilization, interaction with viral nucleic acids, and regulation of pathogen fitness, ILF3 has not previously been described to regulate the function of myeloid immune cells.

Here, we demonstrate that both major isoforms of *ILF3*, NF90 and NF110, restrain myeloid DC maturation and type I IFN responses. Analysis of deletion mutants reveals that the nuclear localization sequences of both NF90 and NF110 are required for this function. Interestingly, mutation of the domain associated with zinc finger (DZF) domain ablated the ability of NF110 to suppress DC maturation, but not NF90. Furthermore, through RNA-seq analysis of DCs expressing mutant or wild type ILF3, we demonstrate that ILF3-dependent genes are strongly enriched for genes associated with cholesterol homeostasis. These data establish *ILF3* as a regulator of DC responses to innate immune stimuli and therefore a potential target for host-directed therapies to fine-tune inflammation and innate immunity.

Results:

Temporal promoter and transcriptome analysis predict ILF3 as a regulator of DC maturation in response to HIV-1-GFP infection

To probe the DC response to innate immune stimuli, we employed HIV-1-GFP, a VSV-pseudotyped, single-cycle, HIV-derived reporter virus that lacks all accessory proteins and expresses GFP in place of Nef. Normally, HIV-1 infection is severely limited in DCs due to expression of the restriction factor SAMHD1, which prevents reverse transcription of viral RNA (70, 136). Providing the SIV accessory protein Vpx, *in trans*, leads to SAMHD1 degradation, allows for reverse transcription to proceed, and enables efficient, productive infection (33, 124). This system is a well-established model for examining DC maturation and type I IFN responses (33, 34, 137). Infection of MDDCs with HIV-1-GFP robustly induces type I IFN through the DNA sensing pathway cGAS-STING, a key initiator of DC maturation via the transcription factor IRF3 and antiviral immunity through the induction of ISGs.

To identify molecules that restrain maturation and IFN responses in myeloid DCs, we reanalyzed existing datasets that were generated from an Assay for Transposase-Accessible Chromatin using sequencing (ATAC-Seq), together with microarray datasets from MDDCs infected with HIV-1-GFP-infected MDDCs (34, 126). We compared changes in genome-wide chromatin accessibility and the transcriptome over time to search for genes that had increased chromatin accessibility near their transcription start sites and decreased gene expression, profiles that could suggest negative transcriptional regulation (Fig. S1A). As expected, chromatin accessibility was increased at the promoters of numerous genes with established roles in DC maturation (*CD40, CIITA, CD80, CD86*) and IFN responses (*IFNB1, ISG15, OASL, IFIT1*) at 24 hours post infection (Fig. S1B) (126) and these increases were associated with altered expression of these genes at later timepoints (Fig S1C). We defined a set of 85 genes that had both large increases in chromatin accessibility (fold-change (FC) > 10, $p < 0.01$) and significantly reduced expression (FC < 1, FDR < 0.05) at 24 hours following infection with HIV-1-GFP. Of those 85 genes, only five were transcription factors, as defined by the Transcriptional Regulatory Relationships Unraveled by Sentence-based Text mining (TRRUST) list of human transcription factors: CDK2AP2, ERCC2, HSF1, ILF3, and KLF2. We were particularly intrigued by the transcription factor ILF3, as it has been reported to negatively regulate IFN production during influenza infection in primary human bronchial epithelial cells (121). Additionally, under different experimental conditions in HeLa and A549 cells, ILF3 has been shown to promote the IFN response upon dsRNA stimulation (115, 123). The gene encoding ILF3 produces two major isoforms, NF90 and NF110 (collectively named ILF3 for the purposes of this study), and both of which are known to act as transcriptional regulators (86-88, 134, 138, 139). We found that human CD14+ monocytes isolated from whole blood express low levels of ILF3 isoforms, but

these are dramatically upregulated over the course of differentiation into immature MDDC in the presence of IL-4 and GM-CSF (Fig. S1D). Since our data in MDDCs suggested that accessibility of the ILF3 promoter is altered during innate immune stimulation, and the transition from immature to mature MDDC coincides with a decrease in ILF3 expression (Fig. S1E,F), we pursued ILF3 as a candidate regulator of innate immune function in human DCs to better clarify its role.

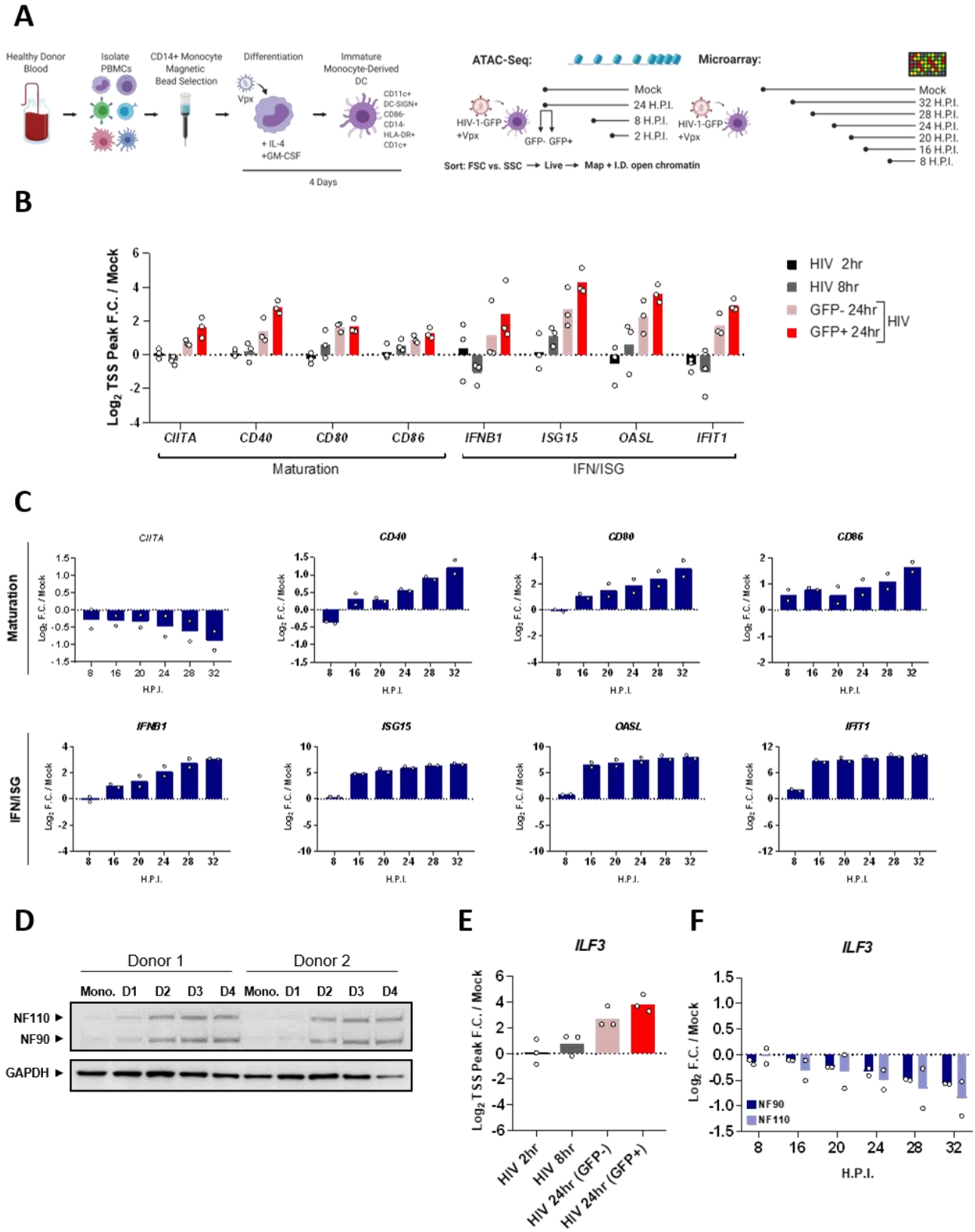
A
Healthy Donor Blood
Isolate PBMCs
CD14+ Monocyte Magnetic Bead Selection
Differentiation
Vpx
+ IL-4
+GM-CSF
4 Days
Immature Monocyte-Derived DC
CD11c+
DC-SIGN+
CD86-
CD14-
HLA-DR+
CD1c+
ATAC-Seq:
HIV-1-GFP +Vpx
Mock
24 H.P.I.
8 H.P.I.
2 H.P.I.
GFP- GFP+
Sort: FSC vs. SSC → Live → Map + I.D. open chromatin
Microarray:
Mock
32 H.P.I.
28 H.P.I.
24 H.P.I.
20 H.P.I.
16 H.P.I.
8 H.P.I.
B
Log2 TSS Peak F.C. / Mock
HIV 2hr
HIV 8hr
GFP- 24hr
GFP+ 24hr
HIV
CIITA
CD40
CD80
CD86
IFNB1
ISG15
OASL
IFIT1
Maturation
IFN/ISG
C
Maturation
IFN/ISG
Log2 F.C. / Mock
H.P.I.
D
Donor 1
Donor 2
Mono. D1 D2 D3 D4 Mono. D1 D2 D3 D4
NF110
NF90
GAPDH
E
ILF3
Log2 TSS Peak F.C. / Mock
HIV 2hr
HIV 8hr
HIV 24hr (GFP-)
HIV 24hr (GFP+)
F
ILF3
Log2 F.C. / Mock
NF90
NF110
H.P.I.

Figure S1. **Changes in chromatin accessibility and gene expression over time for select genes in MDDCs during infection with HIV-1-GFP.** (**A**) Schematic illustrating MDDC derivation and subsequent HIV-1 infection at different timepoints for ATAC-seq and transcriptome analysis as described in (34). (**B**) Log_2 fold change compared to mock infection of the normalized signal at the transcription start sites (TSS) of the indicated genes, averaged over 3 independent donors, at 2, 8, or 24 (GFP+/GFP-) hours following of HIV-1-GFP infection of MDDCs (See Materials and Methods). (**C**) Expression changes relative to mock infection for genes at the indicated time points following HIV-1-GFP infection of MDDCs, averaged over two donors, for the genes shown in (B). **(D)** Western blot from 2 donors of CD14+ monocytes (Mono. Day 0) differentiated with IL-4 and GM-CSF through Day 4 with samples taken every 24 hours. Stained for ILF3 and GAPDH as a loading control. (**E**) Log_2 fold change of *ILF3*'s TSS peak as described in (B). (**F**) Log_2 of *ILF3* gene expression, separated by isoform (NF90 and NF110) as described in (C).

ILF3 restrains monocyte-derived dendritic cell (MDDC) maturation

To determine the set of genes regulated by ILF3 in unstimulated myeloid cells, we transduced MDDCs with two independent shRNAs targeting all isoforms of *ILF3* and analyzed their transcriptomes by microarray (Fig. 1A). Knockdown of ILF3 in resting MDDCs (Fig. 1B) altered the expression of 106 genes (FDR < 0.05; |FC > 1.5|). Gene Set Enrichment Analysis (GSEA) revealed that this set of genes was enriched for members of curated gene sets associated with DC maturation in response to inflammatory stimuli. Up-regulated genes were significantly enriched in three of the four "Lindstedt Dendritic Cell Maturation" gene sets (A-C) (140) (Fig. 1C,S2A). Genes down-regulated during DC maturation showed enrichment in the remaining set (set D), demonstrating the concordance of the effects. (Fig. 1D). The set of 106 genes whose expression was affected by ILF3 knockdown also contained additional genes that are not in the Lindstedt gene sets but have established associations with innate immune activation and myeloid DC maturation (*CHI3L1, PPARG, TLR3, WFDC21P (Lnc-DC), CCR2, ST6GAL1, VENTX*, and *CCL23*) (Fig. 1D) (141-148). Together, these transcriptomic analyses suggested that ILF3 functions as a negative regulator of MDDC maturation and innate immune responses. To

determine whether phenotypic changes to DC maturation accompanied these transcriptional changes, we measured surface expression of the costimulatory factors CD86, CD40, and the MHC II cell surface receptor HLA-DR by flow cytometry following shRNA-mediated knockdown of ILF3. In agreement with the transcriptomic data, knockdown of ILF3 led to significantly elevated surface expression of CD86, HLA-DR, and CD40 (Figs. 1E, S2B), while having a minimal effect on cell viability (Fig. S2C). Upregulation of CD86 correlated with expression HLA-DR in a subset of cells and was associated with reduced expression of CD1c, which are characteristic expression patterns of mature, heterogeneous MDDC cultures (Fig. 1F) (8, 149). In agreement with these findings, we also observed upregulation of CD83 (an additional marker of MDDC maturation) following ILF3 knockdown, although the sh2 condition did not reach statistical significance (Fig. S2D). Nearly all cells in these cultures expressed high levels of CD1c, suggesting that ILF3 knockdown does not alter differentiation of monocytes into MDDCs but rather affects MDDC maturation (Fig. S2E,F).

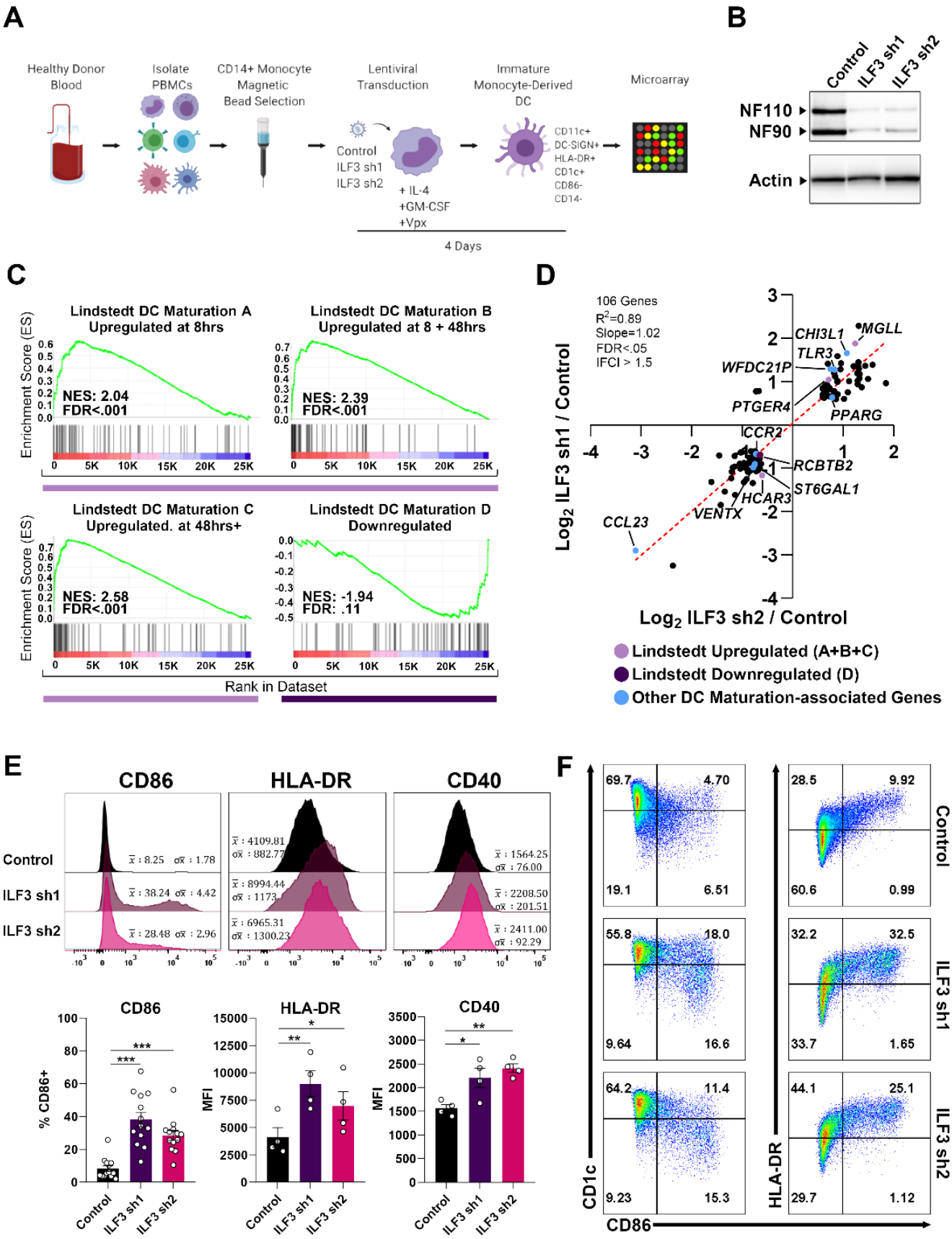
A
Healthy Donor Blood
Isolate PBMCs
CD14+ Monocyte Magnetic Bead Selection
Lentiviral Transduction
Control
ILF3 sh1
ILF3 sh2
+ IL-4
+GM-CSF
+Vpx
Immature Monocyte-Derived DC
CD11c+
DC-SIGN+
HLA-DR+
CD1c+
CD86-
CD14-
Microarray
4 Days
B
Control
ILF3 sh1
ILF3 sh2
NF110
NF90
Actin
C
Lindstedt DC Maturation A
Upregulated at 8hrs
NES: 2.04
FDR<.001
Lindstedt DC Maturation B
Upregulated at 8 + 48hrs
NES: 2.39
FDR<.001
Lindstedt DC Maturation C
Upregulated. at 48hrs+
NES: 2.58
FDR<.001
Lindstedt DC Maturation D
Downregulated
NES: -1.94
FDR: .11
Enrichment Score (ES)
Rank in Dataset
D
106 Genes
R2=0.89
Slope=1.02
FDR<.05
IFCI > 1.5
Log2 ILF3 sh1 / Control
Log2 ILF3 sh2 / Control
CHI3L1
MGLL
TLR3
WFDC21P
PTGER4
PPARG
CCR2
RCBTB2
ST6GAL1
HCAR3
VENTX
CCL23
Lindstedt Upregulated (A+B+C)
Lindstedt Downregulated (D)
Other DC Maturation-associated Genes
E
CD86
HLA-DR
CD40
Control
ILF3 sh1
ILF3 sh2
% CD86+
MFI
F
CD1c
CD86
HLA-DR
Control
ILF3 sh1
ILF3 sh2

Figure 1. ILF3 restrains monocyte-derived dendritic cell (MDDC) maturation. (**A**) Schematic illustration for transcriptomic analyses of MDDCs transduced with shRNAs targeting ILF3. Cells from three unique donors were transduced with a control shRNA or one of two shRNAs targeting ILF3. After 4 days, mRNA was isolated and analyzed by microarray. (**B**) Representative Western blot of MDDC whole cell lysates prepared as in (A), 4 days after transduction with the indicated shRNAs. (**C**) GSEA plots for the Lindstedt DC maturation gene sets, in each case comparing the mean expression values from ILF3 sh1 and sh2 conditions to the control sh condition. Gene sets A-C (light purple) contain genes up-regulated during DC maturation and gene set D (dark purple) contains genes down-regulated during DC maturation (**D**) Scatter plot of expression changes for genes significantly differentially expressed following transduction with at least one of two shRNAs targeting ILF3 plotted on a log2 scale ($|FC| > 1.5$, $FDR < 0.05$). (**E**) Flow cytometry analysis of MDDCs after ILF3 knockdown. Plots show a representative histogram of CD86, HLA-DR, and CD40 expression from one donor and corresponding graphs showing pooled data from 13 donors across 4 individual experiments for CD86, 4 donors from 1 experiment for HLA-DR, and 4 donors from 1 experiment for CD40, gated on FSC vs. SSC, singlets, and live cells. Statistics were calculated by matching each donor in a mixed-effects model using Dunnet's test for multiple comparisons. Mean and SEM for each marker in a given lentiviral treatment across all represented donors indicated on each histogram used throughout the paper. Significance of $*P < 0.05$, $**P < 0.01$, $***P < 0.001$ used for the entirety of the paper. (**F**) Flow cytometry plots of CD86 vs CD1c or HLA-DR of one representative donor, gated as in E.

As various interferons and pro-inflammatory cytokines can influence DC maturation, we examined whether ILF3's effect on maturation is solely cell intrinsic or mediated by secreted factors. We prepared immature DCs transduced with either a control shRNA or ILF3-targeting shRNAs and after four days we replaced the culture media. 24 hours later, the supernatants of the cultures with control or ILF3-targeting shRNAs were exchanged and incubated for another 24 h before measuring CD86 levels by flow cytometry (Fig S2G). Supernatants from cultures transduced with ILF3-targeting shRNAs induced baseline maturation in control DCs to levels similar to those in DCs transduced with ILF3 shRNAs (Fig. S2H). Supernatants from control cells applied to ILF3 knockdown cells had no additional effect on CD86 expression (Fig. S2H). Together, these data indicate that loss of ILF3 promotes steady-state maturation of MDDCs and that secreted factors contribute to this effect.

To further decipher the molecular mechanisms involved in ILF3-mediated regulation of myeloid cell biology, we perturbed ILF3 expression using two complementary approaches in THP-1 cells, a myeloid leukemia-derived monocytic cell line. Knockdown of ILF3 with shRNAs

led to elevated expression of the maturation marker *CD80*, the differentiation markers *CD209* and *SAMHD1,* as well as the IFN-related markers *CXCL10* and *ISG15* (Fig. S2I). Additionally, we generated ILF3 knockout THP-1 cells using CRISPR-Cas9 (Fig. S2J). We found that expression of the maturation marker *CD86* and the differentiation markers *CD209*, *SAMHD1*, and *CD14* were all significantly elevated after ILF3 was knocked out using either of two independent guide RNA sequences nine days post-transduction (Fig. S2K). These data further support the role of ILF3 as a negative regulator of IFN-related genes and myeloid cell maturation. Given that THP-1 monocytic cell lines do not fully recapitulate primary cell behavior, we chose to focus on primary MDDCs for further studies.

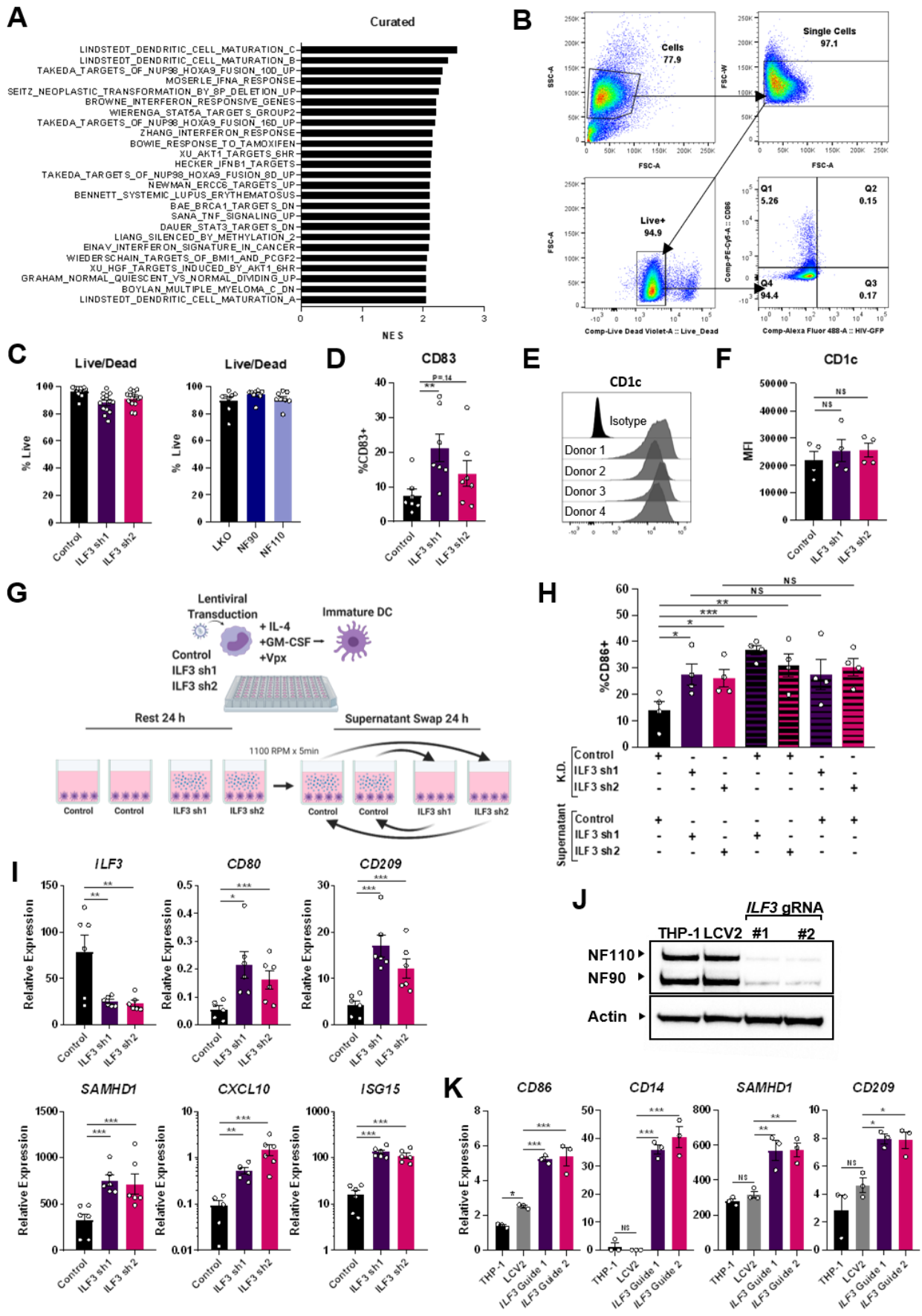
A
Curated
LINDSTEDT_DENDRITIC_CELL_MATURATION_C
LINDSTEDT_DENDRITIC_CELL_MATURATION_B
TAKEDA_TARGETS_OF_NUP98_HOXA9_FUSION_10D_UP
MOSERLE_IFNA_RESPONSE
SEITZ_NEOPLASTIC_TRANSFORMATION_BY_8P_DELETION_UP
BROWNE_INTERFERON_RESPONSIVE_GENES
WIERENGA_STAT5A_TARGETS_GROUP2
TAKEDA_TARGETS_OF_NUP98_HOXA9_FUSION_16D_UP
ZHANG_INTERFERON_RESPONSE
BOWIE_RESPONSE_TO_TAMOXIFEN
XU_AKT1_TARGETS_6HR
HECKER_IFNB1_TARGETS
TAKEDA_TARGETS_OF_NUP98_HOXA9_FUSION_8D_UP
NEWMAN_ERCC6_TARGETS_UP
BENNETT_SYSTEMIC_LUPUS_ERYTHEMATOSUS
BAE_BRCA1_TARGETS_DN
SANA_TNF_SIGNALING_UP
DAUER_STAT3_TARGETS_DN
LIANG_SILENCED_BY_METHYLATION_2
EINAV_INTERFERON_SIGNATURE_IN_CANCER
WIEDERSCHAIN_TARGETS_OF_BMI1_AND_PCGF2
XU_HGF_TARGETS_INDUCED_BY_AKT1_6HR
GRAHAM_NORMAL_QUIESCENT_VS_NORMAL_DIVIDING_UP
BOYLAN_MULTIPLE_MYELOMA_C_DN
LINDSTEDT_DENDRITIC_CELL_MATURATION_A
NES
B
Cells
77.9
Single Cells
97.1
Live+
94.9
Q1
5.26
Q2
0.15
Q4
94.4
Q3
0.17
SSC-A
FSC-A
FSC-W
Comp-Live Dead Violet-A :: Live_Dead
Comp-Alexa Fluor 488-A :: HIV-GFP
Comp-PE-Cy5-A :: CD86
C
Live/Dead
% Live
Control
ILF3 sh1
ILF3 sh2
LKO
NF90
NF110
D
CD83
%CD83+
P=.14
E
CD1c
Isotype
Donor 1
Donor 2
Donor 3
Donor 4
F
CD1c
MFI
NS
G
Lentiviral
Transduction
+ IL-4
+GM-CSF
+Vpx
Immature DC
Control
ILF3 sh1
ILF3 sh2
Rest 24 h
Supernatant Swap 24 h
1100 RPM x 5min
H
%CD86+
K.D.
Supernatant
I
ILF3
CD80
CD209
SAMHD1
CXCL10
ISG15
Relative Expression
J
ILF3 gRNA
THP-1 LCV2 #1 #2
NF110
NF90
Actin
K
CD86
CD14
SAMHD1
CD209
THP-1
LCV2
ILF3 Guide 1
ILF3 Guide 2

Figure S2. ILF3 regulates expression of genes associated with myeloid cell maturation. (**A**) Top 25 Curated gene sets (gene set member size 200 > x > 15) with an FDR < 0.05 from GSEA analysis of sh1+sh2 ILF3 vs Control shRNA ranked by t-test. Results represented as Normalized Enrichment Scores. (**B**) Gating scheme for all flow cytometry experiments listed in this manuscript. Day 6 MDDCs were prepared as described for flow cytometry analysis (see Materials and Methods). Relevant cells were gated on SSC vs. FSC, then singlets were selected, then "live" cells were selected via an amine reactive fixable viability dye, and subsequent surface markers, intracellular markers, and GFP from HIV-1-GFP were analyzed. **(C)** Live/Dead staining of % Live MDDCs in either ILF3 knockdown (Control, ILF3 sh1, ILF3 sh2) or NF90/NF110 overexpression experiments (LKO, NF90, NF110). **(D)** Quantification of CD83 expression on live-gated MDDCs, n=7 donors over 2 separate experiments. **(E)** Histogram of CD1c expression across n=4 donors compared to relevant isotype control (Donor 1 used as a representative isotype example) using control MDDCs. **(F)** CD1c MFI quantification in control, ILF3 sh1, and ILF3 sh2 conditions across n=4 donors. (**G**) Illustration of MDDC supernatant swap experiment in control or ILF3 knockdown MDDCs. MDDCs were transduced with control shRNAs or shRNAs targeting ILF3. At day 4 post-transduction, the culture media was replaced with fresh media and the cells were cultured for an additional 24 hours. Media was then exchanged across conditions as indicated and the cells were cultured for another 24 hours before scoring surface expression of CD86 by flow cytometry. **(H)** Quantification of CD86 expression in the experiment described in G. n = 4 donors. (**I**) qPCR analysis of the indicated genes following shRNA knockdown of ILF3 in THP-1 cells. n = 6 independent transductions. Statistics were calculated using a one-way ANOVA with Dunnet's test for multiple comparisons. (**J**) Western blot depicting expression of NF90, NF110, and actin from whole cell lysates of parental THP-1 cells compared to cells transduced with a non-targeting lentiCRISPR control vector (LCV2) or two independent vectors targeting *ILF3*, at day 9 post-transduction. (**K**) qPCR analysis of targets from Day 9 CRISPR knockout of *ILF3* in THP-1 cells. n = 3 technical replicates, one-way ANOVA using Dunnet's test for multiple comparisons.

ILF3 restrains DC Maturation and antiviral IFN responses to HIV-1-GFP infection

Our transcriptomic analysis of unstimulated MDDCs indicated a role for ILF3 in regulating myeloid cell maturation, so we also examined the impact of ILF3 knockdown or overexpression on MDDC responses to infection with HIV-1-GFP. Knockdown of ILF3 resulted in significantly elevated expression of CD86 (Fig. 2A), CD80, and HLA-DR (Fig. S3A,B) in HIV-1-GFP-infected cells compared to controls. In contrast to markers of mature MDDCs, expression of *CCL23*, a chemokine marker of immature MDDCs, was suppressed by knockdown of ILF3, as measured at the levels of mRNA and protein (Fig. 2B). Similarly, expression of *CIITA*, which typically decreases during DC maturation (150), was further decreased by ILF3 knockdown during HIV-1-GFP infection (Fig. 2C). In addition, knockdown of ILF3 increased expression and secretion of type I IFN (Fig. S3C,D) and expression of the hallmark IFN-stimulated gene ISG15 in response to HIV-1-GFP infection (Fig. 2D).

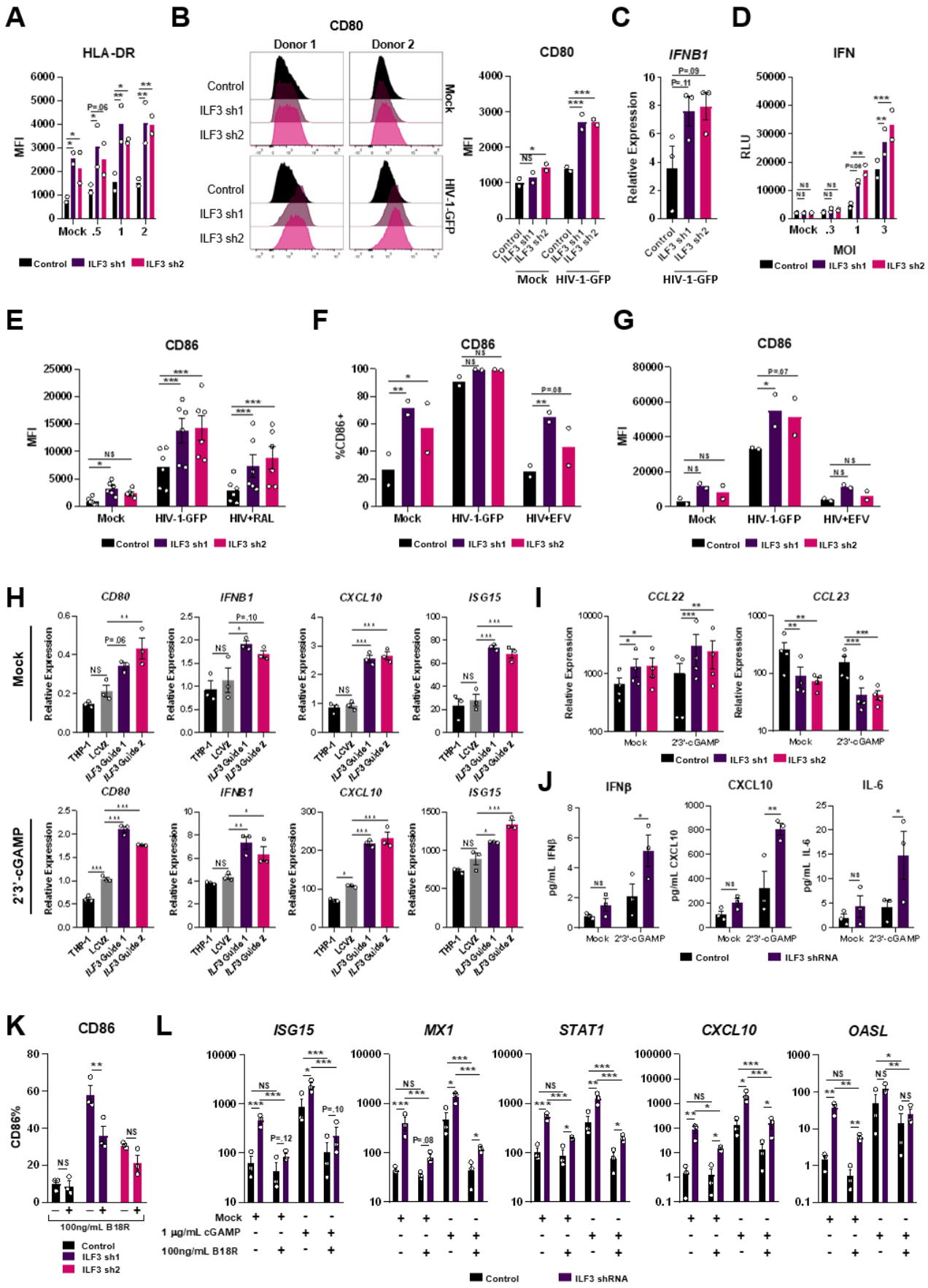
A
HLA-DR
MFI
Mock .5 1 2
Control ILF3 sh1 ILF3 sh2
B
CD80
Donor 1
Donor 2
Control
ILF3 sh1
ILF3 sh2
Mock
HIV-1-GFP
CD80
MFI
Mock HIV-1-GFP
C
IFNB1
Relative Expression
HIV-1-GFP
D
IFN
RLU
Mock .3 1 3
MOI
Control ILF3 sh1 ILF3 sh2
E
CD86
MFI
Mock HIV-1-GFP HIV+RAL
F
CD86
%CD86+
Mock HIV-1-GFP HIV+EFV
G
CD86
MFI
Mock HIV-1-GFP HIV+EFV
H
Mock
2'3'-cGAMP
CD80
IFNB1
CXCL10
ISG15
Relative Expression
THP-1 LCV2 ILF3 Guide 1 ILF3 Guide 2
I
CCL22
CCL23
Relative Expression
Mock 2'3'-cGAMP
Control ILF3 sh1 ILF3 sh2
J
IFNβ
CXCL10
IL-6
pg/mL IFNβ
pg/mL CXCL10
pg/mL IL-6
Mock 2'3'-cGAMP
Control ILF3 shRNA
K
CD86
CD86%
100ng/mL B18R
Control
ILF3 sh1
ILF3 sh2
L
ISG15
MX1
STAT1
CXCL10
OASL
Mock
1 µg/mL cGAMP
100ng/mL B18R
Control ILF3 shRNA

Figure S3. ILF3 regulates innate responses to HIV-1-GFP and cGAMP. (**A**) Flow cytometry analysis of HLA-DR MFI from n=2 donors in MDDCs at the indicated MOIs of HIV-1-GFP 48 hours post-infection, (**B**) Histogram and flow cytometry analysis of %CD80+ cells at an HIV-1-GFP MOI of 2, 48 hours post-infection. n = 2 donors. (**C**) qPCR expression of *IFNB1* in HIV-1-GFP-infected MDDCs at an MOI of 1. n=3 donors. **(D)** Type I IFN bioassay of supernatants from MDDCs infected with HIV-1-GFP at the indicated MOIs for 48 h. n = 2 donors. (**E**) Flow cytometry analysis of CD86 MFI in MDDCs infected with HIV-1-GFP (MOI = 3) for 48 h, ± RAL. n = 6 donors from 2 experiments. (**F**) Flow cytometry analysis of CD86%+ in MDDCs infected with HIV-1-GFP (MOI = 3) for 48 h, ± EFV. n = 2 donors. (**G**) Flow cytometry analysis of CD86 MFI from (E). (**H**) qPCR analysis of targets from day 9 CRISPR knockout of ILF3 in THP-1 cells untreated or treated with 2'3'-cGAMP (3ug/mL, 7 hours). n = 3 technical replicates. **(I)** qPCR expression of DC maturation chemokine markers *CCL22* and *CCL23* in mock or 1μg/mL 2'3'-cGAMP-treated control or ILF3 knockdown MDDCs in n=4 donors. **(J)** ELISAs for IFNβ, CXCL10, and IL-6 secretion in control or ILF3 knockdown MDDCs in mock or 1μg/mL 2'3'-cGAMP-treated conditions in n=4 donors. **(K)** Flow cytometry analysis of CD86 expression on live-gated control or ILF3 knockdown MDDCs 48 hours post-media refresh on day 4. n=3 donors were mock or B18R-treated at 100ng/mL at t=0 and t=24. **(L)** qPCR analysis of ISGs in control or ILF3 knockdown MDDCs. Cell were either mock or 1μg/mL 2'3'-cGAMP-treated for 7 hours. B18R was added 1 hour prior to 2'3'-cGAMP stimulation at 100ng/mL. For (A-G, I-L), statistics were calculated with a paired mixed-effects model using Dunnet's test for multiple comparisons. For (H) a one-way ANOVA was used with Dunnet's test for multiple comparisons.

To confirm that the negative regulation of DC maturation and IFN responses was specific to modulation of ILF3, we overexpressed each of its two major isoforms, NF90 and NF110 (Fig. 2E), and tested responses to HIV-1-GFP infection. We observed inverse effects compared to knockdown, as overexpression of either isoform suppressed surface expression of CD86 in resting MDDCs relative to controls (Fig. 2F). In HIV-1-GFP-infected MDDCs, both isoforms suppressed surface expression of CD86 (Fig. 2F). Similarly, overexpression of either ILF3 isoform potentiated CCL23 mRNA and secreted protein (Fig. 2G), enhanced expression of *CIITA* in response to HIV-1-GFP infection, and suppressed expression of *CCL22*, an additional chemokine marker of mature DCs (Fig. 2H). We also found that overexpression of NF90 or NF110 suppressed *IFNB1* in HIV-1-GFP-infected MDDCs and trended toward suppression of ISG15, with only the NF110 isoform reaching statistical significance (Fig. 2H,I). Taken together, these experiments demonstrate that ILF3 negatively regulates myeloid DC maturation and innate immune responses driven by HIV-1-GFP.

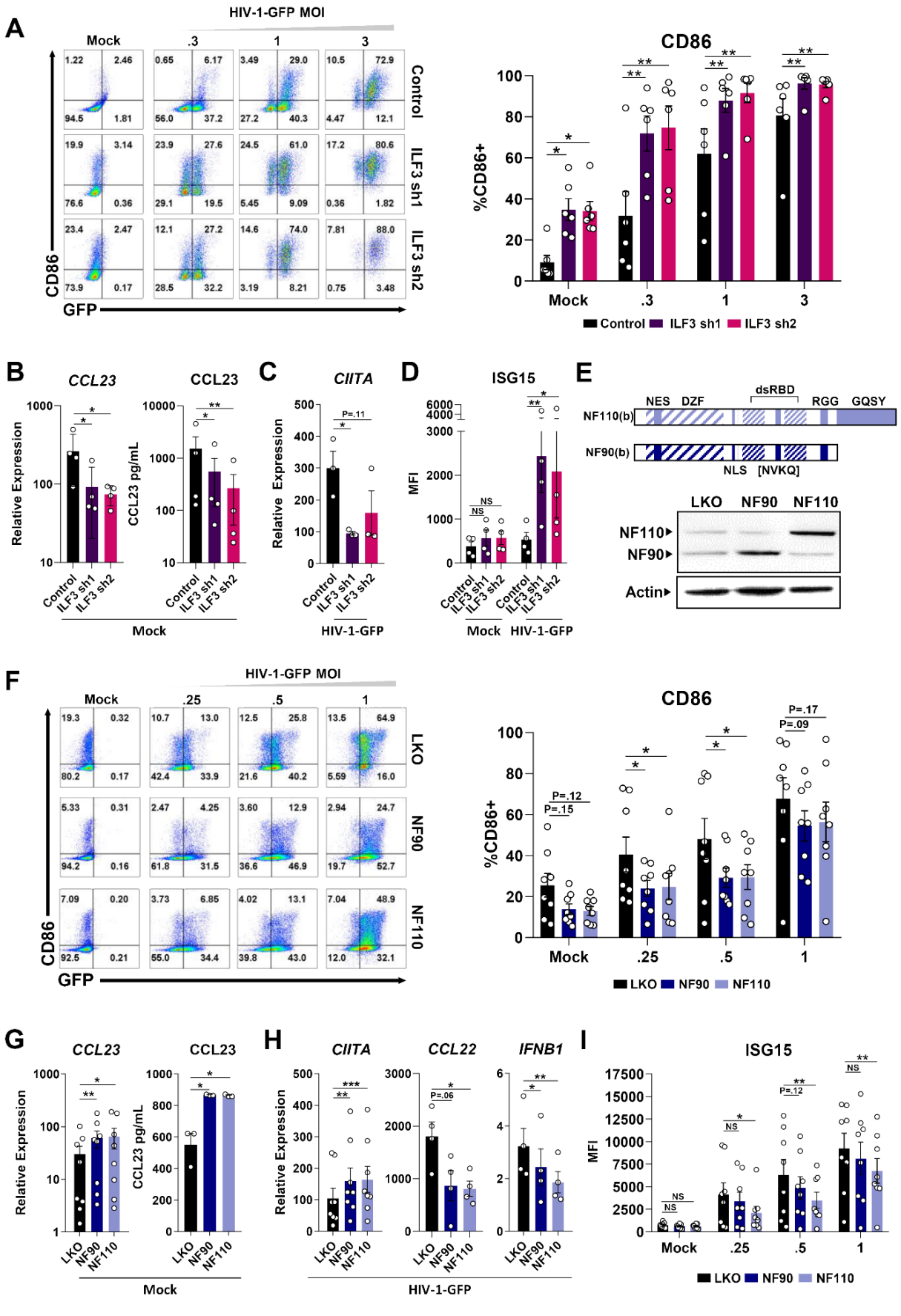
A
HIV-1-GFP MOI
Mock
.3
1
3
Control
ILF3 sh1
ILF3 sh2
CD86
GFP
CD86
%CD86+
Mock
.3
1
3
Control
ILF3 sh1
ILF3 sh2
B
CCL23
CCL23
Relative Expression
CCL23 pg/mL
Control
ILF3 sh1
ILF3 sh2
Mock
C
CIITA
Relative Expression
P=.11
HIV-1-GFP
D
ISG15
MFI
NS
Mock
HIV-1-GFP
E
NES
DZF
dsRBD
RGG
GQSY
NF110(b)
NF90(b)
NLS
[NVKQ]
LKO
NF90
NF110
NF110
NF90
Actin
F
HIV-1-GFP MOI
Mock
.25
.5
1
LKO
NF90
NF110
CD86
GFP
CD86
%CD86+
P=.12
P=.15
P=.17
P=.09
Mock
.25
.5
1
LKO
NF90
NF110
G
CCL23
CCL23
Relative Expression
CCL23 pg/mL
LKO
NF90
NF110
Mock
H
CIITA
CCL22
IFNB1
Relative Expression
P=.06
HIV-1-GFP
I
ISG15
MFI
P=.12
NS
Mock
.25
.5
1
LKO
NF90
NF110

Figure 2. ILF3 restrains MDDC maturation and IFN signaling in response to HIV-1-GFP viral challenge. (**A**) Flow cytometry analysis of CD86 expression in ILF3 knockdown MDDCs that were either mock treated or infected with HIV-1-GFP at the indicated MOIs, gated on FSC vs. SSC, singlets, and live cells. n = 6 donors quantified over 2 individual experiments. (**B**) qPCR of *CCL23* and CCL23 ELISA data of mock-treated MDDCs. n=4 donors. **(C)** qPCR of *CIITA* expression in MDDCs infected with HIV-1-GFP for 32 hours. n = 3 donors. (**D**) MFI of ISG15 expression in MDDCs infected with HIV-1-GFP for 48 h. n = 4 donors over 2 experiments. (**E**) Major protein isoforms of ILF3 and their domains: Nuclear export signal (NES), Domain associated with Zinc Finger (DZF), double-stranded RNA-binding domain (dsRBD), RGG-repeat motif (RGG=RGG-repeat), GQSY-repeat motif (GQSY-repeat), Nuclear localization signal (NLS), and NVKQ motif (NVKQ). Western blot of NF90 and NF110 expression in MDDC whole cell lysates after transduction with LKO, NF90, or NF110 overexpression vectors. (**F**) Flow cytometry analysis of CD86 surface expression in MDDCs overexpressing NF90 or NF110 that were infected with HIV-1-GFP for 48 hours. n = 8 donors from 2 individual experiments. (**G**) qPCR of *CCL23* and CCL23 ELISA data of mock-treated MDDCs. n=4 donors. **(H)** Expression of *CIITA, CCL22,* and *IFNB1* in MDDCs infected with HIV-1-GFP (MOI=1 for *CIITA*, MOI=.5 for *CCL22* and *IFNB1*) for 32 h. n=8 donors over 2 experiments for *CIITA* and n = 4 donors for *CCL22 and IFNB1*. (**I**) MFI of ISG15 expression under the conditions shown in (E). For (A, B, C, D, F, G, H & I), statistics were calculated by matching each donor in a mixed-effects model using Dunnet's test for multiple comparisons.

ILF3 dampens innate sensing of HIV-1-GFP and of other innate stimuli

Under permissive conditions, HIV-1 is detected in myeloid cells primarily through the cGAS-STING pathway (58, 137). These responses depend on reverse transcription of the incoming HIV-1 RNA, which in MDDCs is allowed to proceed by providing Vpx *in trans* to disable SAMHD1 (33). They are also facilitated by capsid destabilization (151), are limited by the exonuclease TREX1 (152), and can occur both before and after integration (34). Detection of HIV-1 components has also been reported to occur through TLR7/TLR8 (153, 154), through the MAVS pathway (155, 156), through NONO (54), and through other cellular sensors (157). To determine whether ILF3 impacts sensing of HIV-1-GFP at different stages of the virus life cycle, we inhibited reverse transcription using EFV, or blocked integration using RAL, and tested innate responses to HIV-1-GFP in ILF3 knockdown cells (Fig. 3A). RAL treatment did not affect ILF3's ability to restrain MDDC maturation upon HIV-1-GFP infection as measured by the percentage of live, CD86+ cells (Fig. 3B) or CD86 MFI (Fig. S3E). We noted that blocking reverse transcription inhibited responses to HIV-1-GFP as expected (33, 34) and did not affect baseline increases in maturation in ILF3 knockdown conditions as measured by CD86 (Fig.

S3F,G). These data suggested that loss of ILF3 potentiates baseline maturation and innate immune signaling in MDDCs and that these responses persist during stimulation with HIV-1 when reverse transcription is allowed to proceed.

We next sought to determine whether loss of ILF3 potentiated responses to stimulation specifically through the cGAS-STING and TLR-MyD88 pathways, which are known to act through several shared downstream kinases and transcription factors (Fig 3C). cGAS can be directly activated by transfection of immunostimulatory DNA (ISD). Alternatively, robust cGAS activation can by phenocopied by exogenous delivery of its enzymatic product, 2′3′-cGAMP, a secondary messenger that binds to and activates the adapter protein STING. We also tested the ssRNA mimetic R848, which is detected through TLR8 and relays innate immune activation of inflammatory genes downstream of the adapter protein MyD88 (Fig. 3D). Stimulation with 2′3′-cGAMP in ILF3 knockdown MDDCs led to increased expression *IFNB1,* the maturation factor *WFDC21P,* the ISGs *CXCL10,* and *ISG15* and the pro-inflammatory cytokine *IL6,* and decreased expression of *CIITA* compared to controls (Fig. 3E). Stimulation with ISD similarly potentiated expression of *IFNB1, CXCL10, ISG15,* and *IL6.* This result supports a role for ILF3 as a negative regulator of DC responses to cGAS-STING stimuli. Following stimulation with R848, knockdown of ILF3 increased expression of *IL1B* and *IL6,* pro-inflammatory cytokines downstream of MyD88 and NF-κB, as well as *ISG15,* and *WFDC21P,* while also decreasing *CIITA* (Fig. 3E). Knockdown of ILF3 also significantly increased surface expression of HLA-DR and CD86 in response to 2’3’-cGAMP and R848 stimulation, respectively, compared to controls (Fig. 3F,G). In THP-1 cells lacking ILF3, expression of *CD80, IFNB1, CXCL10,* and *ISG15* were also significantly increased at baseline and when stimulated with 2′3′-cGAMP (Fig. S3H). Knockdown of ILF3 in MDDCs also led to elevated expression of *CCL22* and a reciprocal

suppression of *CCL23*, both at baseline and following 2’3’-cGAMP stimulation (Fig. S3I). These data indicate that ILF3 dampens responses through both STING and MyD88 pathways, suggesting that ILF3 might function broadly as a negative regulator of innate responses.

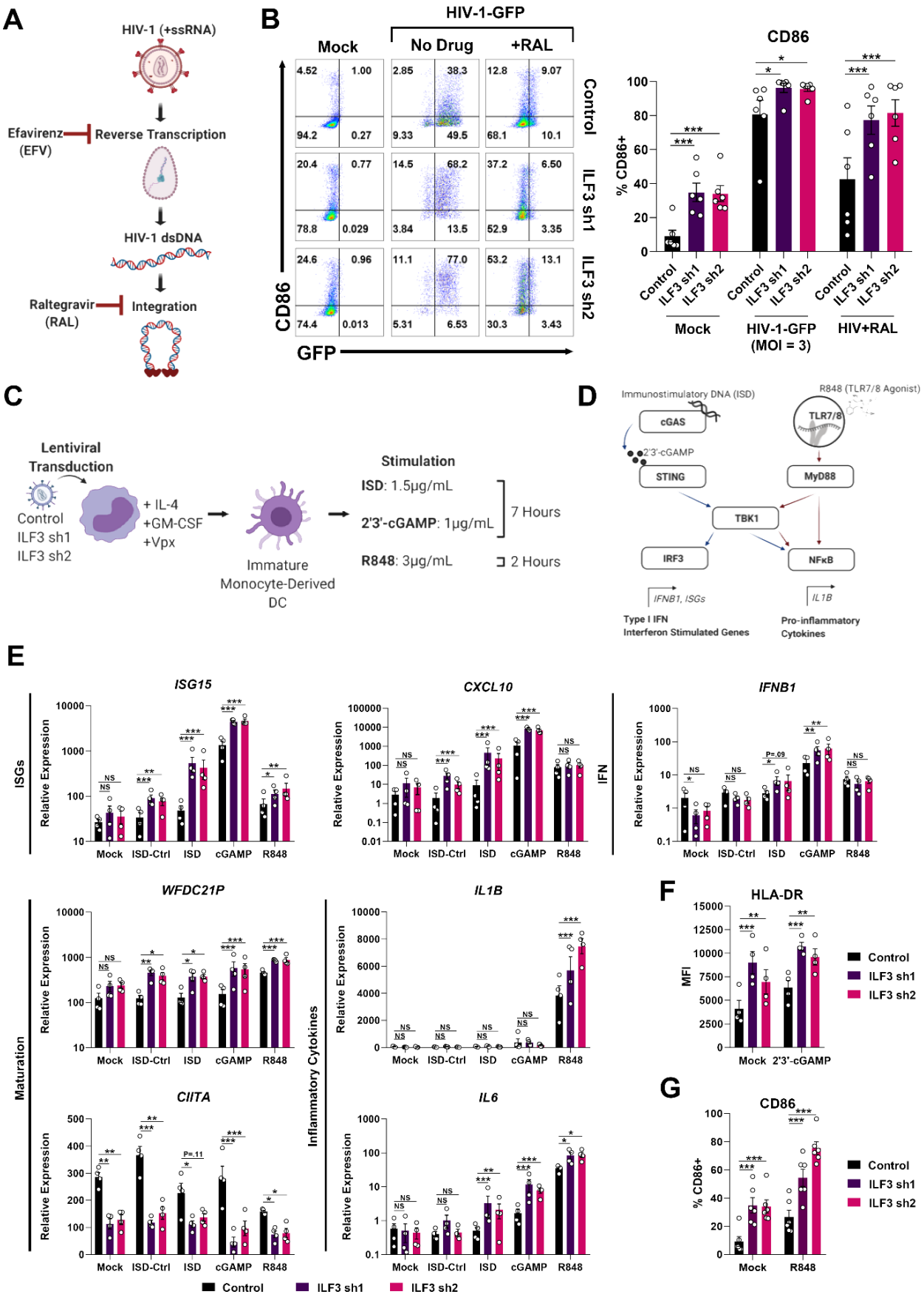
A
HIV-1 (+ssRNA)
Efavirenz (EFV)
Reverse Transcription
HIV-1 dsDNA
Raltegravir (RAL)
Integration
B
HIV-1-GFP
Mock
No Drug
+RAL
Control
ILF3 sh1
ILF3 sh2
CD86
GFP
CD86
% CD86+
Control
ILF3 sh1
ILF3 sh2
Mock
HIV-1-GFP (MOI = 3)
HIV+RAL
C
Lentiviral Transduction
Control
ILF3 sh1
ILF3 sh2
+ IL-4
+GM-CSF
+Vpx
Immature Monocyte-Derived DC
Stimulation
ISD: 1.5µg/mL
2'3'-cGAMP: 1µg/mL
7 Hours
R848: 3µg/mL
2 Hours
D
Immunostimulatory DNA (ISD)
R848 (TLR7/8 Agonist)
cGAS
TLR7/8
2'3'-cGAMP
STING
MyD88
TBK1
IRF3
NFκB
IFNB1, ISGs
IL1B
Type I IFN
Interferon Stimulated Genes
Pro-inflammatory Cytokines
E
ISGs
IFN
Maturation
Inflammatory Cytokines
ISG15
CXCL10
IFNB1
WFDC21P
IL1B
CIITA
IL6
Relative Expression
Mock
ISD-Ctrl
ISD
cGAMP
R848
Control
ILF3 sh1
ILF3 sh2
F
HLA-DR
MFI
Mock
2'3'-cGAMP
G
CD86
% CD86+
Mock
R848

Figure 3. ILF3 dampens innate sensing of HIV-1 and other PAMPs. (**A**) Illustration of the first half of the HIV-1 lifecycle and the point of action of inhibitors that target reverse transcription (efavirenz (EFV)) and integration (raltegravir (RAL)). (**B**) Flow cytometry analysis of CD86 expression on MDDCs infected with HIV-1-GFP for 48 h that were treated or untreated with RAL. n = 6 donors from 2 individual experiments. (**C**) Illustration of ILF3 knockdown in MDDCs and stratification of stimulation with either immunostimulatory DNA (ISD, 1.5μg/mL), 2'3'-cGAMP (1μg/mL), or R848 (3μg/mL). (**D**) Illustration of signaling pathways downstream of cGAS and TLR7/8. (**E**) qPCR analysis of the indicated targets in MDDCs that were mock treated or stimulated with the agonists depicted in (C). n = 4 donors. **(F)** Flow cytometry analysis of HLA-DR expression on MDDCs that were mock-treated or stimulated with 2'3'-cGAMP (1μg/mL), for 24 hours. n=4 donors. (**G**) Flow cytometry analysis of CD86 expression on MDDCs that were mock-treated or stimulated with R848 (3μg/mL). n = 6 donors from 2 individual experiments. For (B, E, F, & G), statistics were calculated by matching each donor in a mixed-effects model using Dunnet's test for multiple comparisons.

To verify that these changes in expression of IFN and maturation-related genes in ILF3 knockdown MDDCs correspond to increases in protein expression, we measured secretion of IFNβ, CXCL10, and IL-6 under mock or 2'3'-cGAMP conditions (Fig. S3J). Knockdown of ILF3 elaborated secretion of all three cytokines following stimulation with 2'3'-cGAMP and a trend toward increased secretion at baseline. Because we observed significant potentiation of IFNβ upon ILF3 knockdown, we sought to neutralize IFN produced in culture using the vaccina virus IFN receptor decoy protein B18R to evaluate IFN's contribution to ILF3-dependent gene expression. Interestingly, treatment with B18R only partially suppressed CD86 induction in unstimulated ILF3 knockdown MDDCs, which suggested that IFNs might contribute to, but are not solely responsible for MDDC maturation under these conditions (Fig. S3K). Neutralization of IFN was effective, as B18R treatment efficiently blocked induction of *ISG15*, *MX1*, and *STAT1* and reduced expression of *CXCL10* and *OASL* in cells stimulated with 2'3'-cGAMP (Fig. S3L). In ILF3 knockdown conditions, B18R treatment reduced expression of these ISGs, and yet, similar to observations for CD86, differences between control and ILF3 sh conditions persisted, particularly for *STAT1*, *CXCL10*, and *OASL*. Since B18R did not completely block elevated expression of ISGs and CD86 in ILF3 knockdown conditions, we can interpret these results in one of two ways: 1) B18R neutralization was insufficient to block all IFN-driven

signaling, or 2) IFN-dependent and IFN-independent signaling pathways contribute to the ILF3 phenotype. The latter interpretation should be strongly considered, given that induction of ISGs and MDDC maturation can occur through IFN-independent signals (126, 158). This would suggest that ILF3 negatively regulates innate immune responses and MDDC maturation through IFN-dependent and -independent mechanisms.

Nuclear localization of NF90 and N110 are required for suppression of innate responses

Having established a role for NF90 and NF110 in restraining MDDC maturation and innate responses to various stimuli, we sought to determine the specific domains of each protein required for their function. Both NF90 and NF110 forms of *ILF3* have been reported to exist predominantly in the nucleus (159, 160). To test whether nuclear localization is required for suppression of DC maturation and type I IFN responses, we overexpressed versions of NF90 and NF110 lacking the bipartite nuclear localization sequence (a.a. 370-394: KRPMEEDGEEKSPSKKKKKIQKKE) (NF90/NF110ΔNLS) in MDDCs (Fig. 4A) and confirmed via immunofluorescence microscopy that NF90/NF110ΔNLS mutants were localized to the cytosol (Fig. 4B), as indicated by the shift in the ratio of total nuclear to cytosolic ILF3 (Fig. 4C). We also confirmed overexpression of wild type and ΔNLS forms of NF90 and NF110 by qPCR (Fig. 4D). In MDDCs challenged with HIV-1-GFP, full-length NF90 and NF110 were able to suppress *CD86*, *WFDC21P*, and *ISG15* induction, and deletion of the NLS from either isoform prevented suppression of these markers (Fig. 4D). By flow cytometry, we saw concordant effects on protein expression of CD86 and ISG15 (Fig. 4E,F). NF90 and NF110 have been previously found to translocate to the cytosol during influenza infection of epithelial cells (161). To determine whether HIV infection could influence ILF3 localization, we compared the

nuclear vs cytosolic ratios of endogenous NF90 and NF110 in uninfected or HIV-1-GFP+ MDDCs, and we found no significant shift in their localization (Fig 4G). These experiments suggest that nuclear localization is essential to the function of both of ILF3's isoforms in regulating myeloid maturation and IFN responses, and in this context, infection with HIV-1-GFP does not impact ILF3 localization.

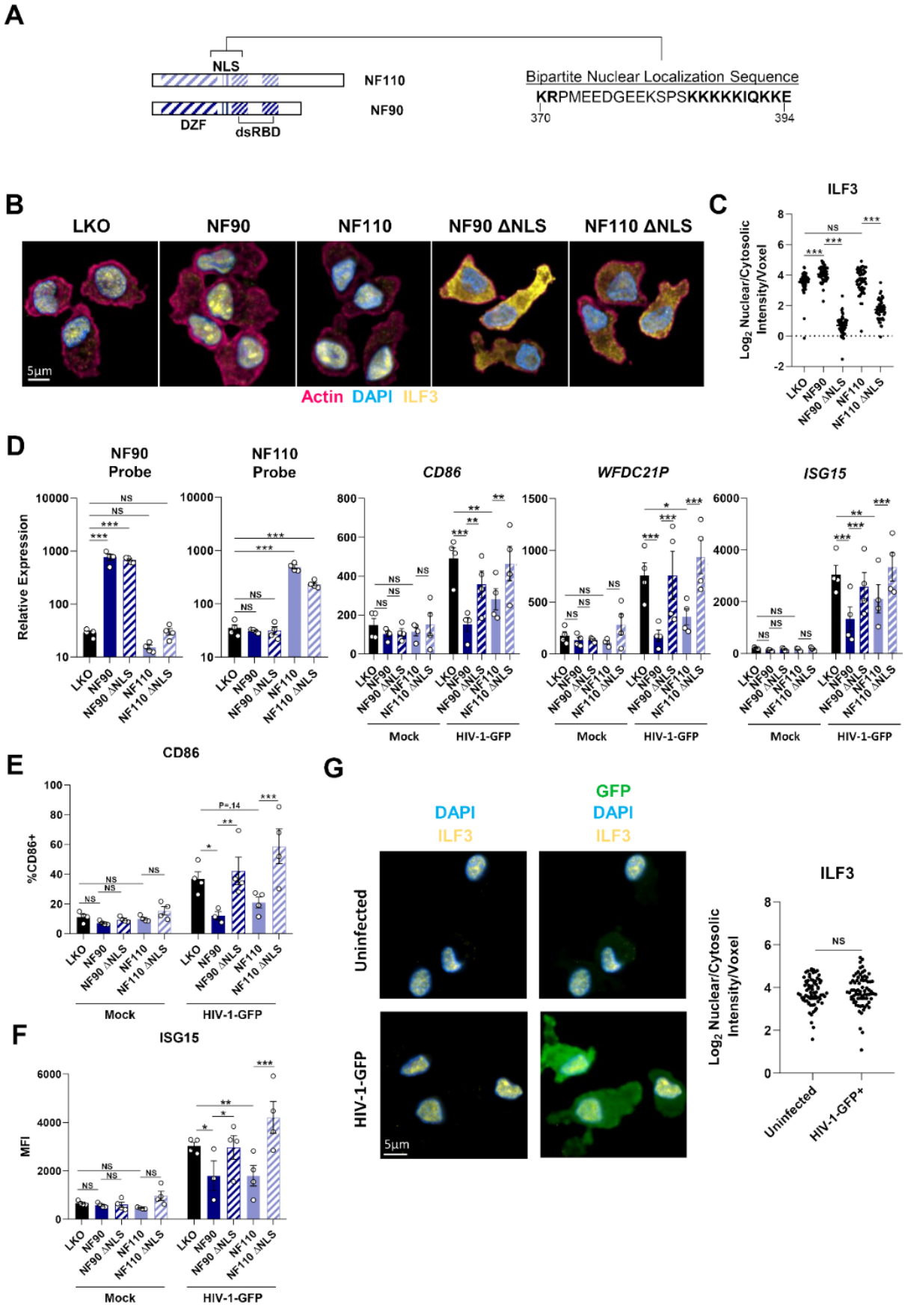
A
NLS
NF110
NF90
DZF
dsRBD
Bipartite Nuclear Localization Sequence
KRPMEEDGEEKSPSKKKKKIQKKE
370
394
B
LKO
NF90
NF110
NF90 ΔNLS
NF110 ΔNLS
5μm
Actin DAPI ILF3
C
ILF3
Log2 Nuclear/Cytosolic Intensity/Voxel
D
NF90 Probe
NF110 Probe
CD86
WFDC21P
ISG15
Relative Expression
Mock
HIV-1-GFP
E
CD86
%CD86+
F
ISG15
MFI
G
DAPI
ILF3
GFP
DAPI
ILF3
Uninfected
HIV-1-GFP
5μm
ILF3
Log2 Nuclear/Cytosolic Intensity/Voxel
Uninfected
HIV-1-GFP+

Figure 4. Nuclear localization of NF90 and N110 are required for suppression of innate responses to HIV-1-GFP. (**A**) Illustration of the bipartite nuclear localization sequence in NF90 and NF110. (**B**) Immunofluorescence of mock-treated MDDCs that were transduced with the indicated constructs and stained for actin (magenta), ILF3 (yellow, staining endogenous and overexpression constructs), and DNA (cyan, DAPI). (**C**) Quantification of three-dimensional immunofluorescence microscopy of total ILF3 antibody staining represented as the intensity of signal over voxel space, presented as a ratio between nuclear and cytosolic compartment. Data is from one representative donor using 50 cells per condition. Statistics were calculated using a one-way ANOVA with Sidak's test for multiple comparisons. (**D**) qPCR quantification of *NF90* and *NF110* expression using SybrGreen probes to detect endogenous and overexpressed isoforms of *ILF3*. **(E)** Flow cytometry analysis of CD86 expression in MDDCs that were transduced with the indicated overexpression constructs and either mock treated or infected with HIV-1-GFP for 48 h. n = 4 donors. (**F**) MFI quantification of ISG15 expression. n = 4 donors. Donor #2 was excluded from the HIV-1-GFP condition for aberrant activation. For (D, E, & F), statistics were calculated using a paired mixed-effects model with Dunnet's test for multiple comparisons. (**G**) Representative three-dimensional immunofluorescence microscopy quantification of total NF90 and NF110 from one donor, demonstrating the intensity of signal over voxel space as a ratio of nuclear versus cytosolic space. 75 cells were quantified from each condition: mock infected or HIV-1-GFP+ infected MDDCs at 27 hours post-infection (selecting GFP+ cells). Image channels depict total ILF3 (yellow), DNA (cyan, DAPI), and GFP. An unpaired, two-tailed t-test was used for statistical analysis.

The DZF domain of NF110 is required for suppression of MDDC maturation and type I IFN responses

To determine the domains of NF90 and NF110 that are required for regulation of DC responses, we designed constructs that lacked the dual double-stranded RNA-binding domains (dsRBDs) (ΔdsRBD1: a.a. 402-465, ΔdsRBD2: a.a. 531-576) or lacked the DZF domain (ΔDZF: a.a. 89-342) (Fig. 5A). These constructs were robustly overexpressed at the mRNA level in MDDCs (Fig. 5B) and were translated to significantly higher levels than the corresponding native proteins (Fig. 5C). Deletion of the dsRBDs in either NF90 or NF110 had no effect on levels of the maturation transcripts *CD86*, *CD80*, or *CCL23* or surface expression of CD86 following HIV-1-GFP infection (Fig. 5D,E). Surprisingly, deletion of the DZF domain eliminated the ability of NF110 to suppress MDDC maturation, whereas deletion of the same domain in NF90 had no effect (Fig. 5D,E). We also quantified IFNβ secretion during HIV-1-GFP infection in MDDCs that overexpressed wild type or mutant ILF3 constructs. Although none of these experimental conditions reached statistical significance, all ILF3 constructs except

for the NF110 DZF-deletion mutant trended toward IFNβ suppression (Fig. 5F).

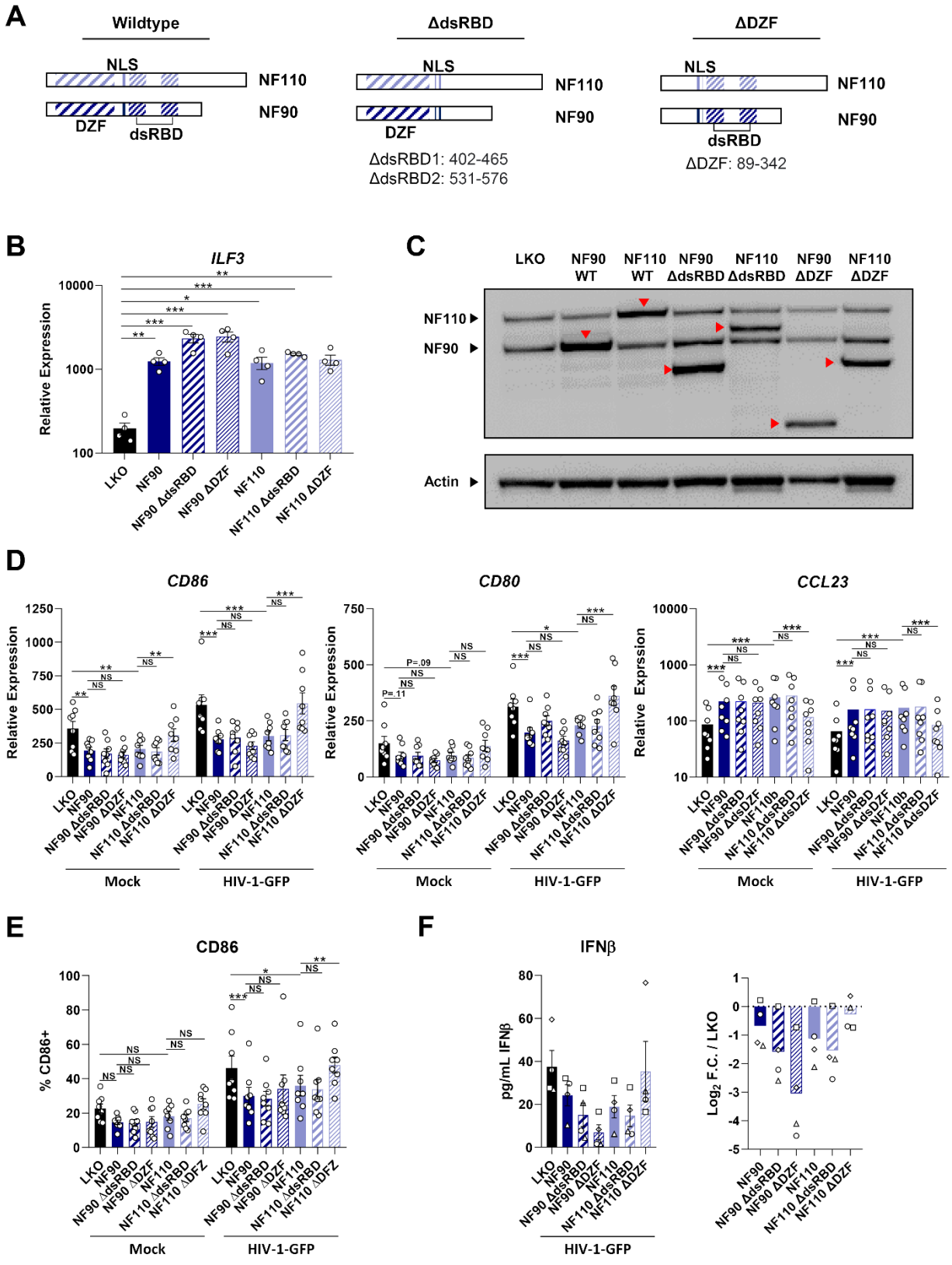

Figure 5. The DZF domain of NF110 suppresses MDDC maturation. (**A**) Illustration of wt NF90 and NF110 constructs and the corresponding domain mutants with deletions in either the dsRBD or the DZF domains. (**B**) Representative qPCR quantification of both endogenous and overexpressed *ILF3*. n = 4 donors. (**C**) Representative western blot of MDDC whole cell lysates depicting overexpression of NF90 and NF110 constructs. Red arrowheads indicate overexpressed mutant constructs. (**D**) qPCR quantification of *CD86, CD80,* and *CCL23* expression in MDDCs that were transduced with the indicated overexpression constructs and either mock treated or infected with HIV-1-GFP (MOI = 0.5) for 32 h. n = 8 donors from 2 independent experiments. (**E**) Flow cytometry quantification of CD86 expression in MDDCs infected with HIV-1-GFP (MOI = 0.5) for 48 h. n = 8 donors from 2 independent experiments. (**F**) ELISA of IFNβ in supernatants from MDDCs infected with HIV-1-GFP (MOI = 0.5) for 32 h. n = 4 donors. Shapes represent individual donors. For (B, D, & E), statistics were calculated using a paired mixed-effects model with Dunnet's test for multiple comparisons.

RNA-seq analysis of NF110 reveals DZF-dependent genes associated with DC maturation and metabolic pathways

In order to more comprehensively define the molecular pathways regulated by ILF3 in DCs, we performed RNA-seq analysis of mock MDDCs transduced with the LKO control vector, a vector expressing full-length NF110, or the NF110 DZF-deletion mutant (ΔDZF). 355 genes were significantly differentially expressed in cells overexpressing wildtype NF110 compared to the LKO control ($|\log_2(\text{NF110/LKO})| > \log_2(1.5)$, FDR < 0.05, for genes with an average $\log_2(\text{CPM})>1$). For 97 of these genes, more than 50% of the expression change induced by overexpression of NF110 was retained when NF110ΔDZF was overexpressed. We termed these genes "DZF-independent" with respect to the ILF3-mediated effect (Fig. S4A). Many of the most strongly down-regulated, DZF-independent genes were found to be non-coding RNAs (Fig. 6A), consistent with ILF3's known role as a binder and modulator of lncRNAs (94-99). Interestingly, genes that were up-regulated by NF110 overexpression in a DZF-independent manner were generally protein-coding (Fig. S4A). Of note, NF110 overexpression led to upregulation of *AQP7*, *CD163L1, CD14, C3AR1, CD300a, ABCA9, MAFB, FMN1*, *STEAP4, CD163, IL10,* and *CFH* (Fig.6B), which are all associated with immature or tolerogenic myeloid/DC phenotypes (162-172). Conversely, *DCSTAMP, CHI3L1, CH25H, ALDH1A2, BHLHE41*, and *CCL22*, which are characteristic genes expressed in mature DCs (9, 141, 173-

176), were down-regulated in a DZF-dependent manner (Fig. 6B). Together, these data demonstrate that NF110 restrains maturation in uninfected DCs and that this activity is dependent on the DZF domain.

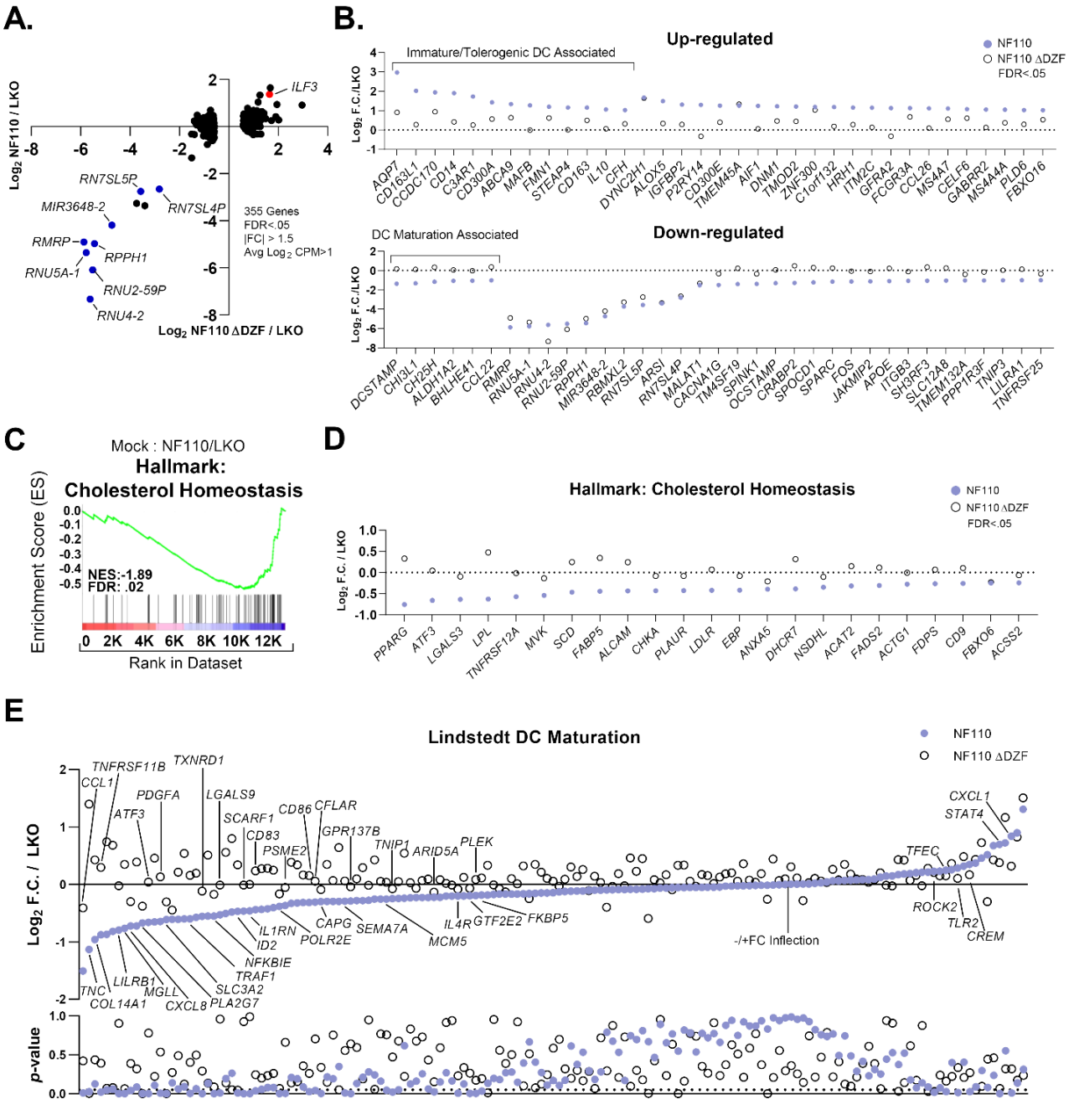

Figure 6. RNA-Seq analysis of NF110 overexpression reveals DZF-dependent genes associated with DC maturation and metabolic pathways. (**A**) Plot of 355 differentially expressed genes on log2 scale, averaged across n=4 donors, with a |FC| > 1.5, average Log_2 CPM > 1, and FDR < 0.05 of NF110 and NF110 ΔDZF constructs under unstimulated conditions. Blue points indicate noncoding-RNAs down-regulated by NF110 and NF110 ΔDZF. Red point indicates overexpression of NF110 (ILF3), as expected. (**B**) Genes represented in (A), |FC| > 2, ordered by magnitude of fold change by group. (**C**) GSEA plot of top-ranking Cholesterol Homeostasis Hallmark gene set from analysis of MDDCs overexpressing NF110 compared to the LKO control. (**D**) Log_2 fold change of core enrichment genes (FDR < 0.05) from (C), pre-ranked by t-test. (**E**) Average Log_2 fold change for genes from the Lindstedt DC Maturation gene sets (Groups A-C) in MDDCs overexpressing NF110 (closed circles) or NF110 ΔDZF (open circles) compared to the LKO control. Highlighted genes represent genes with a *p*-value < 0.05.

We also examined the set of genes that were differentially expressed following overexpression of NF110 wt compared to the LKO control by GSEA (177). Of note, the expression of genes belonging to the Cholesterol Homeostasis (32/74) and Oxidative Phosphorylation (111/200) gene sets was suppressed under conditions of NF110 overexpression. These were the only statistically significantly enriched gene sets out of all tested Hallmark Gene Sets in the Molecular Signatures Database (178) containing between 15 and 200 genes (Fig. 6C, S4B). Inspection of individual genes belonging to the Oxidative Phosphorylation gene set revealed they had subtle changes in magnitude compared to the control (Fig. S4C). Genes in the Cholesterol Homeostasis gene set were suppressed to a greater degree by NF110, and included *PPARG, ATF3, LGALS3, LPL,* and *TNFRSF21* (FDR<0.05) (Fig. 6D). The top DZF-dependent gene in the Cholesterol Homeostasis group, *PPARG* (the gene that encodes PPARγ), was also significantly up-regulated in ILF3 KO THP-1 populations (Fig. S4D).

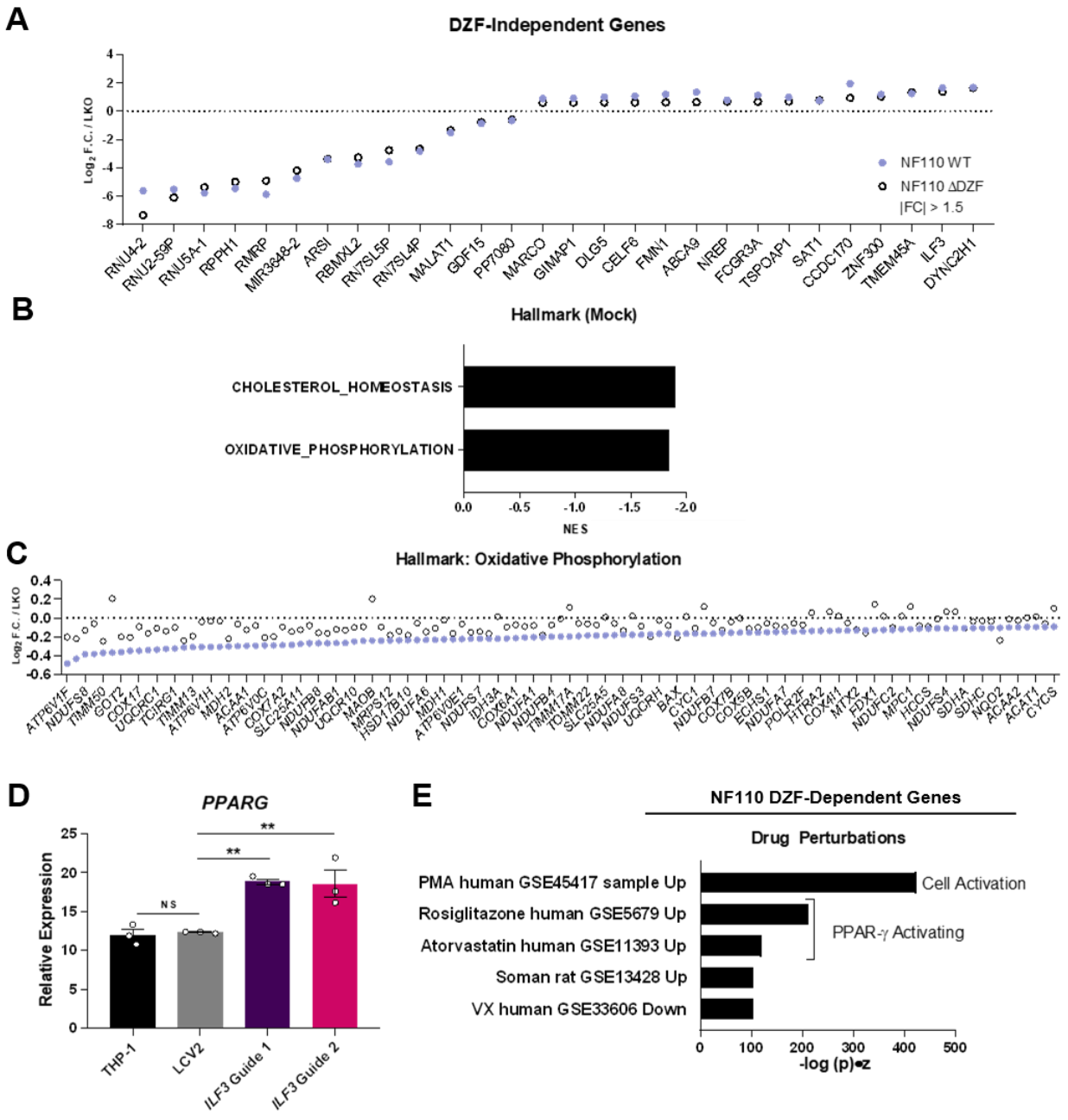

Figure S4. Overexpression of NF110 impacts expression of non-coding RNAs and protein coding genes associated with cholesterol homeostasis. (**A**) Dot plot of DZF-independent genes as defined as more than 50% of the expression change in a gene induced by overexpression of NF110 being retained when NF110ΔDZF is overexpressed with an FDR < 0.05, Avg Log_2 CPM > 1. NF110 wt differential gene expression represented in closed circles and NF110ΔDZF is represented in open circles. Points represent averaged data from n = 4 donors. (**B**) GSEA Hallmark gene set analysis (gene sets containing 15 < x < 200 members) of untreated MDDCs overexpressing NF110 wt, ranked by t-test, represented as Normalized Enrichment Score, FDR < 0.05. (**C**) Hallmark Oxidative Phosphorylation core enrichment from (B) represented as NF110 wt or ΔDZF compared to LKO control, with no set FDR. Every other gene is labeled on the x-axis due to space constraints. (**D**) qPCR analysis of targets from Day 9 CRISPR knockout of ILF3 in untreated THP-1 cells. Representative of 3 technical replicates, using a one-way ANOVA using Dunnet's test for multiple comparisons. (**E**) EnrichR Drug Perturbation analysis of NF110 DZF-dependent genes (defined as less than 50% of the expression change in a gene induced by

overexpression of NF110 being retained when NF110ΔDZF is overexpressed with an FDR < 0.05). Scores represented as Combined Score (-log (p) • z).

To determine if our RNA-seq data from NF110 overexpression reflected known biological perturbations, we compared our set of NF110-regulated DZF-dependent genes with public datasets using EnrichR (179). We found significant overlap with genes affected by the PPARγ agonists rosiglitazone and atorvastatin in MDDCs and monocytes, respectively (Fig. S4E). This overlap is noteworthy, considering that PPARγ is known to control oxidation of fatty acids and regulate NF-κB-mediated proinflammatory responses (180). Taken together, these data suggest that ILF3 shapes the transcriptome of myeloid DCs through pathways that may intersect, at least in part, with PPARγ and lipid metabolism.

We also observed that many genes in the Lindstedt DC maturation gene sets were moderately suppressed by NF110 overexpression (Fig. 6E), although these gene sets did not exhibit high GSEA scores when analyzed in full. This is likely due to the fact that we tested MDDCs in an immature state, with expression of these genes already being low, thereby making further gene suppression difficult to detect. Nevertheless, the majority of genes (75%) in gene sets A-C (elevated in mature DCs in Fig.1) were down-regulated by overexpression of NF110, predominantly in a DZF-dependent manner (Fig. 6E). Apart from the significantly down-regulated genes by NF110, the majority of genes down-regulated by the wildtype form of NF110 had consistently lower *p*-values than those down-regulated by NF110 ΔDZF. These data are in agreement with what we observed in ILF3 knockdown experiments (as expression of these genes associated with DC maturation was increased) and support a specific role for NF110 in negatively regulating myeloid DC maturation.

Discussion

Delineating the mechanisms that regulate DC maturation and innate responses is critical to understanding antiviral immunity and can inform design of new therapeutic agents to modulate inflammation. Here, we have identified that the transcription factor ILF3 acts as a negative regulator of DC maturation and innate immune responses. We discovered that CD14+ monocytes express minimal levels of ILF3 and then increase its expression upon derivation into immature dendritic cells. As DCs are exquisitely sensitive to IFN signaling compared to circulating monocytes (126), it is plausible that DCs change expression levels of ILF3 in order to deploy or withdraw an additional regulator of innate immune responses. Although several previous studies have examined the role of ILF3 in regulating innate immune responses during stimulation, they have not reached a consensus on the role of ILF3, as these functions are likely context dependent. Our findings are consistent with the only other study of ILF3 in primary human cells during virus infection, which demonstrated that knockdown of ILF3 in primary human bronchial epithelial cells led to an increase in IFNβ production in response to infection with influenza virus (121). However, this effect is not observed in all experimental systems, since siRNA knockdown of ILF3 in HeLa and mouse embryonic fibroblast cells did not affect levels of type I IFNs following stimulation with the double-stranded RNA-mimetic polyI:C (polyinosinic:polycytidylic acid) (122). Other examples suggest that ILF3 may positively regulate IFN responses under certain conditions. In one case, A549 cells infected with Sendai virus exhibited decreased IFN upon siRNA knockdown of ILF3 (115). A more recent study in HeLa cells found that NF110 enhanced translation of *IFNB1* mRNA and a subset of ISGs (123). Given that the mechanisms regulating innate immune sensing and IFN production are known to

be different between cell lines of immune and non-immune origin (42), it is not particularly surprising that ILF3's function is context-dependent. Our data, based on knockdown, knockout, and overexpression studies, demonstrate that ILF3 acts to restrain IFN and downstream ISGs in MDDCs and myeloid cell lines, and is a significant contributing factor in regulating DC maturation state.

More broadly, the role of ILF3 in regulating innate immune responses has been evaluated primarily during RNA virus infection (115, 121). Previous studies have also established that NF90 and NF110 isoforms inhibit replication of RNA viruses by physical association with the ISG PKR via their dsRBDs to block viral translation (181, 182). Until now, it has not been established whether ILF3 also has a role in regulating DNA sensing pathways. Here, we have used HIV-1-GFP to model retrovirus infection and innate immune stimulation through the cGAS-STING pathway and have used antiretroviral drugs to separate stages of the virus life cycle. We found that in ILF3 knockdown conditions, the elevated innate immune responses and DC maturation phenotype persisted during infection with HIV-1-GFP. Responses to HIV-1-GFP were dependent on reverse transcription, as previously described (33, 34, 58, 137). Our observation that the ILF3 phenotype was sustained during stimulation with ISD, 2'3'-cGAMP, or R848 suggest that ILF3 acts broadly to negatively regulate pathways in the innate immune response. Placed in context with earlier publications, our data emphasize the varied roles of ILF3, not only across different cell types but across different pathogen sensing pathways.

ILF3 has been described to affect several aspects of HIV-1 infection. Many of these studies focused on a variant of *ILF3,* NF90ctv, that contains a two base-pair CT insertion that results in a frame-shift and translation of a highly acidic C-terminus (117). This variant does not appear to be expressed in the human transcriptome (117, 138) but has been implicated in the

positive regulation of ISGs (117), interactions with HIV-1 Rev and the Rev-responsive element in HIV-1 RNA (183), and binding to HIV-1 TAR RNA (118). In light of our results demonstrating that loss of ILF3 is associated with heightened innate responses and DC maturation, we speculate that the NF90ctv variant may behave as a dominant negative to influence ILF3-dependent gene transcription. Interestingly, NF90 has been shown to enhance HIV gene expression through cyclin T1 regulation (184). Testing these roles for ILF3 and ILF3 variants is beyond the scope of our study, but future work will likely uncover whether these effects dovetail with our findings that ILF3 modulates myeloid cell activation.

Another unresolved question that has emerged from our studies is why the DZF domain in NF110, but not in NF90, is required for suppression of DC maturation. Of the two major isoforms of *ILF3*, NF110 has been shown to be more effective than NF90 at stimulating transcription through a proliferating cell nuclear antigen (PCNA) promoter in a transient reporter assay, whereas NF90 appears to have a greater capacity to bind RNA (138, 161). We note that the dsRBDs have been found to be dispensable for transcriptional coregulatory activity in other experimental systems (139). One hypothesis for why NF110 is a more effective transcriptional regulator is that its GQSY-repeat-containing C-terminus sterically interferes with the double-stranded RNA-binding domain (dsRBD), thereby reducing its activity relative to the DZF domain, which is required for interactions with DNA and for protein-protein interactions with binding partners like NF45 or NF90 (161), and increasing the DZF domain's relative importance in transcriptional regulation. Thus, it is possible that the DZF domain in NF110 plays a key role in regulating transcription in MDDCs, likely through interactions with its binding partners that are not impacted by mutation of the DZF domain in NF90. We speculate that ILF3 transcriptional phenotypes may arise from disruptions in the balance of NF90 and NF110

interactions with other protein partners due to the following observations: 1) overexpression of either full-length NF90 or an NF90 mutant lacking the DZF domain suppressed MDDC maturation, and 2) NF90 and NF110 are known to form large heterodimeric complexes (185, 186), the stoichiometry of which will be impacted by isoform expression and availability. Future studies are required to disentangle the functional role of the DZF domain of each isoform.

The largest effects resulting from manipulation of ILF3 levels in uninfected MDDCs occurred in gene expression pathways related to cholesterol homeostasis. Though the Oxidative Phosphorylation gene set members were affected, dendritic cells have been found to exhibit unique plasticity with respect to their ability to generate ATP from either glycolysis or oxidative phosphorylation during stimulation (187). GSEA analysis of MDDCs overexpressing NF110 identified the Cholesterol Homeostasis pathway as the most significantly enriched Hallmark gene set (FDR < 0.05). *PPARG, ATF3*, *LGALS3*, *LPL*, *TNFRSF12A*, and other genes in this pathway were suppressed by NF110. Expression of *PPARG* was also significantly elevated in unstimulated THP-1 ILF3 knockout cells that displayed elevated maturation and IFN responses at baseline. Decreased expression of genes such as *PPARG* and *CH25H* would be expected to result in a buildup of cholesterol through suppressed efflux and conversion of lipid products, which could impact IFN signaling, inflammatory responses, and myeloid cell maturation as others have shown (188, 189).

PPARγ is known to heterodimerize with retinoid X receptor family members (RXR) and the resulting transcriptional complex has an important function in regulating energy balance, including roles in triglyceride metabolism, fatty acid processing and storage, and glucose homeostasis (190). RXRs can partner with retinoic acid receptor family members (RARs) as well as PPARs (191). We recently reported that RAR alpha (RARA) functions as negative regulator

of DC maturation (126) and we speculate that this phenotype intersects with our observations reported here regarding ILF3. Along these lines, activation of PPARγ has been found to result in retinoid synthesis in dendritic cells (192), and RAR/RXR signaling can be activated through certain retinoids in DCs to suppress maturation (193, 194). Additionally, natural agonists of PPARγ (such as 15d-PGJ_2) and synthetic agonists (such as troglitazone and ciglitizone) have been shown to inhibit NF-κB and mitogen-activated protein (MAP) kinase inflammatory pathways, resulting in the decreased surface expression of DC maturation markers (195, 196). PPARγ has been shown in murine DCs to be important for sustained expression of *Aldh1a2* which promotes tolerogenic CD103+ DCs, and for suppressing the Th17-skewing cytokines IL-6 and IL-23p19 in all CD11c+ DCs (197). Given that that PPARγ was recently found to interact with both ILF3 and RXRA (RARA's heterodimeric partner) (198), it is likely that ILF3 isoforms can also impact PPARγ/RXR and RARA/RXR transcriptional control of lipid metabolism by altering these heteromeric transcriptional complexes, and consequently influence innate immune responses and DC maturation. Additional studies are required to determine whether there is a direct link between ILF3, PPARγ, and RARA as a transcriptional coregulatory complex in the context of lipid metabolism, myeloid cell inflammatory responses, and DC maturation.

Importantly, there is evidence that ILF3 could have a critical role in inflammatory pathophysiology *in vivo*. Small nucleotide polymorphisms within the *ILF3* locus are correlated with more frequent cardiac events in individuals with high and low HDL cholesterol profiles (199). These findings are congruent with a role for ILF3 in regulating cholesterol/lipid metabolism and inflammation. A separate small nucleotide polymorphism within the *ILF3* locus is associated with increased susceptibility to rheumatoid arthritis (200), further reinforcing the principal findings from our study which indicate that ILF3 perturbations are linked with

spontaneous induction of inflammatory gene expression. Taken together, our data identify ILF3 as an important negative regulator of inflammation and myeloid cell maturation, which has broad implications for how innate immune responses are governed during viral infection and inflammatory disease.

CHAPTER 4: Clinical implications for ILF3 in infectious disease and beyond

Introduction

Having explored the role ILF3 serves within the human myeloid immune compartment, it is important to examine the broader implications that studies surrounding ILF3, innate sensing, and DC maturation may have clinically in other disease contexts. Chapter 3 raised the possibility that ILF3-mediated innate immune responses may be impacted in the context other viral pathogens through pathways beyond the cGAS/STING signaling axis. Our work reveals that ILF3 negatively regulates dsDNA signaling, but could this extend to RNA viruses that do not produce DNA species? Use of TLR7/8 agonists in this work suggest that this is likely in myeloid DCs. However, other sensors of RNA exist such as TLR3, RIG-I, and MDA5. Does ILF3 regulate innate immune responses to other viral pathogens detected by these sensors? In addition to examining viral pathogens, what is ILF3's impact on hyperinflammatory diseases that involve dysregulated IFN and inflammatory cytokine responses? ILF3's role in myeloid DCs in the above contexts is likely to be broad-acting, yet our work and the literature suggest that its function in relation to innate immunity may be specific to this cell type. This begs the question, is there the potential for use of a therapeutic intervention targeting ILF3 to ameliorate conditions of hyperinflammation?

Genetic Variants of ILF3

In Chapter 3, we previously noted 2 single nucleotide polymorphisms (SNPs) that exist in the ILF3 locus that correlate with cholesterol levels and susceptibility to rheumatoid arthritis. Upon examination of potential single nucleotide variants within exons of *ILF3*, we found that mutations that could cause loss-of-function through truncation or mutation are highly selected against (Fig. 1A). This is in agreement with ILF3 homozygous knockout mouse models that

result in perinatal lethality but conditional knockouts in certain immune cell types are viable, suggesting that *ILF3* is an essential gene for certain cell types (182, 201). Thus, there is potential that these two SNPs may instead result in changes to the level of expression of *ILF3* in non-exonic regions of the *ILF3* locus, for example via the generation or perturbation of intronic splicing enhancers or perturbation of regulatory factor sites in the flanking untranslated regions rather than causing loss-of-function mutations (202). As an example, the SNV rs2569512 associated with myocardial infarction and altered cholesterol levels, falls within exon 8 and exon 9 in *ILF3*. Specifically, this T to C mutation occurs in a stretch of five T bases (-UUUUU- in the resulting mRNA) in a T rich intron, which is a binding motif for the RNA-binding protein hnRNP C. hnRNP C is involved in splicing and it is possible that this mutation could displace hnRNP C binding and cause intro retention creating altered expression levels of *ILF3* rather than a complete loss-of-function mutation(92, 203).

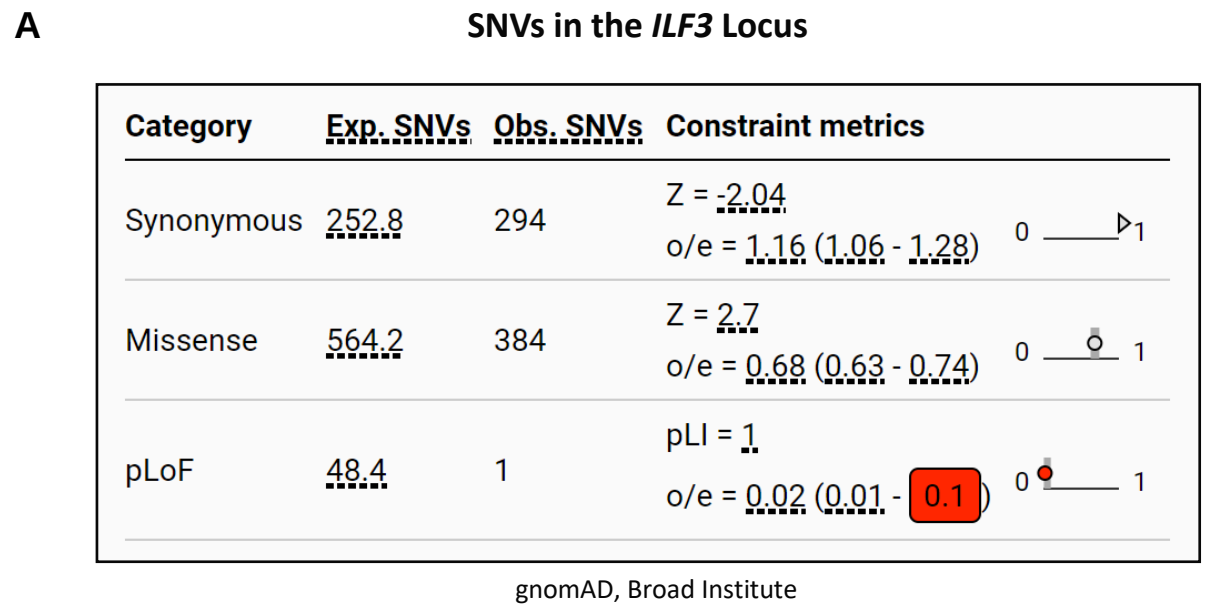

Figure 1. Lack of Loss of Function (LoF) Single Nucleotide Variants (SNVs) in the human *ILF3* locus suggest that ILF3 is essential. A. Single nucleotide variants present in the *ILF3* locus from data from gnomAD via the Broad Institute. pLoF (predicted loss of function).

Associations between ILF3 and other viral infections

As we have shown, myeloid DCs are capable of transiently downregulating *ILF3* in response to HIV-1-GFP (Ch.3 Fig. S1E,F). Others have also shown this effect on *ILF3* using the HIV-1-GFP+Vpx system (54). Interestingly, when MDDCs are infected with HIV-2-GFP, we see that *ILF3* expression trends towards lower expression compared to HIV-1-GFP + Vpx infection (Fig. 2A). This correlates with higher maturation responses as measured by *CD86, CD40,* and *TLR3* with HIV-2-GFP infection as compared to HIV-1-GFP + Vpx. This is noteworthy as we know from the literature that not only does HIV-2 encode the required accessory protein to disable SAMHD1, but its capsid has a unique association with host CypA and NONO, allowing for viral cDNA to escape the shielding of the capsid core to become available for intracellular detection by sensors like cGAS (54). In this context, we hypothesize that downregulation of ILF3 in response to viral infection may be closely tied to innate signaling in an effort to boost innate responses against a pathogen.

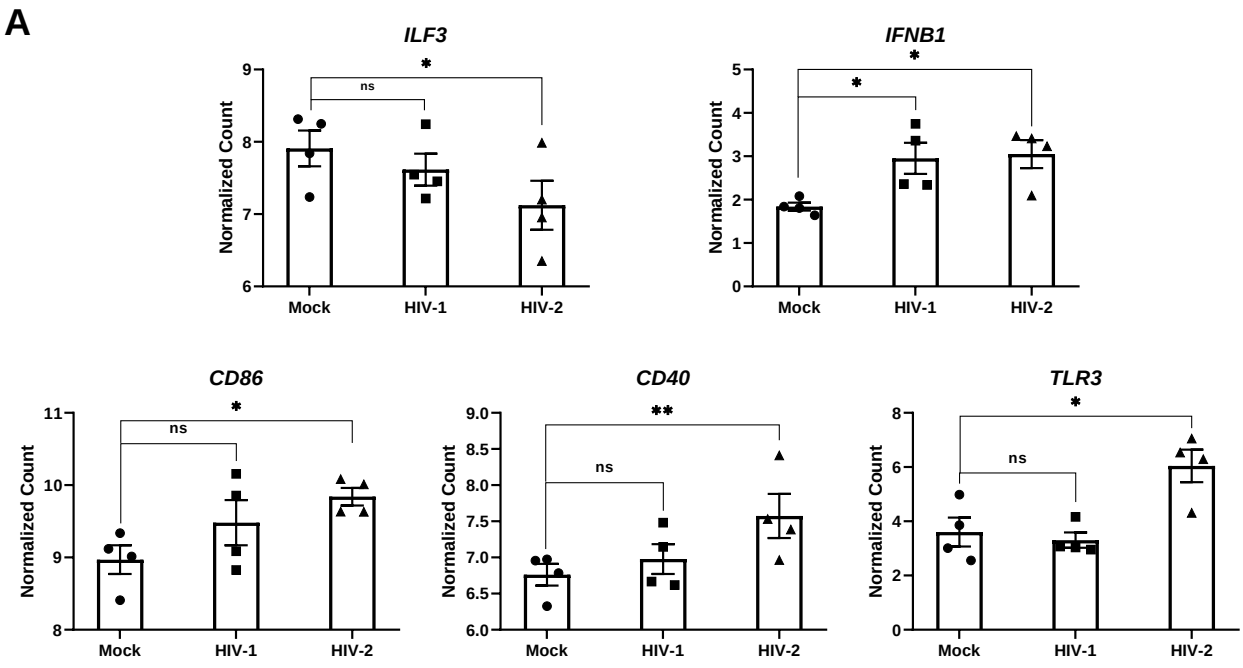

Figure 2. *ILF3* expression inversely associates with IFN during HIV-1-GFP and HIV-2-GFP infection of MDDCs, but only inversely correlates with DC maturation markers during HIV-2-GFP. A. Normalized count microarray data from GSE109554 for the indicated transcripts. Statistics were calculated using an ordinary one-way ANOVA, using Dunnett's test for multiple comparisons. HIV-1 and HIV-2 denote HIV-1-GFP and HIV-2-GFP, respectively.

Additionally, we wondered if this decreased expression of *ILF3* was true in myeloid DCs in the context of other viral infections that do not produce dsDNA species. Indeed, it has been reported that upon infection with a Chicago-1 strain of measles virus, a single-stranded, negative-sense, enveloped RNA virus, MDDCs downregulate *ILF3* over time (204). (Fig. 3A) Similar to our finding, this decrease occurs reciprocally to increases in IFN and maturation markers like *CD86* at these timepoints. Interestingly, it is known that measles virus can be detected via TLR2 (by detection of hemagglutinin) (205) or via TLR3/7 or RIG-I receptors for the detection of viral RNA species of the *Paramyxoviridae* family. Thus, this further supports future investigation of ILF3's role in sentinel myeloid APCs in the context of other viral pathogens.

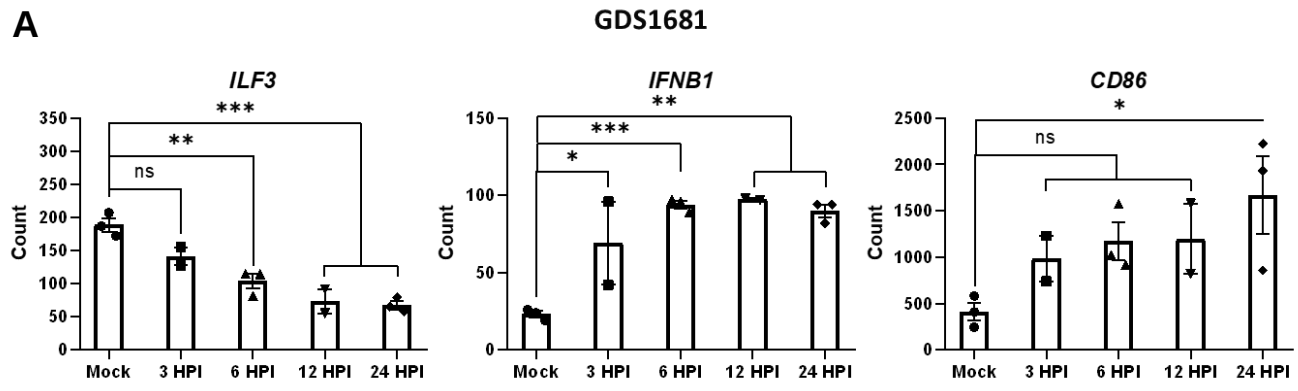

Figure 3. *ILF3* expression inversely associates with IFN and *CD86* expression during measles virus infection of MDDCs. A. Normalized count microarray data from GDS1681 for the indicated transcripts. MDDCs were infected with a Chicago-1 strain of measles virus over the indicated timepoints. Statistics were calculated using an ordinary one-way ANOVA, using Dunnett's test for multiple comparisons.

Clinical observations between ILF3 and autoimmunity

Apart from the evidence that exists to support ILF3-mediated regulation of innate immune responses and myeloid DC maturation, there is also evidence to suggest that ILF3 also may play a crucial role in regulating inflammatory diseases of autoimmune origin. For example, cutaneous lupus erythematosus (CLE) and psoriasis are both forms of autoimmune diseases involving hyperinflammation and immune cell infiltration. In the case of CLE which often occurs in systemic lupus erythematosus (SLE) (206), IFN signatures have been identified in the blood of CLE patients (207). Murine models of lupus-like disease involve type I IFN signaling downstream of TLR7, activated through the use of overexpression models or TLR7/8 small molecules (208, 209). The role of pDCs and TLR7 signaling in autoimmune diseases like systemic lupus erythematosus has been increasingly appreciated (210, 211). Our studies in Chapter 3 have already identified ILF3 as a negative regulator R848-induced TLR7/8 signaling in myeloid DCs. It is tempting to make a connection between ILF3's role in endosomal TLR signaling and lupus-like disease. Importantly, a randomized, double-blind, placebo-controlled phase II clinical trial of 305 adults with moderate-to-severe SLE using an anti-IFNAR monoclonal antibody (Anifrolumab) demonstrated a significant reduction in cutaneous lesions as measured by Cutaneous Lupus Erythematosus Disease Are and Severity Index (CLASI) (212). When examining skin biopsy data from patients with discoid lupus erythematosus (DLE), *ILF3* expression is negatively asssociated with diseased cutaneous lesions compared to healthy surrounding skin, inversely associating with disease state (213). Beyond type I IFNs, autoantibodies are a hallmark feature of lupus-like disease, indicating a critical B-cell immune component of disease (214). Interestingly, ILF3 and its binding partner ILF2, have been found to

be antigens targeted by autoantibodies in both murine and canine systemic autoimmune disease further implicating ILF3's role in autoimmunity (215, 216).

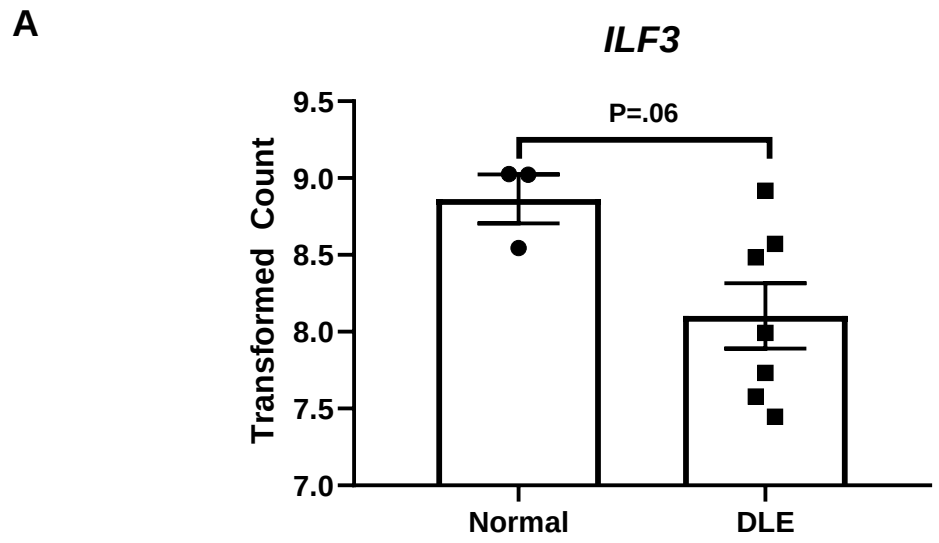

Figure 4. *ILF3* expression is inversely correlated with discoid lupus erythematosus skin biopsies versus normal skin tissue. A. Transformed count of microarray data from GDS4891 in skin biopsies from either discoid lupus erythematosus (DLE) lesions or surrounding normal skin. cDNA batches represented in this figure were prepared using "Ovation Kit." Statistics were calculated using an unpaired, two-tailed t-test.

Psoriasis is another chronic autoimmune disease whose main manifestation is cutaneous lesions. IFN signaling has also been associated with exacerbation of psoriatic disease in humans and murine models of disease (217-220). pDC infiltration is a common hallmark of psoriatic lesions marked by elevated expression of maturation markers CD80, CD83, and CD86 (221) in human patients. In AGR129 mice engrafted with human skin biopsies, a model of spontaneous psoriasis-like disease (222), IFNAR-blocking antibodies in mice engrafted with psoriatic lesional skin inhibited activation and proliferation of pathogenic T-cells, suggesting pDC-derived IFN is crucial to pathology of psoriatic disease (221). Like DLE skin biopsies, psoriatic biopsy lesions from the same study have significantly lower levels of *ILF3* compared to normal surrounding

tissue. One possibility is that ILF3 may play a similar inhibitory role in pDCs regulating type I IFN secretion, as cutaneous psoriatic lesions are enriched for infiltrating pDCs. Supporting this hypotehsis, murine *ILF3* levels in pDCs heterozygous for the pDC master transcription factor E2-2 are significantly higher than WT controls (213). This correlates with decreased levels of serum IFNα in CpG-stimulated E2-2 heterozygous mice compared to wildtype controls (223). In humans with a loss-of-function monoallelic mutation in TCF4, CpG-stimulated pDCs also secrete significantly less IFNα (223). Interestingly, our work in Chapter 3 (Ch.3 Fig. 6B) showed overexpression of NF110 induced expression of *CD300A* in a DZF-dependent manner and CD300a has been shown in pDCs to be inversely correlated with IFN in the context of TLR7 stimulation (166). Further work should consider and explore the potential role of ILF3 in other DC subsets such as pDCs as a negative regulator that can provide balance to inflammation promoted by positive regulators of IFN in pDCs via TLR7, such as BCAP (224).

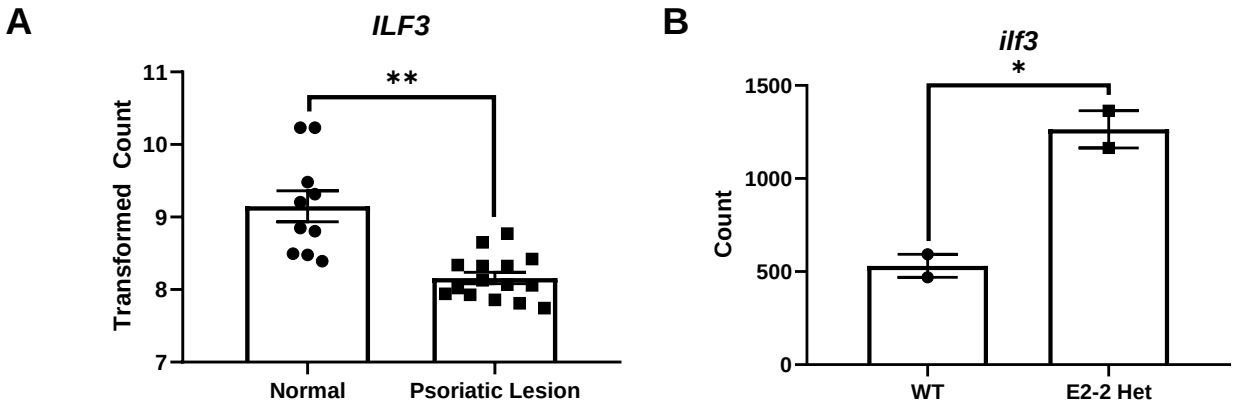

Figure 5. *ILF3* expression inversely correlated in psoriatic lesion skin biopsies versus healthy skin, and in mice partially deficient in pDCs. A. Transformed count of microarray data from GDS4891 in skin biopsies from either psoriatic lesions or surrounding normal skin. cDNA batches represented in this figure were prepared using "Affy Kit." Statistics were calculated using an unpaired, two-tailed t-test. **B.** Murine *ilf3* expression from GSD3519 in wildtype vs. E2-2 heterozygous 129/SvEv mice. Statistics were calculated using a paired, two-tailed t-test.

YM115: an NF110-specific inhibitor with implications for innate immunity

Given this evidence, one clinically relevant question that can be raised is if there are other targets aside from type I IFNs or IFNAR that can help suppress production of inflammatory IFNs and cytokines. Our work has found that monocytes minimally express either form of ILF3 (NF90 or NF110) but do so once differentiated into immature MDDCs. Interestingly, this mirrors another DZF-family member ZFR whose expression is absent in monocytes but is expressed in monocyte-derived macrophages (225). Given this unique innate immune cell specificity, we wondered if there was a therapeutic available that might specific target ILF3 to see if it could modulate innate immune responses related to DC maturation that could potentially influence autoimmune diseases pathogenesis. We came across a small molecule compound, YM155 (IC50=.54nM), which specifically targets the C-terminus NF110 isoform of *ILF3* (226). This molecule was originally used to inhibit Survivin (encoded by the gene *BIRC5*) expression, controlled by NF110 in the context of cancer (227). Interestingly, myeloid DCs do not express appreciable levels of Survivin allowing us to interrogate ILF3's function related to maturation. Treatment of MDDCs with either 5nM or 50nM YM155 during HIV-1-GFP infection demonstrated reduced levels of CD86, HIV-1-GFP integration events, and increased MDDC viability (Fig. 6A-C). We then asked if CD86 potentiation in ILF3-knockdown MDDCs would be impacted by treatment with YM155 at concentrations similar to where maturation was suppressed in HIV-1-GFP infection by YM155. Ideally, ILF3-depleted MDDCs should not have any significant impact on CD86 if YM155-treatment is specific to NF110. YM155 treatment of ILF3-knockdown DCs have minimal impact of CD86 potentiation compared to mock (Fig. 7A). This data could suggest that effects seen in MDDCs treated with YM155 with HIV-1-GFP are specific to the targeting of NF110. However, as these cells do not appreciably express *BIRC5* to

validate YM155's effectiveness as a positive control, it is important that further work validate these findings.

This data could suggest that a small molecule targeting NF110 could disrupt the transcriptional complex controlling innate immune responses and DC maturation in an alternative manner compared to targeting IFNα/β or IFNAR which are far more ubiquitously expressed. Further investigation is required into the role small molecules like YM155 that target ILF3 to more specifically fine-tuning innate immune responses against chronic viral pathogens or autoimmune interferonopathies.

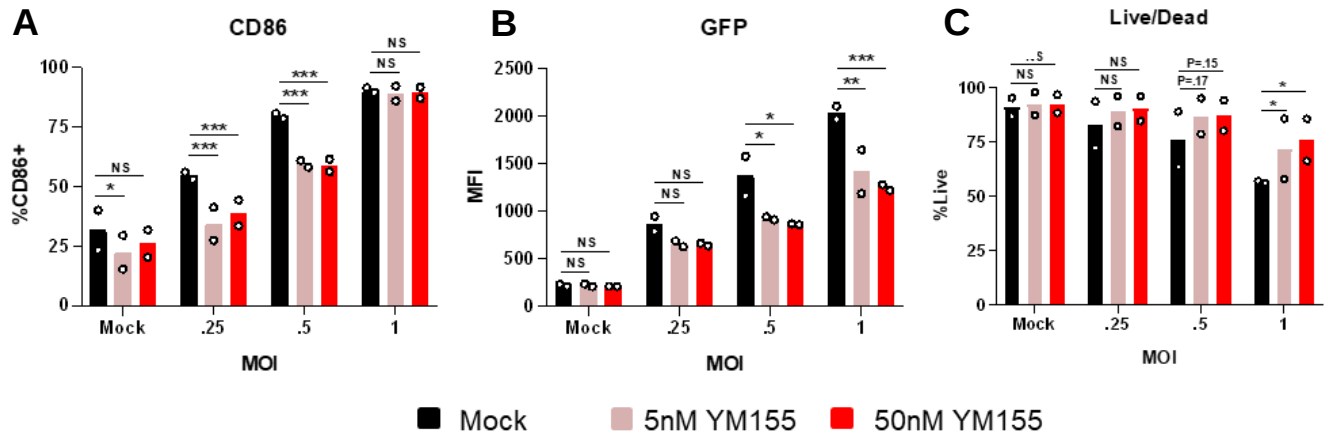

Figure 6. YM155 treatment of MDDCs suppresses DC maturation, GFP expression from HIV-1-GFP, and increases cell viability during HIV-1-GFP infection. A. CD86 measured via flow cytometry in MDDCs mock or HIV-1-GFP-infected over the indicated MOIs. Mock or infected MDDCs were either mock or YM155-treated at the indicated concentrations for 48 hours. n=2. Statistics were calculated using a mixed-effected model using Dunnett's test for multiple comparisons. **B.** GFP expression from HIV-1-GFP as described in A. **C.** %Live in Live/Dead stained MDDCs as described in A.

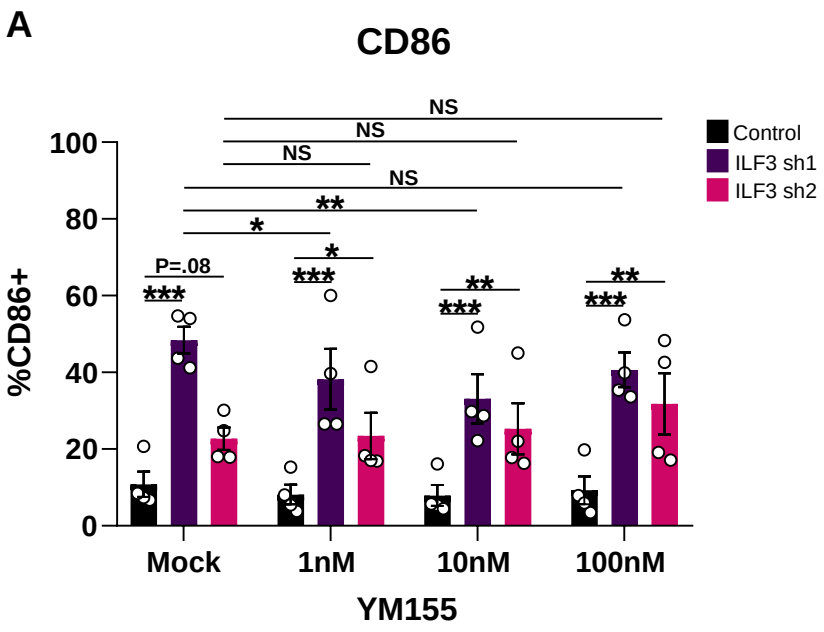

Figure 7. YM155 treatment of ILF3-knockdown MDDCs has minimal effect on ILF3-regulated baseline maturation. A. CD86 measured via flow cytometry in ILF3-knockdown or control MDDCs with mock or HIV-1-GFP-infection over the indicated MOIs. Mock or infected MDDCs were either mock or YM155-treated at the indicated concentrations for 48 hours. n=4. Statistics were calculated using a mixed-effected model using Dunnett's test for multiple comparisons.

Interferon epsilon is unmasked by ILF3 depletion and innate stimulation

While investigating the role of IFNβ in driving DC maturation in the context of ILF3 perturbation, we wondered if ILF3 more broadly affected Type I IFNs. Previous work by our group revealed that the major interferons produced in human monocyte-derived dendritic cells are IFNβ and IFNλ1 in response to stimuli such as LPS, poly I:C, and HIV-1-GFP infection (data not shown). However, we noted that a third type of interferon, *IFNE*, could be unmasked under the specific condition of depleting ILF3 through shRNA knockdown followed by a stimulation. During HIV-1-GFP infection of control MDDCs, *IFNB1* and *IFNL1* are the primary interferons expressed. In ILF3-knockdown MDDCs, we see induction of *IFNE*, a type I IFN, only upon infection with HIV-1-GFP (Fig. 8A). Interestingly, when we directly stimulate the cGAS/STING pathway with the STING agonist 2'3'-cGAMP, we also see the same induction of *IFNE* only

with 2’3’-cGAMP following ILF3 knockdown (Fig. 8B). This is surprising because the promoter of *IFNE* does not have regulatory elements for transcription factors such as IRF3 or NF-κB found at the promoter of other interferons such as *IFNB1* (228). This suggests regulation that could be independent of a pathogen eliciting activation of innate sensing pathways such as TLRs or cGAS. Hormones such as exogenous estrogen are able to induce expression of *IFNE* in cells of the human female reproductive tract (where *IFNE* is constitutively expressed) (228). This suggests that IFNε, while having lower affinity for IFNAR compared to IFNβ, serves as a constitutive first-line defense against a viral pathogen in key mucosal tissues (229). Given our findings in Chapter 3 suggesting a role for proteins involved in cholesterol homeostasis such as PPARγ, it is tempting link clinical trials preformed using PPARγ agonists to treat reproductive syndromes that involve altered levels of hormones such as progesterone and estrogen with potential regulation of *IFNE* (228). This is especially relevant given the fact that *ILF3* expression is highest in tissues of the reproductive system, according to RNA-seq data from the Genotype-Tissue Expression (GTEx) Project. Additional studies examining ILF3, PPARγ, and IFNε might reveal these associations more clearly.

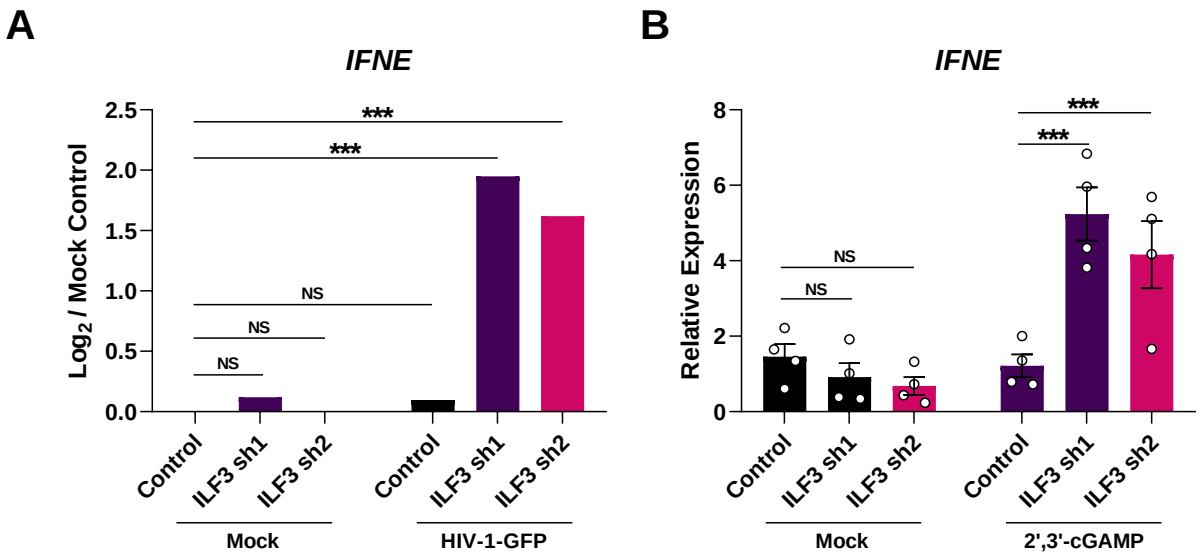

Figure 8. ILF3 knockdown unmasks *IFNE* expression during innate immune stimulation. A. Normalized $\log_2$ microarray expression data for *IFNE* in control or ILF3-knockdown MDDCs from n=1 donor in either mock or HIV-1-GFP infected (32 h) conditions. **B.** qPCR expression of *IFNE* in mock or 2'3'-cGAMP-treated (7h) control or ILF3-knockdown MDDCs. n=4 donors. Statistics performed using a mixed-effects model using Dunnett's test for multiple comparisons.

SUMMARY

This work adds a new regulatory transcriptional node to the human innate immune signaling circuitry, specifically within myeloid dendritic cells. In Chapter 3, we have shown that *ILF3*, which encodes both NF90 and NF110, is able to suppress baseline DC maturation. Restraint of DC maturation by ILF3 is further extended to innate immune stimuli using HIV-1-GFP, immunostimulatory DNA, 2'3' cGAMP, and R848. Effectors of antiviral immunity and DC maturation such as IFN and inflammatory cytokines like IL-6 are similarly suppressed by both isoforms. Through mutagenesis analysis of ILF3's domains, we show that nuclear localization (shown by truncation of the NLS) of both isoforms is required for inhibition of innate immune signaling and DC maturation. By truncating either the dual dsRNA-binding domains or the DZF, we found that this effect is not dependent on NF90 or NF110's capacity to bind RNA. Rather, ILF3's ability to temper innate immune signaling and DC maturation is contingent upon the DZF of the NF110 isoform. RNA-seq analysis of MDDCs overexpressing either wildtype or DZF-truncated NF110 reveal significant enrichment of DZF-dependent genes associated with cholesterol and lipid metabolism, such as *PPARG*. It is likely that perturbation of ILF3 impacts regulators of these pathways that ultimately impact innate immune signaling and subsequently the quality of DC maturation. In Chapter 4, we reveal that implications of ILF3 likely go beyond the pathways we tested and likely impact other non-infectious disease conditions such as autoimmune diseases. We have also shown that an anti-cancer drug could potentially be repurposed to control ILF3-mediated inflammation in a state of chronic infection or autoimmunity. Also, we have revealed ILF3 as a potential target to unmask non-pathogen responsive interferons such as *IFNE* to function similarly to other interferons such as *IFNB1*. It is

our hope that this work will spur additional research in these areas to inform multiple therapeutic designs that have broad-reaching implications in infectious disease and beyond.

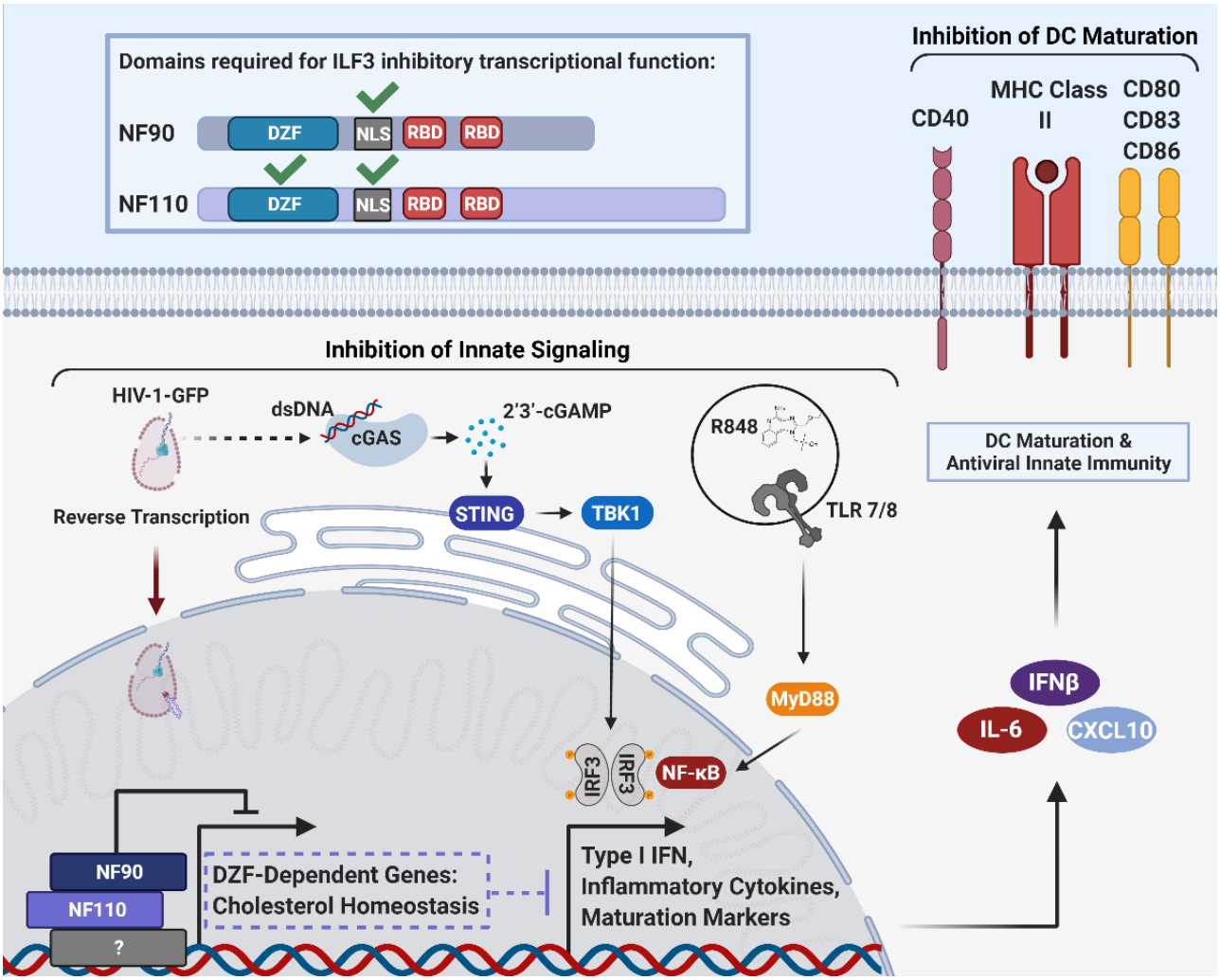

Figure 1. ILF3's role in human monocyte-derived dendritic cells in restraining innate immune signaling and DC maturation.

REFERENCES

1. Steinman, R. M. 1991. The dendritic cell system and its role in immunogenicity. *Annu Rev Immunol* 9: 271-296.
2. Banchereau, J., and R. M. Steinman. 1998. Dendritic cells and the control of immunity. *Nature* 392: 245-252.
3. Liu, K., G. D. Victora, T. A. Schwickert, P. Guermonprez, M. M. Meredith, K. Yao, F. F. Chu, G. J. Randolph, A. Y. Rudensky, and M. Nussenzweig. 2009. In vivo analysis of dendritic cell development and homeostasis. *Science* 324: 392-397.
4. Anderson, D. A., 3rd, C. A. Dutertre, F. Ginhoux, and K. M. Murphy. 2021. Genetic models of human and mouse dendritic cell development and function. *Nat Rev Immunol* 21: 101-115.
5. Tang-Huau, T. L., P. Gueguen, C. Goudot, M. Durand, M. Bohec, S. Baulande, B. Pasquier, S. Amigorena, and E. Segura. 2018. Human in vivo-generated monocyte-derived dendritic cells and macrophages cross-present antigens through a vacuolar pathway. *Nat Commun* 9: 2570.
6. Segura, E., M. Touzot, A. Bohineust, A. Cappuccio, G. Chiocchia, A. Hosmalin, M. Dalod, V. Soumelis, and S. Amigorena. 2013. Human inflammatory dendritic cells induce Th17 cell differentiation. *Immunity* 38: 336-348.
7. Sallusto, F., and A. Lanzavecchia. 1994. Efficient presentation of soluble antigen by cultured human dendritic cells is maintained by granulocyte/macrophage colony-stimulating factor plus interleukin 4 and downregulated by tumor necrosis factor alpha. *J Exp Med* 179: 1109-1118.
8. Sander, J., S. V. Schmidt, B. Cirovic, N. McGovern, O. Papantonopoulou, A. L. Hardt, A. C. Aschenbrenner, C. Kreer, T. Quast, A. M. Xu, L. M. Schmidleithner, H. Theis, L. D. Thi Huong, H. R. B. Sumatoh, M. A. R. Lauterbach, J. Schulte-Schrepping, P. Gunther, J. Xue, K. Bassler, T. Ulas, K. Klee, N. Katzmarski, S. Herresthal, W. Krebs, B. Martin, E. Latz, K. Handler, M. Kraut, W. Kolanus, M. Beyer, C. S. Falk, B. Wiegmann, S. Burgdorf, N. A. Melosh, E. W. Newell, F. Ginhoux, A. Schlitzer, and J. L. Schultze. 2017. Cellular Differentiation of Human Monocytes Is Regulated by Time-Dependent Interleukin-4 Signaling and the Transcriptional Regulator NCOR2. *Immunity* 47: 1051-1066 e1012.
9. Goudot, C., A. Coillard, A. C. Villani, P. Gueguen, A. Cros, S. Sarkizova, T. L. Tang-Huau, M. Bohec, S. Baulande, N. Hacohen, S. Amigorena, and E. Segura. 2017. Aryl

Hydrocarbon Receptor Controls Monocyte Differentiation into Dendritic Cells versus Macrophages. *Immunity* 47: 582-596.e586.

10. Villani, A. C., R. Satija, G. Reynolds, S. Sarkizova, K. Shekhar, J. Fletcher, M. Griesbeck, A. Butler, S. Zheng, S. Lazo, L. Jardine, D. Dixon, E. Stephenson, E. Nilsson, I. Grundberg, D. McDonald, A. Filby, W. Li, P. L. De Jager, O. Rozenblatt-Rosen, A. A. Lane, M. Haniffa, A. Regev, and N. Hacohen. 2017. Single-cell RNA-seq reveals new types of human blood dendritic cells, monocytes, and progenitors. *Science* 356.
11. Bakri, Y., S. Sarrazin, U. P. Mayer, S. Tillmanns, C. Nerlov, A. Boned, and M. H. Sieweke. 2005. Balance of MafB and PU.1 specifies alternative macrophage or dendritic cell fate. *Blood* 105: 2707-2716.
12. Guerriero, A., P. B. Langmuir, L. M. Spain, and E. W. Scott. 2000. PU.1 is required for myeloid-derived but not lymphoid-derived dendritic cells. *Blood* 95: 879-885.
13. Iwakoshi, N. N., M. Pypaert, and L. H. Glimcher. 2007. The transcription factor XBP-1 is essential for the development and survival of dendritic cells. *J Exp Med* 204: 2267-2275.
14. Ghosh, H. S., B. Cisse, A. Bunin, K. L. Lewis, and B. Reizis. 2010. Continuous expression of the transcription factor e2-2 maintains the cell fate of mature plasmacytoid dendritic cells. *Immunity* 33: 905-916.
15. Schotte, R., M. Nagasawa, K. Weijer, H. Spits, and B. Blom. 2004. The ETS transcription factor Spi-B is required for human plasmacytoid dendritic cell development. *J Exp Med* 200: 1503-1509.
16. Lee, J., Y. J. Zhou, W. Ma, W. Zhang, A. Aljoufi, T. Luh, K. Lucero, D. Liang, M. Thomsen, G. Bhagat, Y. Shen, and K. Liu. 2017. Lineage specification of human dendritic cells is marked by IRF8 expression in hematopoietic stem cells and multipotent progenitors. *Nature immunology* 18: 877-888.
17. Kurotaki, D., W. Kawase, H. Sasaki, J. Nakabayashi, A. Nishiyama, H. C. Morse, 3rd, K. Ozato, Y. Suzuki, and T. Tamura. 2019. Epigenetic control of early dendritic cell lineage specification by the transcription factor IRF8 in mice. *Blood* 133: 1803-1813.
18. Hildner, K., B. T. Edelson, W. E. Purtha, M. Diamond, H. Matsushita, M. Kohyama, B. Calderon, B. U. Schraml, E. R. Unanue, M. S. Diamond, R. D. Schreiber, T. L. Murphy, and K. M. Murphy. 2008. Batf3 deficiency reveals a critical role for CD8alpha+ dendritic cells in cytotoxic T cell immunity. *Science* 322: 1097-1100.
19. Klein, U., S. Casola, G. Cattoretti, Q. Shen, M. Lia, T. Mo, T. Ludwig, K. Rajewsky, and R. Dalla-Favera. 2006. Transcription factor IRF4 controls plasma cell differentiation and class-switch recombination. *Nature immunology* 7: 773-782.
20. Park, C. S., P. H. Lee, T. Yamada, A. Burns, Y. Shen, M. Puppi, and H. D. Lacorazza. 2012. Kruppel-like factor 4 (KLF4) promotes the survival of natural killer cells and maintains the number of conventional dendritic cells in the spleen. *J Leukoc Biol* 91: 739-750.
21. Tussiwand, R., B. Everts, G. E. Grajales-Reyes, N. M. Kretzer, A. Iwata, J. Bagaitkar, X. Wu, R. Wong, D. A. Anderson, T. L. Murphy, E. J. Pearce, and K. M. Murphy. 2015. Klf4 expression in conventional dendritic cells is required for T helper 2 cell responses. *Immunity* 42: 916-928.
22. Hacker, C., R. D. Kirsch, X. S. Ju, T. Hieronymus, T. C. Gust, C. Kuhl, T. Jorgas, S. M. Kurz, S. Rose-John, Y. Yokota, and M. Zenke. 2003. Transcriptional profiling identifies Id2 function in dendritic cell development. *Nature immunology* 4: 380-386.

23. Jackson, J. T., Y. Hu, R. Liu, F. Masson, A. D'Amico, S. Carotta, A. Xin, M. J. Camilleri, A. M. Mount, A. Kallies, L. Wu, G. K. Smyth, S. L. Nutt, and G. T. Belz. 2011. Id2 expression delineates differential checkpoints in the genetic program of CD8alpha+ and CD103+ dendritic cell lineages. *EMBO J* 30: 2690-2704.
24. Yanagihara, S., E. Komura, J. Nagafune, H. Watarai, and Y. Yamaguchi. 1998. EBI1/CCR7 is a new member of dendritic cell chemokine receptor that is up-regulated upon maturation. *Journal of immunology* 161: 3096-3102.
25. Orabona, C., U. Grohmann, M. L. Belladonna, F. Fallarino, C. Vacca, R. Bianchi, S. Bozza, C. Volpi, B. L. Salomon, M. C. Fioretti, L. Romani, and P. Puccetti. 2004. CD28 induces immunostimulatory signals in dendritic cells via CD80 and CD86. *Nature immunology* 5: 1134-1142.
26. Gautier, G., M. Humbert, F. Deauvieau, M. Scuiller, J. Hiscott, E. E. Bates, G. Trinchieri, C. Caux, and P. Garrone. 2005. A type I interferon autocrine-paracrine loop is involved in Toll-like receptor-induced interleukin-12p70 secretion by dendritic cells. *J Exp Med* 201: 1435-1446.
27. Zielinski, C. E., F. Mele, D. Aschenbrenner, D. Jarrossay, F. Ronchi, M. Gattorno, S. Monticelli, A. Lanzavecchia, and F. Sallusto. 2012. Pathogen-induced human TH17 cells produce IFN-gamma or IL-10 and are regulated by IL-1beta. *Nature* 484: 514-518.
28. Coombes, J. L., K. R. Siddiqui, C. V. Arancibia-Carcamo, J. Hall, C. M. Sun, Y. Belkaid, and F. Powrie. 2007. A functionally specialized population of mucosal CD103+ DCs induces Foxp3+ regulatory T cells via a TGF-beta and retinoic acid-dependent mechanism. *J Exp Med* 204: 1757-1764.
29. Hickey, F. B., C. F. Brereton, and K. H. Mills. 2008. Adenylate cycalse toxin of Bordetella pertussis inhibits TLR-induced IRF-1 and IRF-8 activation and IL-12 production and enhances IL-10 through MAPK activation in dendritic cells. *J Leukoc Biol* 84: 234-243.
30. McGuirk, P., C. McCann, and K. H. Mills. 2002. Pathogen-specific T regulatory 1 cells induced in the respiratory tract by a bacterial molecule that stimulates interleukin 10 production by dendritic cells: a novel strategy for evasion of protective T helper type 1 responses by Bordetella pertussis. *J Exp Med* 195: 221-231.
31. Jonuleit, H., E. Schmitt, G. Schuler, J. Knop, and A. H. Enk. 2000. Induction of interleukin 10-producing, nonproliferating CD4(+) T cells with regulatory properties by repetitive stimulation with allogeneic immature human dendritic cells. *J Exp Med* 192: 1213-1222.
32. Lugo-Villarino, G., R. Maldonado-Lopez, R. Possemato, C. Penaranda, and L. H. Glimcher. 2003. T-bet is required for optimal production of IFN-gamma and antigen-specific T cell activation by dendritic cells. *Proc Natl Acad Sci U S A* 100: 7749-7754.
33. Manel, N., B. Hogstad, Y. Wang, D. E. Levy, D. Unutmaz, and D. R. Littman. 2010. A cryptic sensor for HIV-1 activates antiviral innate immunity in dendritic cells. *Nature* 467: 214-217.
34. Johnson, J. S., S. Y. Lucas, L. M. Amon, S. Skelton, R. Nazitto, S. Carbonetti, D. N. Sather, D. R. Littman, and A. Aderem. 2018. Reshaping of the Dendritic Cell Chromatin Landscape and Interferon Pathways during HIV Infection. *Cell Host Microbe* 23: 366-381 e369.
35. Dissanayake, D., H. Hall, N. Berg-Brown, A. R. Elford, S. R. Hamilton, K. Murakami, L. S. Deluca, J. L. Gommerman, and P. S. Ohashi. 2011. Nuclear factor-kappaB1 controls the

functional maturation of dendritic cells and prevents the activation of autoreactive T cells. *Nat Med* 17: 1663-1667.

36. Dejean, A. S., D. R. Beisner, I. L. Ch'en, Y. M. Kerdiles, A. Babour, K. C. Arden, D. H. Castrillon, R. A. DePinho, and S. M. Hedrick. 2009. Transcription factor Foxo3 controls the magnitude of T cell immune responses by modulating the function of dendritic cells. *Nature immunology* 10: 504-513.

37. Kato, H., O. Takeuchi, S. Sato, M. Yoneyama, M. Yamamoto, K. Matsui, S. Uematsu, A. Jung, T. Kawai, K. J. Ishii, O. Yamaguchi, K. Otsu, T. Tsujimura, C. S. Koh, C. Reis e Sousa, Y. Matsuura, T. Fujita, and S. Akira. 2006. Differential roles of MDA5 and RIG-I helicases in the recognition of RNA viruses. *Nature* 441: 101-105.

38. Seth, R. B., L. Sun, C. K. Ea, and Z. J. Chen. 2005. Identification and characterization of MAVS, a mitochondrial antiviral signaling protein that activates NF-kappaB and IRF 3. *Cell* 122: 669-682.

39. Jonsson, K. L., A. Laustsen, C. Krapp, K. A. Skipper, K. Thavachelvam, D. Hotter, J. H. Egedal, M. Kjolby, P. Mohammadi, T. Prabakaran, L. K. Sorensen, C. Sun, S. B. Jensen, C. K. Holm, R. J. Lebbink, M. Johannsen, M. Nyegaard, J. G. Mikkelsen, F. Kirchhoff, S. R. Paludan, and M. R. Jakobsen. 2017. IFI16 is required for DNA sensing in human macrophages by promoting production and function of cGAMP. *Nat Commun* 8: 14391.

40. Ishikawa, H., and G. N. Barber. 2008. STING is an endoplasmic reticulum adaptor that facilitates innate immune signalling. *Nature* 455: 674-678.

41. Ishikawa, H., Z. Ma, and G. N. Barber. 2009. STING regulates intracellular DNA-mediated, type I interferon-dependent innate immunity. *Nature* 461: 788-792.

42. Sun, L., J. Wu, F. Du, X. Chen, and Z. J. Chen. 2013. Cyclic GMP-AMP synthase is a cytosolic DNA sensor that activates the type I interferon pathway. *Science* 339: 786-791.

43. Qureshi, S. A., M. Salditt-Georgieff, and J. E. Darnell, Jr. 1995. Tyrosine-phosphorylated Stat1 and Stat2 plus a 48-kDa protein all contact DNA in forming interferon-stimulated-gene factor 3. *Proc Natl Acad Sci U S A* 92: 3829-3833.

44. West, A. P., G. S. Shadel, and S. Ghosh. 2011. Mitochondria in innate immune responses. *Nat Rev Immunol* 11: 389-402.

45. Chen, Q., L. Sun, and Z. J. Chen. 2016. Regulation and function of the cGAS-STING pathway of cytosolic DNA sensing. *Nature immunology* 17: 1142-1149.

46. Prevention, C. f. D. C. a. 2018. HIV Surveillance Report Vol. 81.

47. International, A. S. S. W. G. o. H. I. V. C., S. G. Deeks, B. Autran, B. Berkhout, M. Benkirane, S. Cairns, N. Chomont, T. W. Chun, M. Churchill, M. Di Mascio, C. Katlama, A. Lafeuillade, A. Landay, M. Lederman, S. R. Lewin, F. Maldarelli, D. Margolis, M. Markowitz, J. Martinez-Picado, J. I. Mullins, J. Mellors, S. Moreno, U. O'Doherty, S. Palmer, M. C. Penicaud, M. Peterlin, G. Poli, J. P. Routy, C. Rouzioux, G. Silvestri, M. Stevenson, A. Telenti, C. Van Lint, E. Verdin, A. Woolfrey, J. Zaia, and F. Barre-Sinoussi. 2012. Towards an HIV cure: a global scientific strategy. *Nat Rev Immunol* 12: 607-614.

48. Lusic, M., and R. F. Siliciano. 2017. Nuclear landscape of HIV-1 infection and integration. *Nat Rev Microbiol* 15: 69-82.

49. Luban, J. 2012. Innate immune sensing of HIV-1 by dendritic cells. *Cell Host Microbe* 12: 408-418.

50. Calantone, N., F. Wu, Z. Klase, C. Deleage, M. Perkins, K. Matsuda, E. A. Thompson, A. M. Ortiz, C. L. Vinton, I. Ourmanov, K. Lore, D. C. Douek, J. D. Estes, V. M. Hirsch, and J. M. Brenchley. 2014. Tissue myeloid cells in SIV-infected primates acquire viral DNA through phagocytosis of infected T cells. *Immunity* 41: 493-502.
51. Sandler, N. G., S. E. Bosinger, J. D. Estes, R. T. Zhu, G. K. Tharp, E. Boritz, D. Levin, S. Wijeyesinghe, K. N. Makamdop, G. Q. del Prete, B. J. Hill, J. K. Timmer, E. Reiss, G. Yarden, S. Darko, E. Contijoch, J. P. Todd, G. Silvestri, M. Nason, R. B. Norgren, Jr., B. F. Keele, S. Rao, J. A. Langer, J. D. Lifson, G. Schreiber, and D. C. Douek. 2014. Type I interferon responses in rhesus macaques prevent SIV infection and slow disease progression. *Nature* 511: 601-605.
52. Hardy, G. A., S. Sieg, B. Rodriguez, D. Anthony, R. Asaad, W. Jiang, J. Mudd, T. Schacker, N. T. Funderburg, H. A. Pilch-Cooper, R. Debernardo, R. L. Rabin, M. M. Lederman, and C. V. Harding. 2013. Interferon-alpha is the primary plasma type-I IFN in HIV-1 infection and correlates with immune activation and disease markers. *PLoS One* 8: e56527.
53. Gray, E. E., P. M. Treuting, J. J. Woodward, and D. B. Stetson. 2015. Cutting Edge: cGAS Is Required for Lethal Autoimmune Disease in the Trex1-Deficient Mouse Model of Aicardi-Goutieres Syndrome. *Journal of immunology* 195: 1939-1943.
54. Lahaye, X., M. Gentili, A. Silvin, C. Conrad, L. Picard, M. Jouve, E. Zueva, M. Maurin, F. Nadalin, G. J. Knott, B. Zhao, F. Du, M. Rio, J. Amiel, A. H. Fox, P. Li, L. Etienne, C. S. Bond, L. Colleaux, and N. Manel. 2018. NONO Detects the Nuclear HIV Capsid to Promote cGAS-Mediated Innate Immune Activation. *Cell* 175: 488-501 e422.
55. Braaten, D., and J. Luban. 2001. Cyclophilin A regulates HIV-1 infectivity, as demonstrated by gene targeting in human T cells. *EMBO J* 20: 1300-1309.
56. Braaten, D., E. K. Franke, and J. Luban. 1996. Cyclophilin A is required for the replication of group M human immunodeficiency virus type 1 (HIV-1) and simian immunodeficiency virus SIV(CPZ)GAB but not group O HIV-1 or other primate immunodeficiency viruses. *J Virol* 70: 4220-4227.
57. Yoo, S., D. G. Myszka, C. Yeh, M. McMurray, C. P. Hill, and W. I. Sundquist. 1997. Molecular recognition in the HIV-1 capsid/cyclophilin A complex. *J Mol Biol* 269: 780-795.
58. Lahaye, X., T. Satoh, M. Gentili, S. Cerboni, C. Conrad, I. Hurbain, A. El Marjou, C. Lacabaratz, J. D. Lelievre, and N. Manel. 2013. The capsids of HIV-1 and HIV-2 determine immune detection of the viral cDNA by the innate sensor cGAS in dendritic cells. *Immunity* 39: 1132-1142.
59. Christensen, D. E., B. K. Ganser-Pornillos, J. S. Johnson, O. Pornillos, and W. I. Sundquist. 2020. Reconstitution and visualization of HIV-1 capsid-dependent replication and integration in vitro. *Science* 370.
60. Shibata, R., H. Sakai, M. Kawamura, K. Tokunaga, and A. Adachi. 1995. Early replication block of human immunodeficiency virus type 1 in monkey cells. *J Gen Virol* 76 (Pt 11): 2723-2730.
61. Hofmann, W., D. Schubert, J. LaBonte, L. Munson, S. Gibson, J. Scammell, P. Ferrigno, and J. Sodroski. 1999. Species-specific, postentry barriers to primate immunodeficiency virus infection. *J Virol* 73: 10020-10028.

62. Sheehy, A. M., N. C. Gaddis, J. D. Choi, and M. H. Malim. 2002. Isolation of a human gene that inhibits HIV-1 infection and is suppressed by the viral Vif protein. *Nature* 418: 646-650.
63. Liu, Z., Q. Pan, S. Ding, J. Qian, F. Xu, J. Zhou, S. Cen, F. Guo, and C. Liang. 2013. The interferon-inducible MxB protein inhibits HIV-1 infection. *Cell Host Microbe* 14: 398-410.
64. Li, M., E. Kao, X. Gao, H. Sandig, K. Limmer, M. Pavon-Eternod, T. E. Jones, S. Landry, T. Pan, M. D. Weitzman, and M. David. 2012. Codon-usage-based inhibition of HIV protein synthesis by human schlafen 11. *Nature* 491: 125-128.
65. Neil, S. J., T. Zang, and P. D. Bieniasz. 2008. Tetherin inhibits retrovirus release and is antagonized by HIV-1 Vpu. *Nature* 451: 425-430.
66. Neil, S. J., V. Sandrin, W. I. Sundquist, and P. D. Bieniasz. 2007. An interferon-alpha-induced tethering mechanism inhibits HIV-1 and Ebola virus particle release but is counteracted by the HIV-1 Vpu protein. *Cell Host Microbe* 2: 193-203.
67. Lu, J., Q. Pan, L. Rong, W. He, S. L. Liu, and C. Liang. 2011. The IFITM proteins inhibit HIV-1 infection. *J Virol* 85: 2126-2137.
68. Marin, M., K. M. Rose, S. L. Kozak, and D. Kabat. 2003. HIV-1 Vif protein binds the editing enzyme APOBEC3G and induces its degradation. *Nat Med* 9: 1398-1403.
69. Sheehy, A. M., N. C. Gaddis, and M. H. Malim. 2003. The antiretroviral enzyme APOBEC3G is degraded by the proteasome in response to HIV-1 Vif. *Nat Med* 9: 1404-1407.
70. Laguette, N., B. Sobhian, N. Casartelli, M. Ringeard, C. Chable-Bessia, E. Segeral, A. Yatim, S. Emiliani, O. Schwartz, and M. Benkirane. 2011. SAMHD1 is the dendritic- and myeloid-cell-specific HIV-1 restriction factor counteracted by Vpx. *Nature* 474: 654-657.
71. Goujon, C., L. Riviere, L. Jarrosson-Wuilleme, J. Bernaud, D. Rigal, J. L. Darlix, and A. Cimarelli. 2007. SIVSM/HIV-2 Vpx proteins promote retroviral escape from a proteasome-dependent restriction pathway present in human dendritic cells. *Retrovirology* 4: 2.
72. Goujon, C., V. Arfi, T. Pertel, J. Luban, J. Lienard, D. Rigal, J. L. Darlix, and A. Cimarelli. 2008. Characterization of simian immunodeficiency virus SIVSM/human immunodeficiency virus type 2 Vpx function in human myeloid cells. *J Virol* 82: 12335-12345.
73. Reiser, J., G. Harmison, S. Kluepfel-Stahl, R. O. Brady, S. Karlsson, and M. Schubert. 1996. Transduction of nondividing cells using pseudotyped defective high-titer HIV type 1 particles. *Proc Natl Acad Sci U S A* 93: 15266-15271.
74. Unutmaz, D., V. N. KewalRamani, S. Marmon, and D. R. Littman. 1999. Cytokine signals are sufficient for HIV-1 infection of resting human T lymphocytes. *J Exp Med* 189: 1735-1746.
75. Hofmann, H., E. C. Logue, N. Bloch, W. Daddacha, S. B. Polsky, M. L. Schultz, B. Kim, and N. R. Landau. 2012. The Vpx lentiviral accessory protein targets SAMHD1 for degradation in the nucleus. *J Virol* 86: 12552-12560.
76. Marcoulatos, P., E. Avgerinos, D. V. Tsantzalos, and N. C. Vamvakopoulos. 1998. Mapping interleukin enhancer binding factor 3 gene (ILF3) to human chromosome 19 (19q11-qter and 19p11-p13.1) by polymerase chain reaction amplification of human-rodent somatic cell hybrid DNA templates. *J Interferon Cytokine Res* 18: 351-355.

77. Duchange, N., J. Pidoux, E. Camus, and D. Sauvaget. 2000. Alternative splicing in the human interleukin enhancer binding factor 3 (ILF3) gene. *Gene* 261: 345-353.
78. Saunders, L. R., V. Jurecic, and G. N. Barber. 2001. The 90- and 110-kDa human NFAR proteins are translated from two differentially spliced mRNAs encoded on chromosome 19p13. *Genomics* 71: 256-259.
79. Shiina, N., and K. Nakayama. 2014. RNA granule assembly and disassembly modulated by nuclear factor associated with double-stranded RNA 2 and nuclear factor 45. *J Biol Chem* 289: 21163-21180.
80. Shim, J., H. Lim, R. Y. J, and M. Karin. 2002. Nuclear export of NF90 is required for interleukin-2 mRNA stabilization. *Mol Cell* 10: 1331-1344.
81. Wolkowicz, U. M., and A. G. Cook. 2012. NF45 dimerizes with NF90, Zfr and SPNR via a conserved domain that has a nucleotidyltransferase fold. *Nucleic Acids Res* 40: 9356-9368.
82. Reichman, T. W., L. C. Muniz, and M. B. Mathews. 2002. The RNA binding protein nuclear factor 90 functions as both a positive and negative regulator of gene expression in mammalian cells. *Mol Cell Biol* 22: 343-356.
83. Schmidt, T., P. Knick, H. Lilie, S. Friedrich, R. P. Golbik, and S. E. Behrens. 2016. Coordinated Action of Two Double-Stranded RNA Binding Motifs and an RGG Motif Enables Nuclear Factor 90 To Flexibly Target Different RNA Substrates. *Biochemistry* 55: 948-959.
84. Ting, N. S., P. N. Kao, D. W. Chan, L. G. Lintott, and S. P. Lees-Miller. 1998. DNA-dependent protein kinase interacts with antigen receptor response element binding proteins NF90 and NF45. *J Biol Chem* 273: 2136-2145.
85. Aoki, Y., G. Zhao, D. Qiu, L. Shi, and P. N. Kao. 1998. CsA-sensitive purine-box transcriptional regulator in bronchial epithelial cells contains NF45, NF90, and Ku. *Am J Physiol* 275: L1164-1172.
86. Kao, P. N., L. Chen, G. Brock, J. Ng, J. Kenny, A. J. Smith, and B. Corthesy. 1994. Cloning and expression of cyclosporin A- and FK506-sensitive nuclear factor of activated T-cells: NF45 and NF90. *J Biol Chem* 269: 20691-20699.
87. Kiesler, P., P. A. Haynes, L. Shi, P. N. Kao, V. H. Wysocki, and D. Vercelli. 2010. NF45 and NF90 regulate HS4-dependent interleukin-13 transcription in T cells. *J Biol Chem* 285: 8256-8267.
88. Wu, T. H., L. Shi, A. W. Lowe, M. R. Nicolls, and P. N. Kao. 2019. Inducible expression of immediate early genes is regulated through dynamic chromatin association by NF45/ILF2 and NF90/NF110/ILF3. *PLoS One* 14: e0216042.
89. Sakamoto, S., K. Morisawa, K. Ota, J. Nie, and T. Taniguchi. 1999. A binding protein to the DNase I hypersensitive site II in HLA-DR alpha gene was identified as NF90. *Biochemistry* 38: 3355-3361.
90. Shamanna, R. A., M. Hoque, A. Lewis-Antes, E. I. Azzam, D. Lagunoff, T. Pe'ery, and M. B. Mathews. 2011. The NF90/NF45 complex participates in DNA break repair via nonhomologous end joining. *Mol Cell Biol* 31: 4832-4843.
91. Satoh, M., V. M. Shaheen, P. N. Kao, T. Okano, M. Shaw, H. Yoshida, H. B. Richards, and W. H. Reeves. 1999. Autoantibodies define a family of proteins with conserved double-

stranded RNA-binding domains as well as DNA binding activity. *J Biol Chem* 274: 34598-34604.

92. Gillis, P., and J. S. Malter. 1991. The adenosine-uridine binding factor recognizes the AU-rich elements of cytokine, lymphokine, and oncogene mRNAs. *J Biol Chem* 266: 3172-3177.

93. Corso, C., L. Pisapia, A. Citro, V. Cicatiello, P. Barba, L. Cigliano, P. Abrescia, A. Maffei, G. Manco, and G. Del Pozzo. 2011. EBP1 and DRBP76/NF90 binding proteins are included in the major histocompatibility complex class II RNA operon. *Nucleic Acids Res* 39: 7263-7275.

94. Parrott, A. M., and M. B. Mathews. 2007. Novel rapidly evolving hominid RNAs bind nuclear factor 90 and display tissue-restricted distribution. *Nucleic Acids Res* 35: 6249-6258.

95. Jiang, Z., C. M. Slater, Y. Zhou, K. Devarajan, K. J. Ruth, Y. Li, K. Q. Cai, M. Daly, and X. Chen. 2017. LincIN, a novel NF90-binding long non-coding RNA, is overexpressed in advanced breast tumors and involved in metastasis. *Breast Cancer Res* 19: 62.

96. Huang, W., J. Liu, J. Yan, Z. Huang, X. Zhang, Y. Mao, and X. Huang. 2020. LncRNA LINC00470 promotes proliferation through association with NF45/NF90 complex in hepatocellular carcinoma. *Hum Cell* 33: 131-139.

97. Zhang, H., Y. Liu, L. Yan, M. Zhang, X. Yu, W. Du, S. Wang, Q. Li, H. Chen, Y. Zhang, H. Sun, Z. Tang, and D. Zhu. 2018. Increased levels of the long noncoding RNA, HOXA-AS3, promote proliferation of A549 cells. *Cell Death Dis* 9: 707.

98. Zhang, Y., J. Sun, Y. Qi, Y. Wang, Y. Ding, K. Wang, Q. Zhou, J. Wang, F. Ma, J. Zhang, and B. Guo. 2020. Long non-coding RNA TPT1-AS1 promotes angiogenesis and metastasis of colorectal cancer through TPT1-AS1/NF90/VEGFA signaling pathway. *Aging (Albany NY)* 12: 6191-6205.

99. Sur, S., H. Nakanishi, R. Steele, D. Zhang, M. A. Varvares, and R. B. Ray. 2020. Long non-coding RNA ELDR enhances oral cancer growth by promoting ILF3-cyclin E1 signaling. *EMBO Rep*: e51042.

100. Todaka, H., T. Higuchi, K. Yagyu, Y. Sugiyama, F. Yamaguchi, K. Morisawa, M. Ono, A. Fukushima, M. Tsuda, T. Taniguchi, and S. Sakamoto. 2015. Overexpression of NF90-NF45 Represses Myogenic MicroRNA Biogenesis, Resulting in Development of Skeletal Muscle Atrophy and Centronuclear Muscle Fibers. *Mol Cell Biol* 35: 2295-2308.

101. Higuchi, T., H. Todaka, Y. Sugiyama, M. Ono, N. Tamaki, E. Hatano, Y. Takezaki, K. Hanazaki, T. Miwa, S. Lai, K. Morisawa, M. Tsuda, T. Taniguchi, and S. Sakamoto. 2016. Suppression of MicroRNA-7 (miR-7) Biogenesis by Nuclear Factor 90-Nuclear Factor 45 Complex (NF90-NF45) Controls Cell Proliferation in Hepatocellular Carcinoma. *J Biol Chem* 291: 21074-21084.

102. Higuchi, T., K. Morisawa, H. Todaka, S. Lai, E. Chi, K. Matsukawa, Y. Sugiyama, and S. Sakamoto. 2018. A negative feedback loop between nuclear factor 90 (NF90) and an anti-oncogenic microRNA, miR-7. *Biochem Biophys Res Commun* 503: 1819-1824.

103. Zhou, Q., Y. Zhu, X. Wei, J. Zhou, L. Chang, H. Sui, Y. Han, D. Piao, R. Sha, and Y. Bai. 2016. MiR-590-5p inhibits colorectal cancer angiogenesis and metastasis by regulating nuclear factor 90/vascular endothelial growth factor A axis. *Cell Death Dis* 7: e2413.

104. Lin, J., Z. Chen, S. Wu, W. Huang, F. Chen, and Z. Huang. 2019. An NF90/long noncoding RNA-LET/miR-548k feedback amplification loop controls esophageal squamous cell carcinoma progression. *J Cancer* 10: 5139-5152.
105. Sakamoto, S., K. Aoki, T. Higuchi, H. Todaka, K. Morisawa, N. Tamaki, E. Hatano, A. Fukushima, T. Taniguchi, and Y. Agata. 2009. The NF90-NF45 complex functions as a negative regulator in the microRNA processing pathway. *Mol Cell Biol* 29: 3754-3769.
106. Li, X., C. X. Liu, W. Xue, Y. Zhang, S. Jiang, Q. F. Yin, J. Wei, R. W. Yao, L. Yang, and L. L. Chen. 2017. Coordinated circRNA Biogenesis and Function with NF90/NF110 in Viral Infection. *Mol Cell* 67: 214-227.e217.
107. Liao, H. J., R. Kobayashi, and M. B. Mathews. 1998. Activities of adenovirus virus-associated RNAs: purification and characterization of RNA binding proteins. *Proc Natl Acad Sci U S A* 95: 8514-8519.
108. Shin, H. J., S. S. Kim, Y. H. Cho, S. G. Lee, and H. M. Rho. 2002. Host cell proteins binding to the encapsidation signal epsilon in hepatitis B virus RNA. *Arch Virol* 147: 471-491.
109. Li, Y., T. Masaki, T. Shimakami, and S. M. Lemon. 2014. hnRNP L and NF90 interact with hepatitis C virus 5'-terminal untranslated RNA and promote efficient replication. *J Virol* 88: 7199-7209.
110. Wen, X., X. Huang, B. W. Mok, Y. Chen, M. Zheng, S. Y. Lau, P. Wang, W. Song, D. Y. Jin, K. Y. Yuen, and H. Chen. 2014. NF90 exerts antiviral activity through regulation of PKR phosphorylation and stress granules in infected cells. *Journal of immunology* 192: 3753-3764.
111. Li, T., X. Li, W. Zhu, H. Wang, L. Mei, S. Wu, X. Lin, and X. Han. 2016. NF90 is a novel influenza A virus NS1-interacting protein that antagonizes the inhibitory role of NS1 on PKR phosphorylation. *FEBS Lett* 590: 2797-2810.
112. Wang, P., W. Song, B. W. Mok, P. Zhao, K. Qin, A. Lai, G. J. Smith, J. Zhang, T. Lin, Y. Guan, and H. Chen. 2009. Nuclear factor 90 negatively regulates influenza virus replication by interacting with viral nucleoprotein. *J Virol* 83: 7850-7861.
113. Gomila, R. C., G. W. Martin, and L. Gehrke. 2011. NF90 binds the dengue virus RNA 3' terminus and is a positive regulator of dengue virus replication. *PLoS One* 6: e16687.
114. Shabman, R. S., D. W. Leung, J. Johnson, N. Glennon, E. E. Gulcicek, K. L. Stone, L. Leung, L. Hensley, G. K. Amarasinghe, and C. F. Basler. 2011. DRBP76 associates with Ebola virus VP35 and suppresses viral polymerase function. *The Journal of infectious diseases* 204 Suppl 3: S911-918.
115. Patzina, C., C. H. Botting, A. Garcia-Sastre, R. E. Randall, and B. G. Hale. 2017. Human interactome of the influenza B virus NS1 protein. *J Gen Virol* 98: 2267-2273.
116. Li, Y., and M. Belshan. 2016. NF45 and NF90 Bind HIV-1 RNA and Modulate HIV Gene Expression. *Viruses* 8.
117. Krasnoselskaya-Riz, I., A. Spruill, Y. W. Chen, D. Schuster, T. Teslovich, C. Baker, A. Kumar, and D. A. Stephan. 2002. Nuclear factor 90 mediates activation of the cellular antiviral expression cascade. *AIDS research and human retroviruses* 18: 591-604.
118. Agbottah, E. T., C. Traviss, J. McArdle, S. Karki, G. C. St Laurent, 3rd, and A. Kumar. 2007. Nuclear Factor 90(NF90) targeted to TAR RNA inhibits transcriptional activation of HIV-1. *Retrovirology* 4: 41.

119. Urcuqui-Inchima, S., C. Patino, X. Zapata, M. P. Garcia, J. Arteaga, C. Chamot, A. Kumar, and D. Hernandez-Verdun. 2011. Production of HIV particles is regulated by altering sub-cellular localization and dynamics of Rev induced by double-strand RNA binding protein. *PLoS One* 6: e16686.
120. Doyle, T., C. Goujon, and M. H. Malim. 2015. HIV-1 and interferons: who's interfering with whom? *Nat Rev Microbiol* 13: 403-413.
121. Shapira, S. D., I. Gat-Viks, B. O. Shum, A. Dricot, M. M. de Grace, L. Wu, P. B. Gupta, T. Hao, S. J. Silver, D. E. Root, D. E. Hill, A. Regev, and N. Hacohen. 2009. A physical and regulatory map of host-influenza interactions reveals pathways in H1N1 infection. *Cell* 139: 1255-1267.
122. Pfeifer, I., R. Elsby, M. Fernandez, P. A. Faria, D. R. Nussenzveig, I. S. Lossos, B. M. Fontoura, W. D. Martin, and G. N. Barber. 2008. NFAR-1 and -2 modulate translation and are required for efficient host defense. *Proc Natl Acad Sci U S A* 105: 4173-4178.
123. Watson, S. F., N. Bellora, and S. Macias. 2020. ILF3 contributes to the establishment of the antiviral type I interferon program. *Nucleic Acids Res* 48: 116-129.
124. Mangeot, P. E., K. Duperrier, D. Negre, B. Boson, D. Rigal, F. L. Cosset, and J. L. Darlix. 2002. High levels of transduction of human dendritic cells with optimized SIV vectors. *Mol Ther* 5: 283-290.
125. Sanjana, N. E., O. Shalem, and F. Zhang. 2014. Improved vectors and genome-wide libraries for CRISPR screening. *Nat Methods* 11: 783-784.
126. Johnson, J. S., N. De Veaux, A. W. Rives, X. Lahaye, S. Y. Lucas, B. P. Perot, M. Luka, V. Garcia-Paredes, L. M. Amon, A. Watters, G. Abdessalem, A. Aderem, N. Manel, D. R. Littman, R. Bonneau, and M. M. Menager. 2020. A Comprehensive Map of the Monocyte-Derived Dendritic Cell Transcriptional Network Engaged upon Innate Sensing of HIV. *Cell Rep* 30: 914-931 e919.
127. Iwasaki, A., and R. Medzhitov. 2015. Control of adaptive immunity by the innate immune system. *Nature immunology* 16: 343-353.
128. Banchereau, J., and V. Pascual. 2006. Type I interferon in systemic lupus erythematosus and other autoimmune diseases. *Immunity* 25: 383-392.
129. Fernandez, S., S. Tanaskovic, K. Helbig, R. Rajasuriar, M. Kramski, J. M. Murray, M. Beard, D. Purcell, S. R. Lewin, P. Price, and M. A. French. 2011. CD4+ T-cell deficiency in HIV patients responding to antiretroviral therapy is associated with increased expression of interferon-stimulated genes in CD4+ T cells. *The Journal of infectious diseases* 204: 1927-1935.
130. Belz, G. T., and S. L. Nutt. 2012. Transcriptional programming of the dendritic cell network. *Nat Rev Immunol* 12: 101-113.
131. Shi, L., W. R. Godfrey, J. Lin, G. Zhao, and P. N. Kao. 2007. NF90 regulates inducible IL-2 gene expression in T cells. *J Exp Med* 204: 971-977.
132. Shi, L., D. Qiu, G. Zhao, B. Corthesy, S. Lees-Miller, W. H. Reeves, and P. N. Kao. 2007. Dynamic binding of Ku80, Ku70 and NF90 to the IL-2 promoter in vivo in activated T-cells. *Nucleic Acids Res* 35: 2302-2310.
133. Corthesy, B., and P. N. Kao. 1994. Purification by DNA affinity chromatography of two polypeptides that contact the NF-AT DNA binding site in the interleukin 2 promoter. *J Biol Chem* 269: 20682-20690.

134. Hu, Q., Y. Y. Lu, H. Noh, S. Hong, Z. Dong, H. F. Ding, S. B. Su, and S. Huang. 2013. Interleukin enhancer-binding factor 3 promotes breast tumor progression by regulating sustained urokinase-type plasminogen activator expression. *Oncogene* 32: 3933-3943.
135. Isken, O., C. W. Grassmann, R. T. Sarisky, M. Kann, S. Zhang, F. Grosse, P. N. Kao, and S. E. Behrens. 2003. Members of the NF90/NFAR protein group are involved in the life cycle of a positive-strand RNA virus. *EMBO J* 22: 5655-5665.
136. Hrecka, K., C. Hao, M. Gierszewska, S. K. Swanson, M. Kesik-Brodacka, S. Srivastava, L. Florens, M. P. Washburn, and J. Skowronski. 2011. Vpx relieves inhibition of HIV-1 infection of macrophages mediated by the SAMHD1 protein. *Nature* 474: 658-661.
137. Gao, D., J. Wu, Y. T. Wu, F. Du, C. Aroh, N. Yan, L. Sun, and Z. J. Chen. 2013. Cyclic GMP-AMP synthase is an innate immune sensor of HIV and other retroviruses. *Science* 341: 903-906.
138. Reichman, T. W., A. M. Parrott, I. Fierro-Monti, D. J. Caron, P. N. Kao, C. G. Lee, H. Li, and M. B. Mathews. 2003. Selective regulation of gene expression by nuclear factor 110, a member of the NF90 family of double-stranded RNA-binding proteins. *J Mol Biol* 332: 85-98.
139. Nakadai, T., A. Fukuda, M. Shimada, K. Nishimura, and K. Hisatake. 2015. The RNA binding complexes NF45-NF90 and NF45-NF110 associate dynamically with the c-fos gene and function as transcriptional coactivators. *J Biol Chem* 290: 26832-26845.
140. Lindstedt, M., B. Johansson-Lindbom, and C. A. Borrebaeck. 2002. Global reprogramming of dendritic cells in response to a concerted action of inflammatory mediators. *Int Immunol* 14: 1203-1213.
141. Di Rosa, M., D. Tibullo, S. Saccone, G. Distefano, M. S. Basile, F. Di Raimondo, and L. Malaguarnera. 2016. CHI3L1 nuclear localization in monocyte derived dendritic cells. *Immunobiology* 221: 347-356.
142. Nencioni, A., F. Grunebach, A. Zobywlaski, C. Denzlinger, W. Brugger, and P. Brossart. 2002. Dendritic cell immunogenicity is regulated by peroxisome proliferator-activated receptor gamma. *J Immunol* 169: 1228-1235.
143. Muzio, M., D. Bosisio, N. Polentarutti, G. D'Amico, A. Stoppacciaro, R. Mancinelli, C. van't Veer, G. Penton-Rol, L. P. Ruco, P. Allavena, and A. Mantovani. 2000. Differential expression and regulation of toll-like receptors (TLR) in human leukocytes: selective expression of TLR3 in dendritic cells. *Journal of immunology* 164: 5998-6004.
144. Wang, P., Y. Xue, Y. Han, L. Lin, C. Wu, S. Xu, Z. Jiang, J. Xu, Q. Liu, and X. Cao. 2014. The STAT3-binding long noncoding RNA lnc-DC controls human dendritic cell differentiation. *Science* 344: 310-313.
145. D'Amico, G., G. Frascaroli, G. Bianchi, P. Transidico, A. Doni, A. Vecchi, S. Sozzani, P. Allavena, and A. Mantovani. 2000. Uncoupling of inflammatory chemokine receptors by IL-10: generation of functional decoys. *Nature immunology* 1: 387-391.
146. Videira, P. A., I. F. Amado, H. J. Crespo, M. C. Alguero, F. Dall'Olio, M. G. Cabral, and H. Trindade. 2008. Surface alpha 2-3- and alpha 2-6-sialylation of human monocytes and derived dendritic cells and its influence on endocytosis. *Glycoconj J* 25: 259-268.
147. Wu, X., H. Gao, R. Bleday, and Z. Zhu. 2014. Homeobox transcription factor VentX regulates differentiation and maturation of human dendritic cells. *J Biol Chem* 289: 14633-14643.

148. Skelton, L., M. Cooper, M. Murphy, and A. Platt. 2003. Human immature monocyte-derived dendritic cells express the G protein-coupled receptor GPR105 (KIAA0001, P2Y14) and increase intracellular calcium in response to its agonist, uridine diphosphoglucose. *Journal of immunology* 171: 1941-1949.
149. Jin, P., T. H. Han, J. Ren, S. Saunders, E. Wang, F. M. Marincola, and D. F. Stroncek. 2010. Molecular signatures of maturing dendritic cells: implications for testing the quality of dendritic cell therapies. *J Transl Med* 8: 4.
150. Landmann, S., A. Mühlethaler-Mottet, L. Bernasconi, T. Suter, J. M. Waldburger, K. Masternak, J. F. Arrighi, C. Hauser, A. Fontana, and W. Reith. 2001. Maturation of Dendritic Cells Is Accompanied by Rapid Transcriptional Silencing of Class II Transactivator (Ciita) Expression. In *J Exp Med*. 379-392.
151. Rasaiyaah, J., C. P. Tan, A. J. Fletcher, A. J. Price, C. Blondeau, L. Hilditch, D. A. Jacques, D. L. Selwood, L. C. James, M. Noursadeghi, and G. J. Towers. 2013. HIV-1 evades innate immune recognition through specific cofactor recruitment. *Nature* 503: 402-405.
152. Yan, N., A. D. Regalado-Magdos, B. Stiggelbout, M. A. Lee-Kirsch, and J. Lieberman. 2010. The cytosolic exonuclease TREX1 inhibits the innate immune response to human immunodeficiency virus type 1. *Nature immunology* 11: 1005-1013.
153. Lepelley, A., S. Louis, M. Sourisseau, H. K. Law, J. Pothlichet, C. Schilte, L. Chaperot, J. Plumas, R. E. Randall, M. Si-Tahar, F. Mammano, M. L. Albert, and O. Schwartz. 2011. Innate sensing of HIV-infected cells. *PLoS Pathog* 7: e1001284.
154. Gringhuis, S. I., M. van der Vlist, L. M. van den Berg, J. den Dunnen, M. Litjens, and T. B. Geijtenbeek. 2010. HIV-1 exploits innate signaling by TLR8 and DC-SIGN for productive infection of dendritic cells. *Nature immunology* 11: 419-426.
155. Akiyama, H., C. M. Miller, C. R. Ettinger, A. C. Belkina, J. E. Snyder-Cappione, and S. Gummuluru. 2018. HIV-1 intron-containing RNA expression induces innate immune activation and T cell dysfunction. *Nat Commun* 9: 3450.
156. McCauley, S. M., K. Kim, A. Nowosielska, A. Dauphin, L. Yurkovetskiy, W. E. Diehl, and J. Luban. 2018. Intron-containing RNA from the HIV-1 provirus activates type I interferon and inflammatory cytokines. *Nat Commun* 9: 5305.
157. Yin, X., S. Langer, Z. Zhang, K. M. Herbert, S. Yoh, R. Konig, and S. K. Chanda. 2020. Sensor Sensibility-HIV-1 and the Innate Immune Response. *Cells* 9.
158. Chevrier, N., P. Mertins, M. N. Artyomov, A. K. Shalek, M. Iannacone, M. F. Ciaccio, I. Gat-Viks, E. Tonti, M. M. DeGrace, K. R. Clauser, M. Garber, T. M. Eisenhaure, N. Yosef, J. Robinson, A. Sutton, M. S. Andersen, D. E. Root, U. von Andrian, R. B. Jones, H. Park, S. A. Carr, A. Regev, I. Amit, and N. Hacohen. 2011. Systematic discovery of TLR signaling components delineates viral-sensing circuits. *Cell* 147: 853-867.
159. Parker, L. M., I. Fierro-Monti, and M. B. Mathews. 2001. Nuclear factor 90 is a substrate and regulator of the eukaryotic initiation factor 2 kinase double-stranded RNA-activated protein kinase. *J Biol Chem* 276: 32522-32530.
160. Parrott, A. M., M. R. Walsh, T. W. Reichman, and M. B. Mathews. 2005. RNA binding and phosphorylation determine the intracellular distribution of nuclear factors 90 and 110. *J Mol Biol* 348: 281-293.

161. Reichman, T. W., and M. B. Mathews. 2003. RNA binding and intramolecular interactions modulate the regulation of gene expression by nuclear factor 110. *Rna* 9: 543-554.
162. de Baey, A., and A. Lanzavecchia. 2000. The role of aquaporins in dendritic cell macropinocytosis. *J Exp Med* 191: 743-748.
163. Wacleche, V. S., A. Cattin, J. P. Goulet, D. Gauchat, A. Gosselin, A. Cleret-Buhot, Y. Zhang, C. L. Tremblay, J. P. Routy, and P. Ancuta. 2018. CD16(+) monocytes give rise to CD103(+)RALDH2(+)TCF4(+) dendritic cells with unique transcriptional and immunological features. *Blood Adv* 2: 2862-2878.
164. Pickl, W. F., O. Majdic, P. Kohl, J. Stockl, E. Riedl, C. Scheinecker, C. Bello-Fernandez, and W. Knapp. 1996. Molecular and functional characteristics of dendritic cells generated from highly purified CD14+ peripheral blood monocytes. *Journal of immunology* 157: 3850-3859.
165. Li, K., H. Fazekasova, N. Wang, Q. Peng, S. H. Sacks, G. Lombardi, and W. Zhou. 2012. Functional modulation of human monocytes derived DCs by anaphylatoxins C3a and C5a. *Immunobiology* 217: 65-73.
166. Ju, X., M. Zenke, D. N. Hart, and G. J. Clark. 2008. CD300a/c regulate type I interferon and TNF-alpha secretion by human plasmacytoid dendritic cells stimulated with TLR7 and TLR9 ligands. *Blood* 112: 1184-1194.
167. Van der Borght, K., C. L. Scott, V. Nindl, A. Bouche, L. Martens, D. Sichien, J. Van Moorleghem, M. Vanheerswynghels, S. De Prijck, Y. Saeys, B. Ludewig, T. Gillebert, M. Guilliams, P. Carmeliet, and B. N. Lambrecht. 2017. Myocardial Infarction Primes Autoreactive T Cells through Activation of Dendritic Cells. *Cell Rep* 18: 3005-3017.
168. Liu, T. M., H. Wang, D. N. Zhang, and G. Z. Zhu. 2019. Transcription Factor MafB Suppresses Type I Interferon Production by CD14(+) Monocytes in Patients With Chronic Hepatitis C. *Front Microbiol* 10: 1814.
169. Navarro-Barriuso, J., M. J. Mansilla, M. Naranjo-Gomez, A. Sanchez-Pla, B. Quirant-Sanchez, A. Teniente-Serra, C. Ramo-Tello, and E. M. Martinez-Caceres. 2018. Comparative transcriptomic profile of tolerogenic dendritic cells differentiated with vitamin D3, dexamethasone and rapamycin. *Scientific reports* 8: 14985.
170. Maniecki, M. B., H. J. Moller, S. K. Moestrup, and B. K. Moller. 2006. CD163 positive subsets of blood dendritic cells: the scavenging macrophage receptors CD163 and CD91 are coexpressed on human dendritic cells and monocytes. *Immunobiology* 211: 407-417.
171. Corinti, S., C. Albanesi, A. la Sala, S. Pastore, and G. Girolomoni. 2001. Regulatory activity of autocrine IL-10 on dendritic cell functions. *Journal of immunology* 166: 4312-4318.
172. Olivar, R., A. Luque, S. Cardenas-Brito, M. Naranjo-Gomez, A. M. Blom, F. E. Borras, S. Rodriguez de Cordoba, P. F. Zipfel, and J. M. Aran. 2016. The Complement Inhibitor Factor H Generates an Anti-Inflammatory and Tolerogenic State in Monocyte-Derived Dendritic Cells. *Journal of immunology* 196: 4274-4290.
173. Sanecka, A., M. Ansems, A. C. Prosser, K. Danielski, K. Warner, M. H. den Brok, B. J. Jansen, D. Eleveld-Trancikova, and G. J. Adema. 2011. DC-STAMP knock-down deregulates cytokine production and T-cell stimulatory capacity of LPS-matured dendritic cells. *BMC Immunol* 12: 57.

174. Yokota, A., H. Takeuchi, N. Maeda, Y. Ohoka, C. Kato, S. Y. Song, and M. Iwata. 2009. GM-CSF and IL-4 synergistically trigger dendritic cells to acquire retinoic acid-producing capacity. *Int Immunol* 21: 361-377.
175. Vulcano, M., C. Albanesi, A. Stoppacciaro, R. Bagnati, G. D'Amico, S. Struyf, P. Transidico, R. Bonecchi, A. Del Prete, P. Allavena, L. P. Ruco, C. Chiabrando, G. Girolomoni, A. Mantovani, and S. Sozzani. 2001. Dendritic cells as a major source of macrophage-derived chemokine/CCL22 in vitro and in vivo. *Eur J Immunol* 31: 812-822.
176. Park, K., and A. L. Scott. 2010. Cholesterol 25-hydroxylase production by dendritic cells and macrophages is regulated by type I interferons. *J Leukoc Biol* 88: 1081-1087.
177. Subramanian, A., P. Tamayo, V. K. Mootha, S. Mukherjee, B. L. Ebert, M. A. Gillette, A. Paulovich, S. L. Pomeroy, T. R. Golub, E. S. Lander, and J. P. Mesirov. 2005. Gene set enrichment analysis: a knowledge-based approach for interpreting genome-wide expression profiles. *Proc Natl Acad Sci U S A* 102: 15545-15550.
178. Liberzon, A., C. Birger, H. Thorvaldsdottir, M. Ghandi, J. P. Mesirov, and P. Tamayo. 2015. The Molecular Signatures Database (MSigDB) hallmark gene set collection. *Cell Syst* 1: 417-425.
179. Chen, E. Y., C. M. Tan, Y. Kou, Q. Duan, Z. Wang, G. V. Meirelles, N. R. Clark, and A. Ma'ayan. 2013. Enrichr: interactive and collaborative HTML5 gene list enrichment analysis tool. *BMC Bioinformatics* 14: 128.
180. Croasdell, A., P. F. Duffney, N. Kim, S. H. Lacy, P. J. Sime, and R. P. Phipps. 2015. PPARgamma and the Innate Immune System Mediate the Resolution of Inflammation. *PPAR Res* 2015: 549691.
181. Saunders, L. R., D. J. Perkins, S. Balachandran, R. Michaels, R. Ford, A. Mayeda, and G. N. Barber. 2001. Characterization of two evolutionarily conserved, alternatively spliced nuclear phosphoproteins, NFAR-1 and -2, that function in mRNA processing and interact with the double-stranded RNA-dependent protein kinase, PKR. *J Biol Chem* 276: 32300-32312.
182. Harashima, A., T. Guettouche, and G. N. Barber. 2010. Phosphorylation of the NFAR proteins by the dsRNA-dependent protein kinase PKR constitutes a novel mechanism of translational regulation and cellular defense. *Genes Dev* 24: 2640-2653.
183. Urcuqui-Inchima, S., M. E. Castano, D. Hernandez-Verdun, G. St-Laurent, 3rd, and A. Kumar. 2006. Nuclear Factor 90, a cellular dsRNA binding protein inhibits the HIV Rev-export function. *Retrovirology* 3: 83.
184. Hoque, M., R. A. Shamanna, D. Guan, T. Pe'ery, and M. B. Mathews. 2011. HIV-1 replication and latency are regulated by translational control of cyclin T1. *J Mol Biol* 410: 917-932.
185. Guan, D., N. Altan-Bonnet, A. M. Parrott, C. J. Arrigo, Q. Li, M. Khaleduzzaman, H. Li, C. G. Lee, T. Pe'ery, and M. B. Mathews. 2008. Nuclear factor 45 (NF45) is a regulatory subunit of complexes with NF90/110 involved in mitotic control. *Mol Cell Biol* 28: 4629-4641.
186. Chaumet, A., S. Castella, L. Gasmi, A. Fradin, G. Clodic, G. Bolbach, R. Poulhe, P. Denoulet, and J. C. Larcher. 2013. Proteomic analysis of interleukin enhancer binding factor 3 (Ilf3) and nuclear factor 90 (NF90) interactome. *Biochimie* 95: 1146-1157.

187. Everts, B., E. Amiel, S. C. Huang, A. M. Smith, C. H. Chang, W. Y. Lam, V. Redmann, T. C. Freitas, J. Blagih, G. J. van der Windt, M. N. Artyomov, R. G. Jones, E. L. Pearce, and E. J. Pearce. 2014. TLR-driven early glycolytic reprogramming via the kinases TBK1-IKKvarepsilon supports the anabolic demands of dendritic cell activation. *Nature immunology* 15: 323-332.

188. Baker, A. D., A. Malur, B. P. Barna, M. S. Kavuru, A. G. Malur, and M. J. Thomassen. 2010. PPARgamma regulates the expression of cholesterol metabolism genes in alveolar macrophages. *Biochem Biophys Res Commun* 393: 682-687.

189. York, A. G., K. J. Williams, J. P. Argus, Q. D. Zhou, G. Brar, L. Vergnes, E. E. Gray, A. Zhen, N. C. Wu, D. H. Yamada, C. R. Cunningham, E. J. Tarling, M. Q. Wilks, D. Casero, D. H. Gray, A. K. Yu, E. S. Wang, D. G. Brooks, R. Sun, S. G. Kitchen, T. T. Wu, K. Reue, D. B. Stetson, and S. J. Bensinger. 2015. Limiting cholesterol biosynthetic flux spontaneously engages type I IFN signaling. *Cell* 163: 1716-1729.

190. Plutzky, J. 2011. The PPAR-RXR transcriptional complex in the vasculature: energy in the balance. *Circ Res* 108: 1002-1016.

191. Larange, A., and H. Cheroutre. 2016. Retinoic Acid and Retinoic Acid Receptors as Pleiotropic Modulators of the Immune System. *Annu Rev Immunol* 34: 369-394.

192. Szatmari, I., A. Pap, R. Ruhl, J. X. Ma, P. A. Illarionov, G. S. Besra, E. Rajnavolgyi, B. Dezso, and L. Nagy. 2006. PPARgamma controls CD1d expression by turning on retinoic acid synthesis in developing human dendritic cells. *J Exp Med* 203: 2351-2362.

193. Geissmann, F., P. Revy, N. Brousse, Y. Lepelletier, C. Folli, A. Durandy, P. Chambon, and M. Dy. 2003. Retinoids regulate survival and antigen presentation by immature dendritic cells. *J Exp Med* 198: 623-634.

194. Szatmari, I., and L. Nagy. 2008. Nuclear receptor signalling in dendritic cells connects lipids, the genome and immune function. *EMBO J* 27: 2353-2362.

195. Appel, S., V. Mirakaj, A. Bringmann, M. M. Weck, F. Grunebach, and P. Brossart. 2005. PPAR-gamma agonists inhibit toll-like receptor-mediated activation of dendritic cells via the MAP kinase and NF-kappaB pathways. *Blood* 106: 3888-3894.

196. Coutant, F., S. Agaugue, L. Perrin-Cocon, P. Andre, and V. Lotteau. 2004. Sensing environmental lipids by dendritic cell modulates its function. *Journal of immunology* 172: 54-60.

197. Khare, A., K. Chakraborty, M. Raundhal, P. Ray, and A. Ray. 2015. Cutting Edge: Dual Function of PPARgamma in CD11c+ Cells Ensures Immune Tolerance in the Airways. *Journal of immunology* 195: 431-435.

198. Li, C. G., C. Mahon, N. M. Sweeney, E. Verschueren, V. Kantamani, D. Li, J. K. Hennigs, D. P. Marciano, I. Diebold, O. Abu-Halawa, M. Elliott, S. Sa, F. Guo, L. Wang, A. Cao, C. Guignabert, J. Sollier, N. P. Nickel, M. Kaschwich, K. A. Cimprich, and M. Rabinovitch. 2019. PPARgamma Interaction with UBR5/ATMIN Promotes DNA Repair to Maintain Endothelial Homeostasis. *Cell Rep* 26: 1333-1343 e1337.

199. Yoshida, T., K. Kato, M. Oguri, H. Horibe, T. Kawamiya, K. Yokoi, T. Fujimaki, S. Watanabe, K. Satoh, Y. Aoyagi, M. Tanaka, H. Yoshida, S. Shinkai, Y. Nozawa, and Y. Yamada. 2011. Association of polymorphisms of BTN2A1 and ILF3 with myocardial infarction in Japanese individuals with different lipid profiles. *Mol Med Rep* 4: 511-518.

200. Knevel, R., T. W. J. Huizinga, and F. Kurreeman. 2017. Genomic Influences on Susceptibility and Severity of Rheumatoid Arthritis. *Rheum Dis Clin North Am* 43: 347-361.
201. Shi, L., G. Zhao, D. Qiu, W. R. Godfrey, H. Vogel, T. A. Rando, H. Hu, and P. N. Kao. 2005. NF90 regulates cell cycle exit and terminal myogenic differentiation by direct binding to the 3'-untranslated region of MyoD and p21WAF1/CIP1 mRNAs. *J Biol Chem* 280: 18981-18989.
202. Wang, Y., M. Ma, X. Xiao, and Z. Wang. 2012. Intronic splicing enhancers, cognate splicing factors and context-dependent regulation rules. *Nat Struct Mol Biol* 19: 1044-1052.
203. Zarnack, K., J. Konig, M. Tajnik, I. Martincorena, S. Eustermann, I. Stevant, A. Reyes, S. Anders, N. M. Luscombe, and J. Ule. 2013. Direct competition between hnRNP C and U2AF65 protects the transcriptome from the exonization of Alu elements. *Cell* 152: 453-466.
204. Zilliox, M. J., G. Parmigiani, and D. E. Griffin. 2006. Gene expression patterns in dendritic cells infected with measles virus compared with other pathogens. *Proc Natl Acad Sci U S A* 103: 3363-3368.
205. Bieback, K., E. Lien, I. M. Klagge, E. Avota, J. Schneider-Schaulies, W. P. Duprex, H. Wagner, C. J. Kirschning, V. Ter Meulen, and S. Schneider-Schaulies. 2002. Hemagglutinin protein of wild-type measles virus activates toll-like receptor 2 signaling. *J Virol* 76: 8729-8736.
206. Gronhagen, C. M., C. M. Fored, F. Granath, and F. Nyberg. 2011. Cutaneous lupus erythematosus and the association with systemic lupus erythematosus: a population-based cohort of 1088 patients in Sweden. *Br J Dermatol* 164: 1335-1341.
207. Dey-Rao, R., and A. A. Sinha. 2015. Genome-wide transcriptional profiling of chronic cutaneous lupus erythematosus (CCLE) peripheral blood identifies systemic alterations relevant to the skin manifestation. *Genomics* 105: 90-100.
208. Deane, J. A., P. Pisitkun, R. S. Barrett, L. Feigenbaum, T. Town, J. M. Ward, R. A. Flavell, and S. Bolland. 2007. Control of toll-like receptor 7 expression is essential to restrict autoimmunity and dendritic cell proliferation. *Immunity* 27: 801-810.
209. Barrat, F. J., T. Meeker, J. H. Chan, C. Guiducci, and R. L. Coffman. 2007. Treatment of lupus-prone mice with a dual inhibitor of TLR7 and TLR9 leads to reduction of autoantibody production and amelioration of disease symptoms. *Eur J Immunol* 37: 3582-3586.
210. Rowland, S. L., J. M. Riggs, S. Gilfillan, M. Bugatti, W. Vermi, R. Kolbeck, E. R. Unanue, M. A. Sanjuan, and M. Colonna. 2014. Early, transient depletion of plasmacytoid dendritic cells ameliorates autoimmunity in a lupus model. *J Exp Med* 211: 1977-1991.
211. Baccala, R., R. Gonzalez-Quintial, A. L. Blasius, I. Rimann, K. Ozato, D. H. Kono, B. Beutler, and A. N. Theofilopoulos. 2013. Essential requirement for IRF8 and SLC15A4 implicates plasmacytoid dendritic cells in the pathogenesis of lupus. *Proc Natl Acad Sci U S A* 110: 2940-2945.
212. Furie, R., M. Khamashta, J. T. Merrill, V. P. Werth, K. Kalunian, P. Brohawn, G. G. Illei, J. Drappa, L. Wang, S. Yoo, and C. D. S. Investigators. 2017. Anifrolumab, an Anti-

Interferon-alpha Receptor Monoclonal Antibody, in Moderate-to-Severe Systemic Lupus Erythematosus. *Arthritis Rheumatol* 69: 376-386.

213. Jabbari, A., M. Suarez-Farinas, J. Fuentes-Duculan, J. Gonzalez, I. Cueto, A. G. Franks, Jr., and J. G. Krueger. 2014. Dominant Th1 and minimal Th17 skewing in discoid lupus revealed by transcriptomic comparison with psoriasis. *J Invest Dermatol* 134: 87-95.

214. Dorner, T., and P. E. Lipsky. 2016. Beyond pan-B-cell-directed therapy - new avenues and insights into the pathogenesis of SLE. *Nat Rev Rheumatol* 12: 645-657.

215. Bremer, H. D., N. Landegren, R. Sjöberg, Å. Hallgren, S. Renneker, E. Lattwein, D. Leonard, M. L. Eloranta, L. Rönnblom, G. Nordmark, P. Nilsson, G. Andersson, I. Lilliehöök, K. Lindblad-Toh, O. Kämpe, and H. Hansson-Hamlin. 2018. ILF2 and ILF3 are autoantigens in canine systemic autoimmune disease. *Scientific reports* 8: 4852.

216. Satoh, M., H. B. Richards, V. M. Shaheen, H. Yoshida, M. Shaw, J. O. Naim, P. H. Wooley, and W. H. Reeves. 2000. Widespread susceptibility among inbred mouse strains to the induction of lupus autoantibodies by pristane. *Clin Exp Immunol* 121: 399-405.

217. Funk, J., T. Langeland, E. Schrumpf, and L. E. Hanssen. 1991. Psoriasis induced by interferon-alpha. *Br J Dermatol* 125: 463-465.

218. Erkek, E., A. Karaduman, Y. Akcan, C. Sokmensuer, and G. Bukulmez. 2000. Psoriasis associated with HCV and exacerbated by interferon alpha: complete clearance with acitretin during interferon alpha treatment for chronic active hepatitis. *Dermatology* 201: 179-181.

219. van der Fits, L., L. I. van der Wel, J. D. Laman, E. P. Prens, and M. C. Verschuren. 2004. In psoriasis lesional skin the type I interferon signaling pathway is activated, whereas interferon-alpha sensitivity is unaltered. *J Invest Dermatol* 122: 51-60.

220. Baldwin, H. M., K. Pallas, V. King, T. Jamieson, C. S. McKimmie, R. J. Nibbs, J. M. Carballido, M. Jaritz, A. Rot, and G. J. Graham. 2013. Microarray analyses demonstrate the involvement of type I interferons in psoriasiform pathology development in D6-deficient mice. *J Biol Chem* 288: 36473-36483.

221. Nestle, F. O., C. Conrad, A. Tun-Kyi, B. Homey, M. Gombert, O. Boyman, G. Burg, Y. J. Liu, and M. Gilliet. 2005. Plasmacytoid predendritic cells initiate psoriasis through interferon-alpha production. *J Exp Med* 202: 135-143.

222. Boyman, O., H. P. Hefti, C. Conrad, B. J. Nickoloff, M. Suter, and F. O. Nestle. 2004. Spontaneous development of psoriasis in a new animal model shows an essential role for resident T cells and tumor necrosis factor-alpha. *J Exp Med* 199: 731-736.

223. Cisse, B., M. L. Caton, M. Lehner, T. Maeda, S. Scheu, R. Locksley, D. Holmberg, C. Zweier, N. S. den Hollander, S. G. Kant, W. Holter, A. Rauch, Y. Zhuang, and B. Reizis. 2008. Transcription factor E2-2 is an essential and specific regulator of plasmacytoid dendritic cell development. *Cell* 135: 37-48.

224. Chu, T., M. Ni, C. Chen, S. Akilesh, and J. A. Hamerman. 2019. Cutting Edge: BCAP Promotes Lupus-like Disease and TLR-Mediated Type I IFN Induction in Plasmacytoid Dendritic Cells. *Journal of immunology* 202: 2529-2534.

225. Haque, N., R. Ouda, C. Chen, K. Ozato, and J. R. Hogg. 2018. ZFR coordinates crosstalk between RNA decay and transcription in innate immunity. *Nat Commun* 9: 1145.

226. Nakamura, N., T. Yamauchi, M. Hiramoto, M. Yuri, M. Naito, M. Takeuchi, K. Yamanaka, A. Kita, T. Nakahara, I. Kinoyama, A. Matsuhisa, N. Kaneko, H. Koutoku, M. Sasamata, H.

Yokota, S. Kawabata, and K. Furuichi. 2012. Interleukin enhancer-binding factor 3/NF110 is a target of YM155, a suppressant of survivin. *Mol Cell Proteomics* 11: M111.013243.

227. Yamauchi, T., N. Nakamura, M. Hiramoto, M. Yuri, H. Yokota, M. Naitou, M. Takeuchi, K. Yamanaka, A. Kita, T. Nakahara, I. Kinoyama, A. Matsuhisa, N. Kaneko, H. Koutoku, M. Sasamata, M. Kobori, M. Katou, S. Tawara, S. Kawabata, and K. Furuichi. 2012. Sepantronium bromide (YM155) induces disruption of the ILF3/p54(nrb) complex, which is required for survivin expression. *Biochem Biophys Res Commun* 425: 711-716.

228. Fung, K. Y., N. E. Mangan, H. Cumming, J. C. Horvat, J. R. Mayall, S. A. Stifter, N. De Weerd, L. C. Roisman, J. Rossjohn, S. A. Robertson, J. E. Schjenken, B. Parker, C. E. Gargett, H. P. Nguyen, D. J. Carr, P. M. Hansbro, and P. J. Hertzog. 2013. Interferon-epsilon protects the female reproductive tract from viral and bacterial infection. *Science* 339: 1088-1092.

229. Harris, B. D., J. Schreiter, M. Chevrier, J. L. Jordan, and M. R. Walter. 2018. Human interferon- and interferon-kappa exhibit low potency and low affinity for cell-surface IFNAR and the poxvirus antagonist B18R. *J Biol Chem* 293: 16057-16068.